UNIVERSITY OF CAPE TOWN

Calibration of a FOSIM Model for a Section of the N2 Freeway in Cape Town: Weaving Section at an Off-Ramp

Minor Dissertation

A thesis submitted in partial fulfilment of the requirements for the degree of

Master of Engineering
In Transport Studies

Prepared by
Bongani Dlamini

June 2023

Abstract

Driver behaviour differs from person to person depending on the driver's behavioural characteristics, the vehicle used and road geometry. Traffic models must account for this variation in behaviour to properly analyse this complex reality. Typically, the variation is modelled by distinguishing between different 'vehicle-driver combinations', whose behaviour is established by the settings of model parameters. Adjusting the parameters to make the model deliver realistic results is called model calibration. This is done by comparing the model results with field observations and adjusting the parameters systematically until the model results and empirical data align as much as possible. Subsequently, model validation is carried out to test the applicability of the calibrated parameters on a dataset separate from that used in the calibration process.

This research is aimed at calibrating and validating a microscopic simulation model for a section of the N2 freeway using FOSIM software. FOSIM, a software originally developed to simulate Dutch freeway traffic, is used by road authorities in The Netherlands and some parts of the UK to test freeway capacity. Its simplistic, intuitive, and user-friendly nature makes it a more efficient and cost-effective tool for assessing traffic management and operations and would be of great benefit to the South African market and transport authorities. Since the software is calibrated and validated for the Dutch freeway scenario, it needs to be tested and adapted to the local context in order to be applied on South African freeways.

The selected network of analysis falls within Section 1 of the National Road N2 (Settlers Way) in Cape Town between the M4 off-ramp and Hospital Bend (M3) in the in-bound direction. Peak hour traffic volumes were obtained using CCTV footage supplied by the Cape Town Freeway Management System over a period of three days. Travel time and speed data for the same dates was obtained from floating car runs and supplemented by CCTV observations. Based on this collected data, the Measures of Effectiveness (MoEs) examined in the study were traffic volumes, speed and travel time.

The modelling commenced with coding the road geometry and the applicable traffic demand. The calibration process was carried out using a series of steps, the first of which was a sensitivity analysis. A sensitivity analysis was conducted to determine the relative influence of each of the

parameters on the simulated output. Through this analysis, it was discovered that 36% of the parameters did not have a significant influence on the simulated output and were thus omitted from the calibration. On the other hand, the parameters that showed significant effect were carried over to the next step which included establishing the search range in which the optimum parameter values lie. This was done using the Golden Selection Method (GSM), which is an iterative, single-parameter search technique that seeks to minimize the standard error between the simulated output and empirical data.

The initial model, which was run with default parameters, showed good results when assessed on traffic volumes. This model had a GEH statistic of less than 5 for 97% of the simulated values and an R-squared value of 0.88, both signifying a very high correlation between the simulated and empirical traffic volumes. However, travel time and speed exhibited high discrepancies between the empirical average and model output, with all the simulated values falling outside the acceptable range and the average percentage error reaching 40.5% - clearly indicating problems with the model. When the local conditions were calibrated based on floating car run data, travel time and speed results were improved significantly with only 21% of simulated values falling out of the acceptable range. The average error decreased from 40.5% to 3.8%. On the other hand, the traffic volume MoE worsened, with the GEH being less than 5 for only 63% of the simulated values and the R-squared consequently decreased to 0.42.

The model was then advanced further to be calibrated globally by adjusting model parameters. After several iterations and multiple improvements to the model, the final model with the optimum parameter values demonstrated a significant improvement in the simulated volumes. The average GEH statistic decreased from 4.56 to 2.2. The GEH was also less than 5 for 97% of the simulated values, which was an improvement from the 63% obtained in the previous model. Furthermore, the R-squared increased from 0.42 in the previous model to 0.82. Travel time and speed also exhibited improved results when compared to the previous model, with only 1.6% of the simulated values falling out of the acceptable range as opposed to 21% in the previous model.

Following the calibration process, the model which best estimated the empirical data measurement was validated. The validation results showed that even though the established parameters produced an excellent calibration model, the same parameters failed to produce sufficiently good validation results. The average GEH value had increased to 3 and was less than 5 for only 77% of the simulated values compared to 97% in the calibration model. The travel time and speed were, however, well within the acceptable range. In order to overcome the unsatisfactory GEH results obtained, the calibration parameters had to the fine-tuned further over several models and iterations. The final calibration and validation models both passed the acceptance test on all three MoEs. Statistical analysis also showed that the models were acceptable.

The FOSIM model was thus successfully calibrated and validated, and the objectives of the research were duly met. Some of the take-homes from the findings of this study include the observation that using a single MoE in model calibration can be problematic and misleading. This is exhibited by the initial model that produced excellent volume predictions while travel time and speed were extremely inaccurate. The research also showed that fine-tuning the parameters to explain the calibration too well leads to overfitting the model which causes other problems. This explains why a good calibration model failed when it was initially validated. Finally, it is recommended that future studies explore a sensitivity analysis which will consider interactive effect between model parameters. It is also recommended that a more generalized models with an acceptable margin of error be developed to avoid overfitting and to enable the models to be applicable on a wider network range.

Contents

List of figures

List of Tables

List of Equations

Plagiarism Declaration

I, Bongani Dlamini, hereby declare that the work on which this thesis is based is my original work (except where acknowledgements indicate otherwise) and that neither the whole work nor any part of it has been, is being, or is to be submitted for another degree in this or any other university. I authorize the University to reproduce for the purpose of research either the whole or any portion of the contents in any manner whatsoever.

Student Number: DLMBON018 **Signature:**……………………….

Acknowledgements

I give thanks to God for the love He's shown throughout the course of my life and all while carrying out this research.

A special thanks goes to my late mother who continuously provided a sense of 'home' even though she was very far away and encouraged me to finish this work at a time when I no longer had the intention to do so.

I am grateful to Prof. Mark Zuidgeest for granting me the opportunity to work with him and for making this research possible. I appreciate all the time he spent in guiding me and the insights he shared.

I would also like to thank Mr Angus Rule and the Cape Town Freeway Management System for making the data available, which was a crucial component of this research.

1. Introduction

Traffic simulation modelling has become increasingly prevalent among transportation agencies around the world when evaluating existing and proposed transport infrastructure alternatives (Jobanputra & Vanderschuren , 2012). Traffic simulation provides an efficient way of determining the benefits and limitations of alternative transport and traffic solutions, with minimal cost implications and disruption to existing traffic operations. This apparent surge in their application can partly be attributed to increasing affordability and improvement in the processing power of modern computers. In particular, microsimulation models require significantly higher computing power, since they represent traffic data in greater detail compared to other traffic simulation models, such as macroscopic and mesoscopic. Considering this heightened processing detail, microsimulation models are classified as high-fidelity. To put it more simply, they can produce more accurate simulation results, while studying a larger number of traffic performance measures.

These microsimulation traffic models are hinged on reproducing traffic flows by simulating individual vehicle behaviour. This does not only enable capturing the dynamic aspects of time dependent traffic characteristics, but it also permits the modelling of individual driver reactions and behaviour. The underlying premise is that the dynamic characteristics of a particular traffic stream emerge from a series of driver's efforts to regulate their operating speed, while interacting with other drivers and the road environment according to the perceived information. The individual driver's reaction to the perceived information consists in regulating their speed by either accelerating, decelerating, or maintaining current speed; control of direction (steering); overtaking in order to drive at a higher speed or to place themselves in the appropriate lane so they could perform the desired turning movement.

Many microscopic simulation tools designed to account for these induvial driver behaviours have been developed over the years, for instance, VISSIM, CORSIM, PARAMICS and FOSIM, to mention a few. The models consist of sub-models which account for various types of traffic dynamics or driver behaviours, such as the car-following, acceleration, lane-change and gap acceptance (Jobanputra & Vanderschuren , 2012). There are a set of rules and equations which govern each of these sub-models, and these rules and equations are composed of several model parameters. These model parameters are vast, some are linked to vehicle characteristics and performance, while some account for driver behaviour, and still some are centred around the road network and geometric features. The model software comes with default parameter values, which are calibrated for a particular context. However, these default values are unlikely to produce sufficiently accurate models when applied in a different context (Bloomberg et a., 2003). Given that the traffic model accuracy is inextricably related to the use of appropriate parameters, it is crucial that the default parameters are fine-tuned to replicate the observed local traffic conditions (Dowling et al., 2004) – this is how the need for model calibration comes about.

During the calibration phase, driver behaviour and vehicle performance parameters are fine-tuned until the simulated results reflects, as closely as possible, the observed field data from local conditions being modelled. Though the increased performance detail of the microscopic model (as discussed above) is beneficial to the users, the large number of input parameters and calibration required makes the models prone to significant errors. For this reason, accurate and sufficient data collection, appropriate modelling as well as a systematic calibration process are all paramount to producing an accurate model.

1.1 Background

As an emerging economy, South Africa is faced with a myriad of transport and traffic challenges. In addition to the persisting imbalanced apartheid spatial planning, increasing traffic growth; decreasing infrastructure investment in recent years; deterioration of existing transport infrastructure and evolving transport demand are just a few of the dilemmas the country faces. The public sector together with other stakeholders involved in the transport sector need to work together in developing solutions to overcome these various challenges. Some of these solutions include adequate maintenance of existing transport infrastructure, easing traffic congestion, expanding the existing road network and effective management of transport supply and demand. Developing these interventions requires insight into existing and anticipated traffic operations and capacity assessments that go beyond the scope of existing manuals. Traffic simulation modelling using simulation software such as FOSIM is one of the useful tools which could be used for gaining such insight.

FOSIM is a so-called microscopic simulation model which mimics individual driver behaviour. The collective behaviour of all drivers then determines the characteristics of traffic flow state in the network. The software was originally developed to model Dutch motorway traffic and is owned by the Ministry of Infrastructure and the Environment Public Works and Water Management of Rijkswaterstraat. It is used by the Dutch government and other United Kingdom authorities with the intention of testing transport interventions prior to implementation and to test freeway capacities.

In comparison to the more commercial microsimulation packages, such as VISSIM and AIMSUN, FOSIM is a more rudimentary software, since it was built with a different purpose in mind - to measure the real capacity of a freeway or freeway configuration. It is more focused on traffic volumes, lateral and longitudinal behaviours, speed adaptation and testing of traffic management rules. What's more, it's proved to be an efficient and cost-effective tool for assessing freeway capacity while avoiding exorbitant license fees and laborious training. South African road authorities would benefit immensely from having such a modelling tool at their disposal, while they seek to overcome the various transportation challenges with limited resources.

Since FOSIM is calibrated and validated for the Dutch traffic scenario, which is characterized by right-hand driving, flat topography, dedicated public transport facilities and different driving behaviour in general; the model needs to be tested and calibrated for a South African traffic scenario before it can be applied in the country's local context. Considering this, Enigmatry developers in collaboration with Rijkswaterstaat developed a left-hand driven version (applicable to the South African context) at the request of the University of Cape Town. This study, therefore, seeks to conduct a detailed analysis of a South African freeway by calibrating and validating it accordingly in order that it can be used to assess actual flow capacities along South African freeways.

1.2 Objectives

The primary objective of this research is to calibrate and validate a microscopic simulation model using FOSIM software for a specific section of the freeway. The secondary objectives of the research will involve the following:

- To select a road network and code the geometry.
- To develop a strategy for extracting traffic count and travel time data from video recordings.

- To develop a systematic approach to adjust model parameters and establish acceptance criteria.
- To analyse the FOSIM model and establish a set of optimal calibration parameters.

1.3 Research Design

This research will include a comprehensive study of the literature on traffic simulations in general, including microscopic, mesoscopic, and macroscopic models. A brief evolutionary history of these models will be discussed, with greater emphasis on governing equations. The study will also draw from the previous model calibration literature and various optimization techniques available.

The second task will involve selecting a study area and coding the geometric characteristics and traffic control measures of the road network using geographical data tools such as google aerial maps. This includes road width, section length, number of lanes, on – and – off ramp locations, speed limit etc.

Thirdly, MoEs will be determined and traffic flow data at the area of interest will be collected in accordance with the chosen MoEs. This study will make use of surveillance camera data obtained from the Cape Town Freeway Management System. Traffic count data will be obtained for several days to enable the validation of the model using an independent set of data from a separate day to that used for calibration.

Thereafter, a detailed study of the FOSIM software and the user manual will be undertaken. This is an essential step in any traffic modelling exercise, since the modelling requires the translation of observed data into the input data, which the software can process.

A systematic calibration approach will be developed through a sensitivity analysis and parameter search techniques, which will seek to narrow the search range by computing the parameter values that minimize the objective function. The study will further establish a set of acceptance and evaluation criteria by which the validity of the model will be tested.

The collected data will then be analysed by running a micro simulation model in FOSIM. This simulation model will be calibrated and thereafter validated accordingly, and the output will be extracted to test whether the model has been sufficiently calibrated by comparing the output to the field data. Figure 1-1 depicts a research design flow diagram.

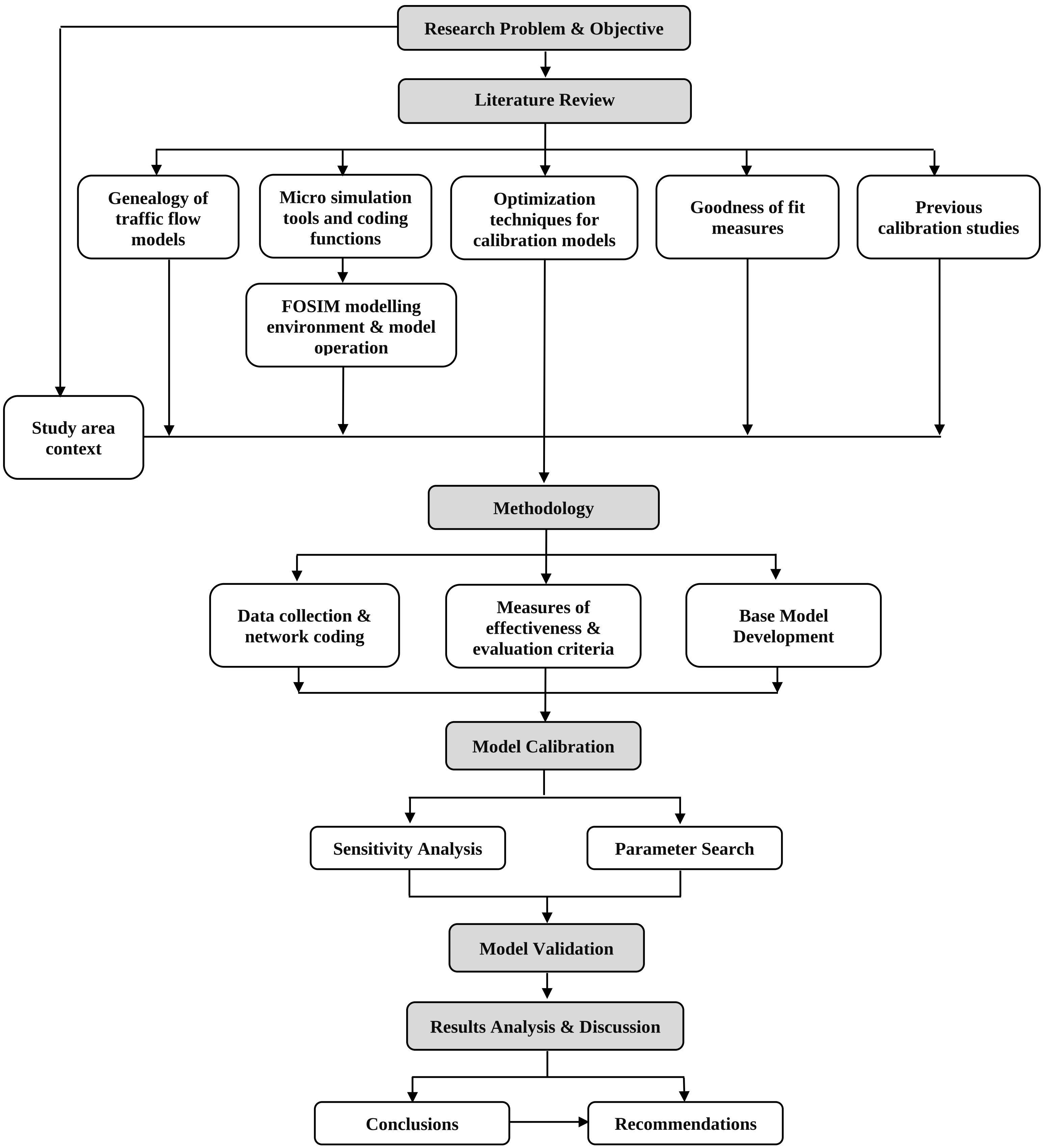

Figure 1-1: Research design

1.4 Limitations of the Study

This study was constrained by time and a lack of resources, and as such, large-scale manual traffic counts on a freeway facility were not feasible. Therefore, the researcher relied on readily available sources of data, which in turn, played a critical role in the selection of a road segment, as well as the segment length. The data was obtained from CCTV footage obtained from the Cape Town FMS, and because the primary function of these cameras is not that of traffic data collection, they do not cover the length of the freeway and ramps in their entirety. To calibrate the weaving patterns of a particular section of the freeway, therefore, required a strategic selection of a camera - one which provided a clear view of a road section, including the ramps, as well as the weaving patterns. This meant that sections beyond which entrance and exit movements could be observed had to be eliminated from the study area. For this reason, the study area beyond the Main Road (M4) off ramp could not be included in this study, since the camera did not provide a clear view of that section and, therefore, traffic counts were not possible. The study area then starts just after the M4 ramp and ends on Hospital Bend.

The analysis in this study was conducted using FOSIM software, version 7.0.1197, which was released in September 2021. Because FOSIM is mainly used by the Dutch road authorities, thus originally coded, calibrated and validated for Dutch freeways, the general assumptions made by the model poses limitations when the model is applied on scenarios in which the operating conditions are not synonymous with those of The Netherlands.

FOSIM does not permit user-specified O-D per lane. The model operates such that at the beginning of each lane is a vehicle generator (also called origin or source). With each time step, the source determines whether vehicles should be placed on the lane, based on the specified volumes and distribution of vehicle types. The input only allows traffic to be specified per carriageway (all lanes combined), and the source later places the vehicles per lane. This could potentially affect lane behaviour.

Two such assumptions are that the road curvature and the longitudinal slopes do not influence the vehicle operating speed. As a result, FOSIM does not explicitly model the restrictive effects of horizontal and vertical curves, as well as the vertical grades. The road geometry can, therefore, only be modelled with straight horizontal tangents. These assumptions are founded in the fact that freeway horizontal curves in The Netherlands are generally large and their effect on the speed is, therefore, deemed negligible. Additionally, The Netherlands is characterized by flat topography and the slopes are generally short, the longitudinal grade is thus also deemed not to have a major impact on the speed. Even though the model attempts to overcome these limitations using localized speed limitation by applying a speed suppression factor, there is a risk that the model input is not being accurately represented, thus impacting the overall behavioural power of the model.

As already stated above, each of the sub-models in FOSIM is composed of several parameters, and the overall simulation model often includes numerous parameters. An explicit measurement of some of the parameter values is complex, if not impossible; not only because they are subtle elements that are difficult to isolate, but also because they require extensive resources and data collection. To this end, data is collected at an aggregate level, which does not describe individual driver behaviour or vehicles. The aggregated data includes measures like classified traffic counts, average speed and travel time, and through calibration, the parameters are tweaked so that the simulation output mimics the field scenario. Calibrating the model using this aggregated data poses a risk of limited behavioural power.

Traffic simulations are often not free from simplification, such as not completely accounting for the effects of local roadside conditions or accidents. When the simulation output is compared to the field conditions, it is often assumed that the simulation accounts for all possible factors which take place in the road environment. This could potentially result in errors during model calibration, which affects the behavioural explanatory power of the model, and there is no means of tackling this issue.

Ideally, we would like to calibrate a large number of parameters, but the limited data and extensive computational requirements render this goal unattainable. This limitation also affects the explanatory power of the model.

1.5 Structure of Thesis

The dissertation comprises of nine chapter which are organized as per the summary below:

Chapter 1: Introduction

As a start, the chapter discusses a general overview of microscopic simulation models, their use, and benefits in engineering practice. It goes on to presents the main idea behind model calibration and its importance in traffic studies. Thereafter, the background to the study is discussed, presenting a case for road authorities to have readily available microsimulation software at their disposal to aid them in addressing everyday traffic challenges and future ones. The objectives of the study and research design is provided. Finally, the limitations of the study and FOSIM are reported.

Chapter 2: Literature Review

This chapter seeks to provide better knowledge and understanding of traffic modelling by collecting relevant historical studies in the field. This is done by firstly, providing the background to traffic simulation models by contrasting some of the definitions from well-known authors in the field. Secondly, it traces traffic simulation models back to their inception when the very first traffic flow model was presented and how they eventually evolved into varying families of traffic flow models. Thirdly, the main differences and governing equation for the three different families of traffic models are provided. Thereafter, some of the most common microsimulation software are discussed, including their differences and how they are coded to produce the desired model outputs. Furthermore, the optimization techniques and search functions for model calibration are examined together with the goodness of fit measures, where a comprehensive list of error measurement equations used to test the model validity against field observations is provided. The chapter ends by reviewing some of the existing literature on microscopic model calibration.

Chapter 3: Modelling Environment

The purpose of this chapter is to familiarize the analyst and the reader of certain intricacies of the FOSIM modelling platform. Like other microsimulation software, FOSIM is unique in the coding and processing of data. Understanding the unique manner in which it functions is essential to the accurate capturing of data, calibration and interpretation of results; and ultimately, to the production of a reliable simulation model. The chapter, therefore, starts by providing details on geometry and driver behaviour principles, vehicle generation process and the simulation process. Thereafter, the vehicle following behaviour is presented by explaining the following distance and collision avoidance models and governing equations. Lastly, lane change behaviour and factors affecting speed are also reported.

Chapter 4: Study Area Context

This chapter provides a brief outline of the area of study selected for this research. This is done through presenting a locality map to show the geographical location of the road. The relevant road section details such as the limits of study and other geometric features are outlined. Then, the observed traffic dynamics and section capacities during the analysis period are briefly discussed.

Chapter 5: Methodology

In this chapter, a detailed report of the adopted methodology is offered. The chapter commences by providing a calibration model process flow chat – describing the various crucial phases of the modelling process. The rest of the chapter expands on the processes shown on the flow chat. This includes the data requirements and method of collection – here a list of the required data is provided. Then, the operations of the Freeway Management System are discussed, followed by the details of the traffic count data. Next, it outlines the road geometry data, traffic regulation data, vehicle characteristics and travel time data. The chosen Measures of Effectiveness and evaluation criteria are also presented before a detailed base model development description. Lastly, the calibration and validation processes are presented.

Chapter 6: Results and Discussions

This chapter presents the results of the models which the analysist felt were worth highlighting. The chapter presents results from the model output before calibration, to the local and global calibration models, until the final model with the optimum calibration parameters. Thereafter, the model validation results are presented together with their effects on the model. Lastly, some detailed discussions on the different models and the statistical significance of the models are presented.

Chapter 7: Conclusions

In this chapter, research conclusions are presented based on the findings presented in Chapter 6. A brief overview of the objectives is provided together with a summary of the key findings and take-homes from the research.

Chapter 8: Recommendations

On the basis of the key result and conclusions, recommendations are presented for future studies.

2. Literature Review

Numerous traffic simulation models have been developed and used for analysing previous, existing and even projected traffic conditions. Since their conception, various authors have presented traffic simulation models for planning, designing or evaluation of alternative design proposals for different transport networks, while some authors have explored these models purely for research purposes and expanded their capabilities (Lieberman, 2015). Traffic simulation models thus enjoy a deep history, dating back in the early 1900s (Lieberman, 2015; van Wageningen-Kessels, et al., 2015). This literature explores the historical background of traffic simulation models. It does so by taking account of the very first traffic simulation model presented in 1930 and how this model ultimately became the steppingstone and foundation upon which all traffic modelling would later be developed with increasing complexity.

Microscopic simulation models are among the earliest in the traffic modelling field (van Wageningen-Kessels et al., 2015). Owing to their ability to analyse the dynamic characteristics of transport systems in a stochastic manner, they have gained significant popularity among researchers and industry professionals – so much so that a myriad of microsimulation software has been developed, with varying underlying logic (Jobanputra & Vanderschuren , 2012). Lane changing, gap acceptance and car-following models, in particular, are at the centre of microsimulation models. This literature will thus explore some of the well-known micro-simulation traffic software and their logic.

The literature further explores the various optimization techniques, which are commonly used in the calibration of these microscopic simulation models. This is followed by a comprehensive list of common goodness-of-fit measures, which are often employed to assess the closeness of the model output to the empirical data. Lastly, a review of some of the previous calibration studies is explored.

2.1 Background of Traffic Simulation Models

The literature shows that various authors have provided definitions of traffic simulation models, with each of the definitions highlighting a different element of traffic simulation models. To illustrate, Gerlough and Huber (1975) refer to traffic simulation as a type of experiment, which is performed on an unreal system that tries mimics reality, while Drew (1968) describes it as a robust representation of traffic conditions in the real-world, which is used to evaluate complex traffic scenarios in a research laboratory. For Wohl and Martin (1967), simulation is a process of mimicking particular traffic flow appearances outside of the real environment. And Liebermann and Rathi (2005), simply describe traffic simulation as an abstraction of the real traffic system. While these definitions may present varying characteristics of the purpose of simulation models, the common theme among them is quite clear, and that is, traffic simulation models are tools that seek to replicate field observed traffic patterns and behaviour in a controlled setting such as computers.

As corroborated by Chiappone et al. (2015) and Kim et al. (2005), it is indeed true that the application of traffic simulation models has been on a surge in recent years due to increased computational abilities and affordability. Yet their conception has been traced back to almost a century ago in the mid-1930s (van Wageningen-Kessels et al., 2015). The very first traffic flow model was presented by Bruce Greenshields at the Annual Meeting of the Highway Research Board, where he demonstrated the relationship between the vehicle's distance headway and their corresponding speed. In the later stages, many traffic simulation tools were developed – incorporating dynamics which enabled prediction studies. Recently, these models have been further advanced to use actual field data for long-term and short-term transport planning and strategic solutions. Figure 2-1 shows a model tree, which illustrates the traffic flow model families and their genealogy; all of which descended from Greenshields's traffic flow model. This model tree indicates the evolution of traffic flow models from a common 'ancestor', namely the fundamental diagram. From the fundamental diagram, further models were then developed such as microscopic, macroscopic and mesoscopic models. These models are discussed briefly in the sections below.

2.2 Fundamental Diagram

The initial fundamental diagram presented by Greenshields in 1934 shown in Figure 2-3 sought to establish the relationship between the distance headway and speed as mentioned above. However, Greenshields became popular for the second round of fundamental diagram, which he presented a year after the original diagram. His second diagram presented the relationship between density and speed as shown in Figure 2-2. Since its inception, the shape of this diagram has been a subject of rigorous debate among several authors who proposed variations of the original shape. Some of the proposed shapes are shown in Table 2-1 along with the corresponding representation of the density vs flow shapes. Del Castillo (2012) proposed a set of requisite criteria by which fundamental diagrams could be evaluated, to which only the Greenshields, Smulders & Daganzo diagrams complied. However, it has been argued that they fail at sufficiently representing the observed density-speed or density-flow scatter plot shown in Figure 2-4.

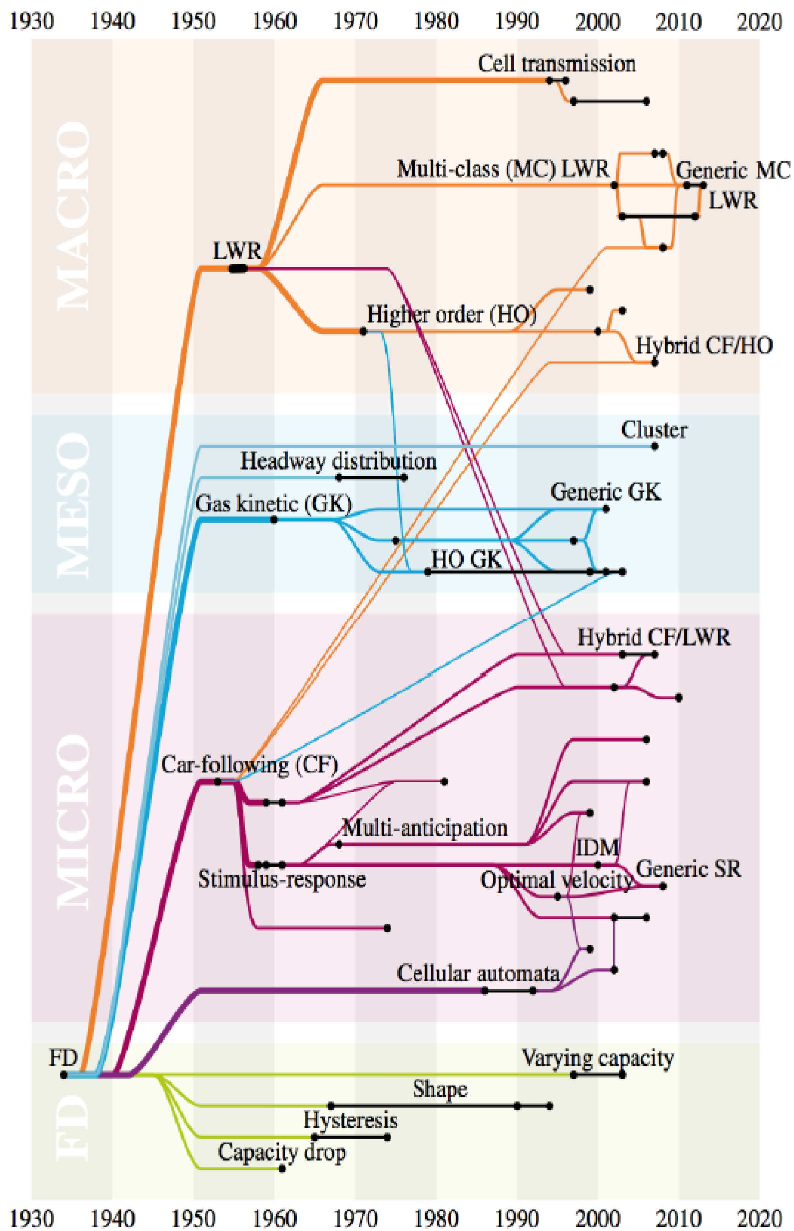

Figure 2-1: Genealogy of traffic flow model. (van Wageningen-Kessels et al., 2015)

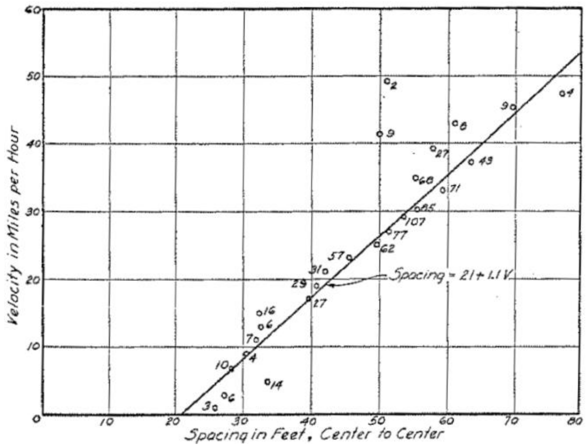

Figure 2-3: Greenshields' original fundamental diagram showing a linear relationship between spacing and speed. (Greenshields et al., 1934)

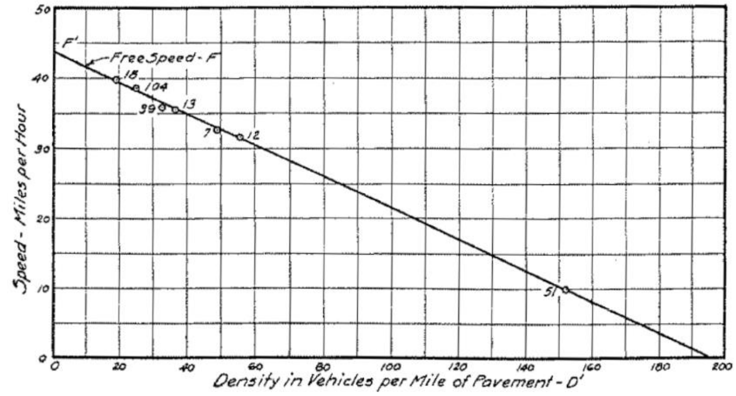

Figure 2-2: Greenshields' fundamental diagram (1935), showing a linear relation between density and speed. (Greenshields et al., 1935)

Table 2-1: Different shapes of fundamental diagrams, in density-flow and density-speed plane.

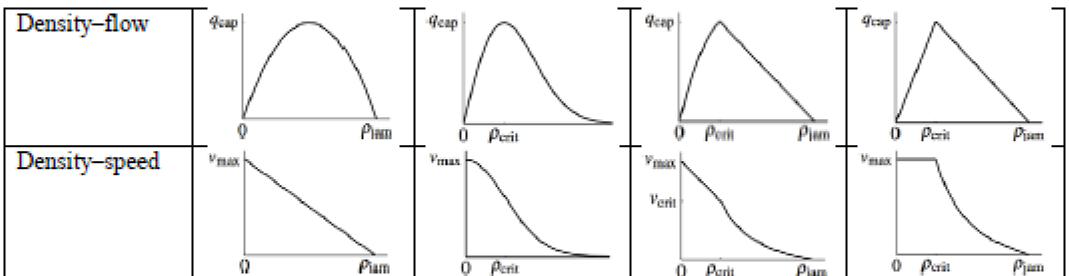

Shape	Parabolic	Bell	Parabolic–linear	Bilinear
Author	Greenshields	Drake	Smulders	Daganzo
Year	1934	1967	1990	1994
Reference	*4*	*5*	*6*	*7*

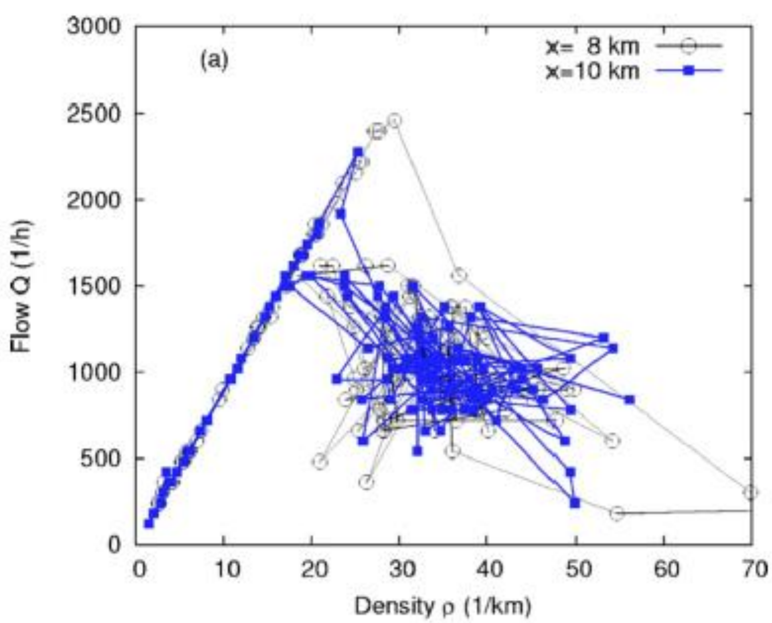

Figure 2-4: Scatter in an observed density-flow plot. (Treiber et al., 2006)

This observed scatter plot is partly due to the methods of measurement and data aggregation. Eddie (1961) proposed a fundamental diagram, which takes account of a capacity drop and showed that this modified diagram better represents the observed scatter plot (Figure 2-5). The capacity drop model shows that the traffic flow leaving a congested traffic state is lower than the flow just before the traffic state breakdown.

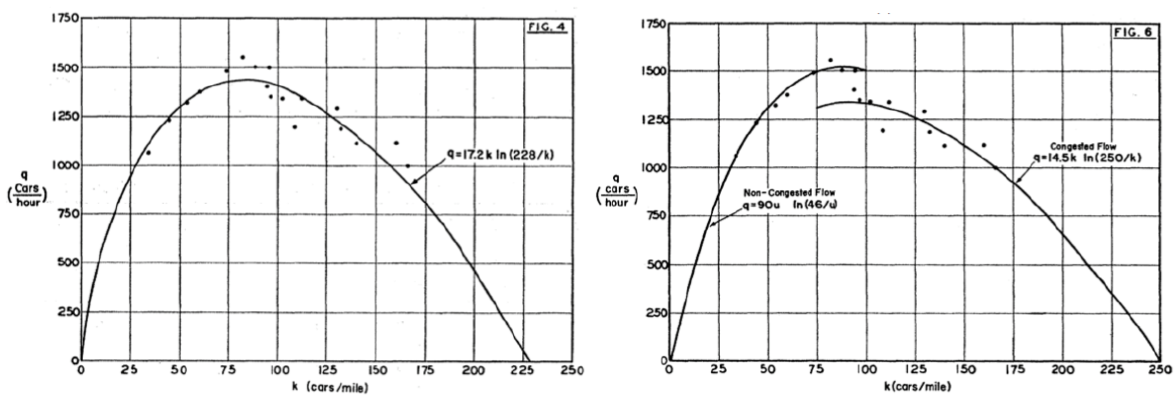

(a) (b)

Figure 2-5: Fundamental diagram (a) without and (b) with capacity drop. The graph shows a better fit with the data of the fundamental diagram with capacity drop. (Edie, 1961)

In 1965, the concept of hysteresis was introduced by Newell (1965), which brought forth the theory that the density-speed relationship is different during acceleration and deceleration (Newell, 1965). This was fortified by Treiterer and Myers (1974) who showed using Figure 2-6 that hysteresis could explain the observed scatter.

Kerner and Rehborn (1997), however, undertook a different approach by suggesting a peculiar relationship between flow and density. In this approach, they argued that during congestion, traffic could be in a synchronized flow state illustrated by the shaded area of Figure 2-7. Ultimately, Chanut and Buisson (2003), proposed a fundamental diagram which takes account of cars and trucks separately as illustrated by Figure 2-8. In this three-dimensional diagram, the same total number of vehicles will lead to lower speeds if the proportion of trucks is large.

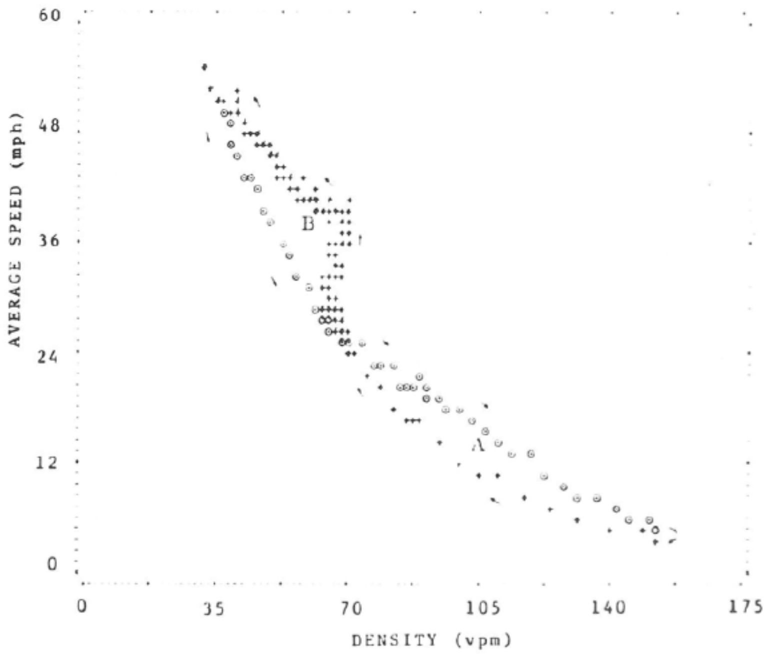

Figure 2-6: Observed densities and speeds showing the hysteresis phenomenon. At relatively low densities, speeds are higher when accelerating (diamonds) than when decelerating (circles), at relatively high densities, it is the other way around.

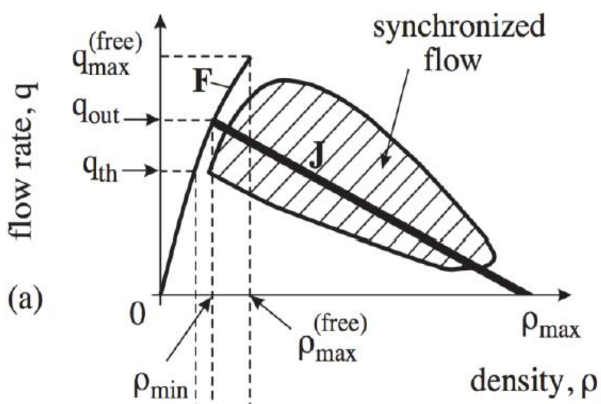

Figure 2-7: Fundamental diagram with infinitely many admissible states in the congestion branch (shaded area). **(Kerner & Rehborn, 1997)**

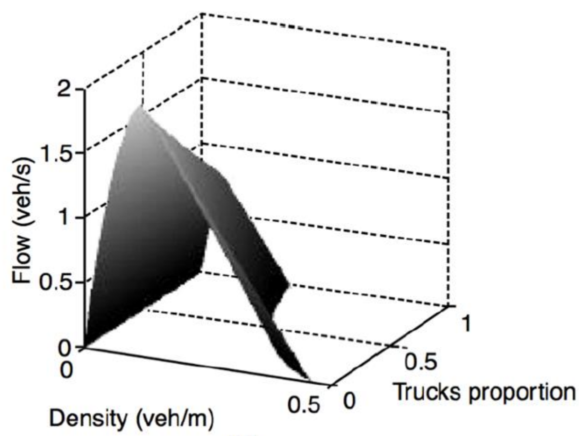

Figure 2-8: Three-dimensional fundamental diagram where a high trucks proportion leads to lower speeds and flow. **(Chanut & Buisson, 2003)**

2.3 Microscopic Simulation Models:

The three other model families involve a more dynamic evaluation and tracks the traffic state evolution over a period of time. The oldest of these families is the microscopic model family (van Wageningen-Kessels et al., 2015). Microsimulation models are concerned with describing individual vehicle movement on the basis of lane-changing, car-following, and gap acceptance models (Alexiadis et al., 2004). These models take cognizance of the vehicle and driver characteristics, interaction with road network geometry, interaction between vehicles and other external factors like weather and lighting conditions. In microscopic models, vehicle entry is through a statistical distribution of arrivals and tracked over the road network over incremental time steps. Each vehicle is assigned a vehicle type, a driver and destination (Alexiadis et al., 2004). As a result, microscopic models require a lot more computational ability.

2.3.1 Safe-Distance Model

Pipes (1953) presented the earliest car-following model named the safe-distance model. According to this model, drivers seek to adjust their speed to maintain a safe following distance to the leading vehicle as shown in Figure 2-9. Gipps (1981) further advanced the safe-distance model by introducing two traffic state regimes. In one regime, free-flow conditions prevail, and speed is influenced by the respective vehicle and the desired speed. The other regime has a congested road network, and vehicle speed is reduced since the driver must keep a safe following distance to the leading vehicle.

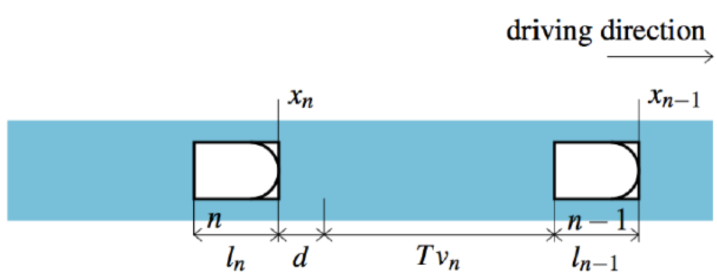

Figure 2-9: Variables and parameters in Pipes' safe-distance model.

In reviving safe-distance models, Newell (1961) and Newell (2002) explored a simplified car-following model. The simplified model was found to be similar to the cellular-automata branch models as well as the kinematic wave branch, which are also shown in Figure 2-1 (Daganzo et al., 2007). This similarity has been used to advance hybrid simulation models that combine both macroscopic and microscopic simulation models (Bourrel & Lesort, 2003; Leclercq, 2007).

2.3.2 Stimulus-Response Models

The logic used to determine the vehicle's acceleration and deceleration rates is central to the accuracy of micro-simulation models. The second car-following model branch shown in the model tree, which became predominant around the 1960s is the stimulus-response model (van Wageningen-Kessels et al., 2015; Chander et al., 1958; Herman et al., 1959; Helly, 1961; Gazis et al., 1961). Several authors have proposed that the deceleration and acceleration of drivers is in response to the three stimuli listed below:

- Driver's current speed,
- Distance to leading vehicle, and
- Relative speed between the leading and subject vehicle.

It is, generally, accepted that under free-flow traffic conditions, drivers do not influence one another, and speed is thus determined by the individual driver's desired speed and legal speed limit. As the density increases, drivers must adapt their speed to the surrounding traffic. When a vehicle travelling at free-flow speed approaches a slow-moving vehicle and cannot overtake, the subject vehicle must reduce its speed to match that of the leading vehicle. This adaptation process is influenced by the driver's psychological state (e.g., level of aggressiveness) and physiological abilities, for example, speed differential and perceived distance gap (Dijker et al., 1997). Once the subject vehicle has reduced its speed to that of the leading vehicle, it will seek to maintain a particular distance gap, which Pipe (1953) has suggested should be at least the length of a vehicle for every ten miles per hour of speed of the following vehicle. In trying to keep a constant gap from the leading vehicle, the subject vehicle will have more or less the same speed as that of the leading vehicle. Similarly, when the leading vehicle increases its speed, the following vehicle will proportionally increase its speed in order to maintain the appropriate gap and small difference in speed between the two vehicles. According to Wiedemann (1974), the moment at which the subject vehicle adjusts its speed to the leading vehicle's depends on a speed difference – distance gap ratio as shown in Figure 2-10.

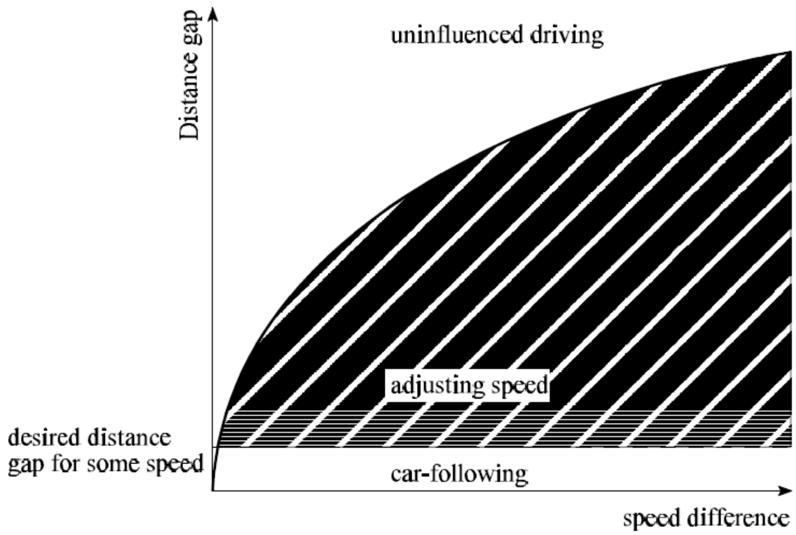

Figure 2-10: Speed adjustment model. **(Wiedemann, 1974)**

To model this relationship, in the late 1950s, General Motors Group performed extensive field tests and mathematical experiments to establish GM models (Herman et al., 1959). The main idea behind these models was to explain notion that driver's sensitivity to deceleration and acceleration is proportional to the degree of the stimulus occurring at time t, beginning after a time lag T. The behavior is commonly expressed with the general form:

$$\boldsymbol{Response}\ (\boldsymbol{t}+\boldsymbol{T}) = \boldsymbol{Sensitivity}\ \times \boldsymbol{Stimulus}\ (\boldsymbol{t}) \qquad \textbf{2-1}$$

The relationship can also be expressed with Equation 2-2 where the parameter α is the sensitivity and relative speed with respect to the leader is the stimulus:

$$\boldsymbol{\ddot{x}_F} = \boldsymbol{\alpha_F}\left(\boldsymbol{\dot{x}_L(t)} - \boldsymbol{\dot{x}_F(t)}\right) \qquad \textbf{2-2}$$

Where:

$\ddot{x}_F$ = acceleration of the following vehicle [m/s^2],

α_F = sensitivity of the following vehicle,

$\dot{x}_F$ = speed of the following vehicle [m/s],

$\dot{x}_L$ = speed of the leading vehicle [m/s], and

t = time [s].

Equation 2-3 is the generalized GM model expressing the following vehicle's deceleration and acceleration.

$$\ddot{x}_F(t+T) = \lambda \frac{[\dot{x}_F(t+T)]^m}{[x_L(t) - x_F(t)]^l} [\dot{x}_L(t) - \dot{x}_F(t)], \qquad \textbf{2-3}$$

Where:

T = following driver's perception-reaction time [s],

λ, m, l = constants relating to driver sensitivity,

x_L = Position of leading vehicle [m], and

x_F = Position of following vehicle [m]

By changing values of m and l, different variations of the GM model can be produced. The two special cases of the GM models are described by Kikuchi et al. (2003) as Gazi's and Pipes' models. Gazi's model sets m to zero and l to 1 - making car-following sensitivity inversely proportional to the distance headway. In the Pipes model, both m and l are set to zero, thus collapsing the generalized GM model to Equation 2-2, with $\alpha = \lambda$.

2.3.3 Action Point Models

Action points form the third branch of the car-following models. These were first introduced by Wiedemann (1974) and they assume that the driver reacts at certain instances in time (the action points) when there is an abrupt change in acceleration or when the change is significant enough to be perceived but held constant in between two action points. This implies that the driver is only influenced by other drivers if the headways are small enough and changes are sufficiently large to be observed (van Wageningen-Kessels et al., 2015).

2.3.4 Cellular-Automata Models

Even though cellular automata models fall within the microscopic family, they are not on the same branch as the car-following models. The first of these models was presented by Cremer & Ludwig (1986), although, the model introduced by Nagel & Schreckenberg (1992) is widely used and considered the prototype cellular-automata model. The vehicle description and tracing is similar to other microsimulation models, however, space and time are discretized. The road is divided into discrete cells and through an algorithm, vehicles are moved from one cell to another in each time (van Wageningen-Kessels et al., 2015).

2.4 Macroscopic Models

The macroscopic family of models are primarily applied in the analysis of larger-scale traffic networks and have been found suitable for transportation planning studies, as well as spatial interaction in transportation systems. In these models, the movement of vehicles is ruled by the deterministic relationship between aggregated variables, such as density, flow, and speed of the traffic stream (Alexiadis et al., 2004). Compared to the microscopic model, macroscopic models do not track individual vehicle trajectory and driver behaviour, and thus have considerably less computational requirements (Owen et al., 2000). In other words, they do not possess the ability to analyse traffic flow dynamics at a level of detail similar to that of a microscopic model. The modelling is applied on a section-by-section basis and assumes that between two sections of a roadway without exist or entrance, the number of vehicles in the road section is conserved (Barceló, 2010). This theory can be represented by the conservation or continuity equation which is analogous with flow of other media such as water or gasses. The equation in hydrodynamics is expressed as follows:

$$\frac{\partial q}{\partial x} + \frac{\partial k}{\partial t} = 0 \qquad \textbf{2-4}$$

Where:

q = traffic volume [veh/h]

x = distance [km]

k = density [veh/km]

t = time [h]

It is empirically known that for a given section of road, speed is dependent on the density. As discussed in the section above, Greenshields (1934) presented a relationship between speed and density represented by the expression in Equation 2-5.

$$u = u_f - \frac{u_f}{k_j} k \tag{2-5}$$

Where:

u = speed [km/h]

u_f = free flow speed [km/h]

k = density [veh/km]

k_j = jam density [veh/km]

It has also been deliberated that this relationship does not accurately represent reality and several researchers developed and proposed non-linear models for these variables. Van Aerde (1995) for example, introduced five equations of non-linear models. These models included more parameters which took account of varying traffic scenarios across diverse road networks.

The relationship between the macroscopic traffic variables is finally expressed by Equation 2-6:

$$q = uk \tag{2-6}$$

Where:

q = traffic flow rate [veh/h]

u = speed [km/h]

k = density [veh/km]

2.5 Mesoscopic Models

Mesoscopic traffic models were fundamentally created to strike a balance between the computationally exacting microscopic models and the lenient macroscopic simulation models. To this effect, mesoscopic models generally combine macroscopic and microscopic model properties, though their use has become less common as the computational abilities required to perform microscopic analysis has becoming more prevalent. In mesoscopic models, there are two ways in which vehicle simulation is carried out (Barceló, 2010). The first attempt seeks to model vehicles as a collection or a platoon moving along the traffic stream. The second approach incorporates the tracking of individual vehicles through a simplified car following simulation model where the traffic movement is influenced by the average speed on the link (Alexiadis, Jeannotte, & Chandra, 2004).

There are two important parameters involved in modelling car following behaviour in mesoscopic simulation models (Barceló, 2010). The first one being the reaction time factor, which governs the rate at which a vehicle reacts to surrounding traffic conditions. The second critical parameter is the look-ahead distance, which determines how far the driver will look in order to identify the next turn and thus start searching for the opportunity to perform the necessary lane changes. Mesoscopic simulation software packages commonly do not model lane change within a link. The vehicle route is rather determined when the vehicle is placed on the roadway ahead of the simulation, and the vehicle chooses the lane that best enables it to reach its predetermined path (Burghout, 2005).

Mesoscopic models include cluster and headway distribution models (Buckley, 1968; Branston, 1976). However, the earliest branch within this family is the gas-kinematic traffic models, which were presented for the first time in the early 1960s (Prigogine & Andrews, 1960). Gas-kinematic models portray traffic flow in a manner analogous to modelling gas particles in a gas-kinematic model.

To bring these models together and establish a notional link between them, Vanderschuren (2007) makes a distinction between road user's differnet types of choices as shown in Figure 2-11.

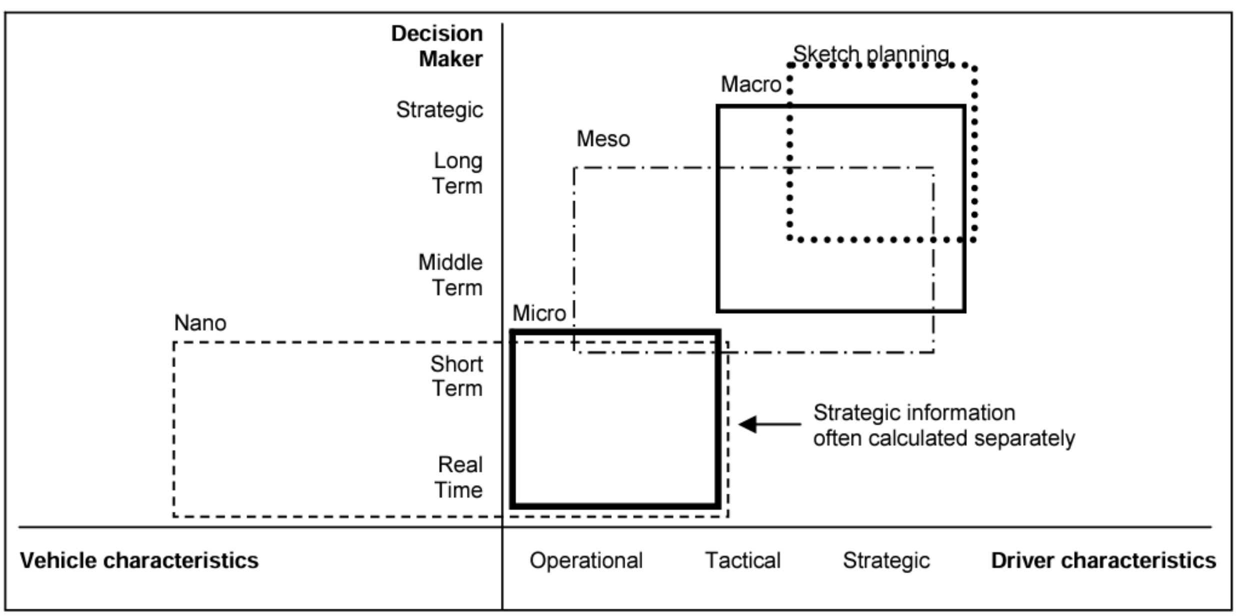

Figure 2-11: Trade-offs between decision horizon and model characteristics

According to this diagram, strategic choices, such as the purchasing of a vehicle or making a trip, are made (long) before the road user gets on the road. Tactical decisions, on the other hand, such as departure time or route choice, generally take place as the trip starts, although some of these decisions can be made during the trip, if new information becomes available. Lastly, operational choices, such as accelerating, lane changes, gap acceptance, etc., are made constantly during the trip. Thus, these decision criteria are also tied to a temporal dimension, such that microscopic models, for example, cater to operational choices which occur in rea time or relatively short term.

2.6 Microscopic Simulation Tools

Microscopic simulation models are an economic and efficient tool used to evaluate transportation strategies. They require complex systematic computations, and their accuracy is contingent on the ability to replicate observed field conditions as closely as possible. For a while, CORSIM was the most commonly used microsimulation software package in industry. However, VISSIM has gained recognition in recent years and is now one of the leading commercial software in many parts of the world (Gazder et al., 2002). Some of the other software packages commonly used include PARAMICS, AIMSUN, INTEGRATION and MITSIM. These microsimulation model packages are detailed below:

2.6.1 CORSIM – CORridor SIMulation

CORSIM is a stochastic microscopic simulation package, which was established by the Federal Highway Administration (FHWA). Traffic Software Integrated Systems (TSIS) is an integrated development environment in which CORSIM and its support tools are hosted and executed (Owen et al., 2000). NETSIM was originally developed in the early 1970s to provide a simulation model which did not require extensive computational requirements and was used to analyse traffic flow in the urban environment. NETSIM was therefore concerned with urban street simulation while FRESIM simulated more complex highways and freeway networks (CORSIM User's Guide, 2006). In fact, FRESIM is an enhanced version which provides a more realistic traffic analysis than its predecessor - INTRAS. In the 1990s, both NETSIM and FRESIM were combined to form CORSIM. The car-following and lane-change logic used in NETSIM and FRESIM are slightly different and thus a vehicle modelled using CORSIM will exhibit different behavioural dynamics depending on the roadside environment, that is, freeway or an urban network.

The model can simulate various intersection controls, such as pre-timed and actuated signals as well as complex geometries and traffic conditions. The model network consists of roadway segments which are modelled as links and intersections, termination points, or roadway changes are represented as nodes (CORSIM User's Guide, 2006). Although CORSIM was developed to primarily model automobiles, it can also model truck and bus lanes. Other features of the model include numerous driver behaviour characteristics and reaction to on-coming traffic, different vehicle classes, clock-time and traffic-responsive ramp metering. In order to replicate real life traffic flow conditions and the variation thereof due to the randomness, the model uses random seed numbers to designate individual driver characteristics and that of the vehicle. The model thus has to be carried out with several runs each time using a different set of random seed to achieve an accurate measure of the network performance.

The CORSIM car-following model descended from two models: NETSIM and FRESIM. The car-following model in FRESIM is similar to that of its predecessor: INTRAS which uses a Pitt car-following model which was developed by the University of Pittsburgh (Halati et al, 1997). In the CORSIM model, the speed differential and distance headway are considered as two independent variables as illustrated by Equation 2-7.

$$h = h_f + c_3 u + b c_3 \Delta u^2 \qquad \textbf{2-7}$$

Where:

h and h_f = the distance headway and jam distance headway respectively [km],

u and Δu = the speed of the subject vehicle and the lead vehicle respectively [km/h]

c_3 = the driver sensitivity

b = the calibration constant.

The NETSIM car-following logic is coded in such a way that the subject vehicle will maintain a particular distance headway relative to the lead vehicle so that even if the lead vehicle applies maximum deceleration, there will be enough reaction time for the subject vehicle to execute the braking action without causing a collision. NETSIM’s car-following model can be expressed with the following equation:

$$h = h_j + \Delta s + \Delta r + S_F - S_L \quad \textbf{2-8}$$

Where:

Δs = the distance travelled by the subject vehicle over the time interval [km]

Δr = the distance travelled by the subject vehicle during its reaction time [km]

S_F = the distance required by the subject vehicle to come to a complete stop [km]

S_L = the distance required by the lead vehicle to come to a complete stop [km]

CORSIM's lane-changing logic follows the Gipps (1981) decision model, which makes a distinction between compulsory and optional lane-changes. During a compulsory lane-change, the driver seeks to leave the current lane in order to make the next exit. On the other hand, the optional lane change is when the driver seeks favourable traffic flow conditions in the neighbouring lanes.

2.6.2 VISSIM – Verkehr In Stadten - Simulationsmodell

VISSIM is a discrete microscopic traffic simulation software which can model freeway and urban traffic operations. It was developed by PTV (Planung Transport Verkehr) AG in Karlsruhe, a German based company (Vissim User Manual - V10, 2018). The software was first developed in the 1970s but was only commercially distributed in 1992. VISSIM is an acronym derived from "**V**erkehr **I**n **S**tadten – **SIM**ulationsmodell" which is German for "Traffic in cities – simulation model" (Gazder et al., 2019). As mentioned above, VISSIM has become one of the leading commercial microsimulation packages globally and is used in various fields, such as transport planning, traffic engineering, urban planning, fire protection as well as computer and architectural animation. Unlike CORSIM, VISSIM is designed to incorporate other special modes such as light rail, heavy rail, pedestrians, and bicycles.

The package comprises of two modules: a traffic simulator and a signal state generator. On the one hand, the traffic simulator consists of network geometry which facilitates the movement of vehicles using links which represent roadway segments and nodes, which represent merging links, crossing links or diverging links. On the other hand, signal state generator has a signal control logic, which is used for modelling traffic control mechanisms such as ramp metering, adaptive, actuated and transit signal priority. The model's vehicle movement logic was developed by Rainer

Wiedemann in 1974. The car-following logic combines the psychological and physical aspects of drivers to optimize traffic flows.

Figure 2-12 illustrates a graphical representation of the Wiedemann 74 model. The X-axis shows the relative speed difference between the subject and leading, while the Y-axis represent the distance headway between the leading and subject vehicle. The various thresholds are represented by unique shapes which have been coded into the model and can be enhanced through the calibration process. The diagram illustrates that the subject vehicle approaches the leading vehicle, which decreases ΔX because of the subject vehicle’s higher speed. Thereafter the subject vehicle crosses SDV and enters a perceptual area where it starts to reduce speed and crosses another threshold CLDV where it further reacts to reduce speed until it enters an unconscious reaction car-following region. The subject vehicle continues in this region as long as it is bound by OPDV, SDX, BX and SDV thresholds.

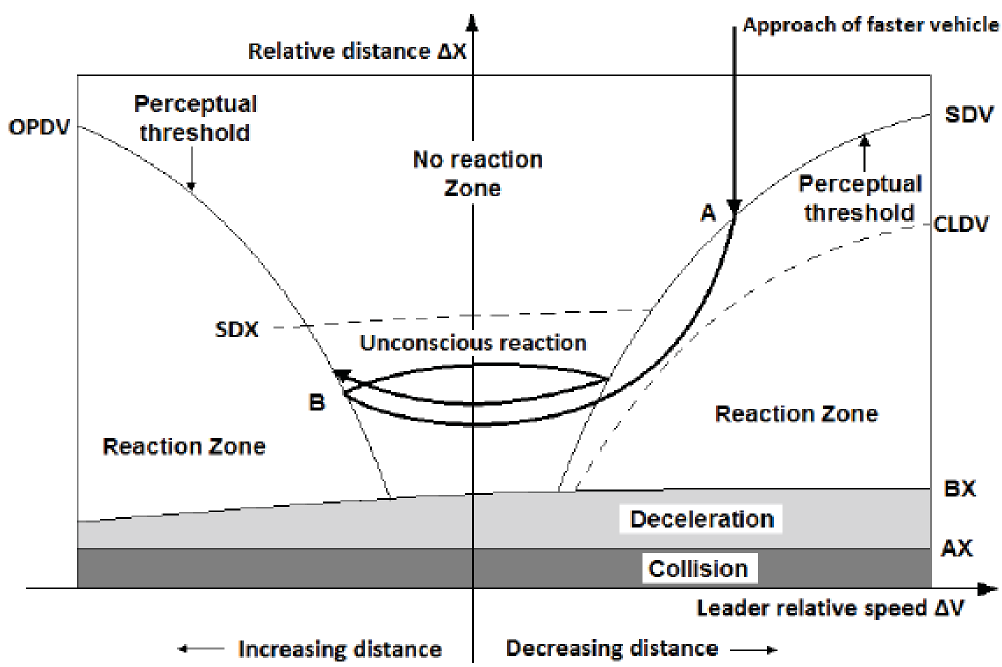

Figure 2-12: Wiedemann psycho-physical car-following model. (Wiedemann, 1974)

VISSIM’s lane-change model, developed by Willmann and Sparmann, divides lane-change behaviour into two main types: Lane change to a slower lane and lane change to a faster lane. In making a lane change decision, three questions need to be considered. The first one being whether the lane change is desired, the second question is whether the traffic condition in the neighbouring lanes are favourable and lastly, whether the lane change is possible (Kan & Bhan, 2007). Like CORSIM and other simulation models, VISSIM also distinguishes between two kinds of lane changing behaviours: necessary, as well as discretionary lane-change. A necessary lane change is executed whenever a driver must exit the current lane for the desired exit while a discretionary lane change is applied when the driver seeks higher speed or more space. In both scenarios, a suitable gap must first be available before the lane-change can be executed.

2.6.3 PARAMICS – Parallel Microscopic Simulation

PARAMICS is a stochastic microsimulation software developed by Quadstone (a software company) in collaboration with SIAS (a traffic engineering company) at the University of Edinburgh in the early 1990s (Druitt, 1998). Like other microsimulation models, PARAMICS uses a combination of links and nodes as well as other related objects to represent real life geometric conditions. It also models vehicle movement based on car-following and lane-changing models on arterials network, freeways, roundabouts, high occupancy vehicles (HOV) lanes, etc. The software is also designed to model various scenarios such as emissions, Intelligent Transport Systems (ITS), public transport and toll plazas. The model requires four input parameters: demand data, geometric characteristics, assignment, and general configuration.

PARAMICS uses the dynamic real-time three-dimensional graphical user interface (GUI), which provides an animation of vehicle movement along the simulated network and helps to make the software easy to use and understand. Unlike other microsimulation packages, PARAMICS does not operate with driver behaviour and vehicle calibration parameters, but rather assumes that sufficient demand data and accurate road geometry will produce satisfactory model output regardless of the local driver characteristics (Druitt, 1998). Driver characteristics such as car-following, lane-changing, gap acceptance, route choice and simulation results can therefore be adapted to match field conditions by using the Application Programming Interface (API).

Like VISSIM, the car-following model in PARAMICS follows a psycho-physical model which was developed by Fritzsche (1994). Figure 2-13 illustrates the perception thresholds and the different regimes, and each regime has its corresponding driver behaviour.

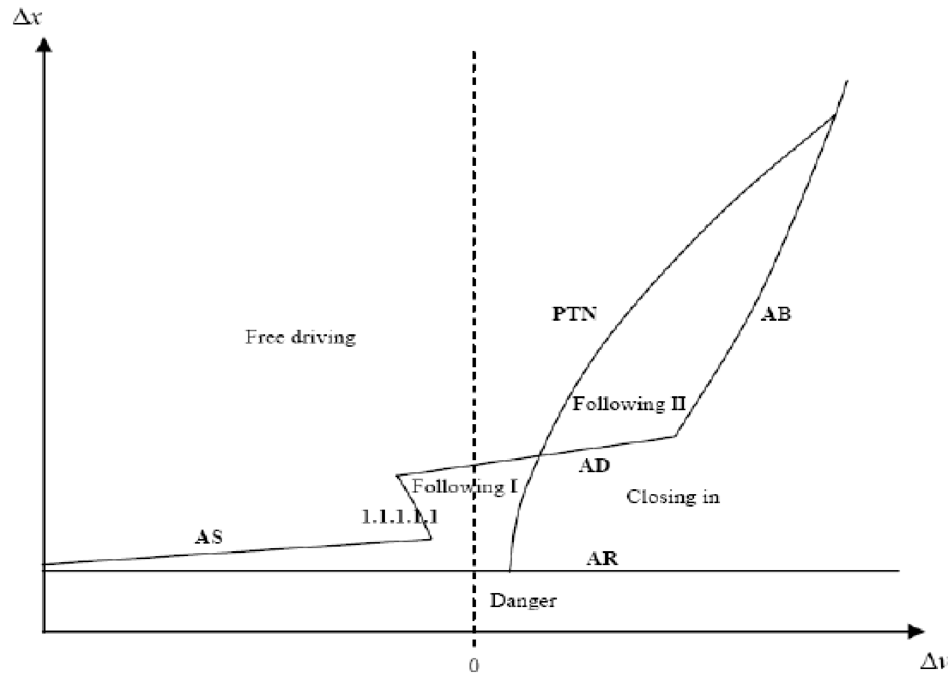

Figure 2-13: Fritzsche car-following model. **(Fritzsche, 1994)**

Each of the thresholds (PTN, AB, AD, AR and AS) shown in Figure 2-13 are modelled in the software using their respective equations. In the danger regime, the distance to the lead vehicle is smaller than the risky distance AR and therefore, the subject vehicle will apply maximum deceleration to increase the headway. The subject vehicle in the closing regime is required to decelerate to maintain a speed similar to that of the leader. In the "following I" regime, the subject vehicle does not need to take any conscious action and a parameter is included in the model to account for the diver's inability to maintain a constant speed. In the "following II" regime, the subject vehicle's driver notices that his vehicle is getting closer to the leader, but the perceived space headway is still too large for him to execute any conscious action. In the free flow regime, the subject vehicle accelerates to attain his desired speed. A parameter is also used to account for cases where the driver is unable to maintain a constant speed.

PARAMICS consists of two lane-change zones. In the first zone, the subject vehicle is at a distance further from the next exit and only changes lanes for the purposes of overtaking a slower vehicle. In the second zone, the subject vehicle is closer to the next exit and may not feel the need to overtake anymore. Lane-change actions are therefore only executed to reach the appropriate lane and for taking an exit. According to Duncan (2000), the lane-changing logic in PARAMIC is operated through a “gap acceptance policy”. This logic is such that in order for the subject vehicle to change lanes, the subject vehicle must first not collide with the leading vehicle in the target lane and secondly, the subject vehicle must not collide with the following vehicle in the target lane.

2.6.4 AIMSUN – Advanced Interactive Microscopic Simulator for Urban and Non-Urban Networks

AIMSUN is a microsimulation tool which was developed by the Department of Statistics and Operational Research, Universitat Poletecnica de Catalunya in Barcelona, Spain. The software can reproduce various real traffic conditions using computational methods. Like other popular microscopic models, AIMSUN models individual driver behaviour through car-following, lane-change and gap acceptance models. It has the API which enables integration with some user-defined applications. It also produces a detailed traffic analysis and can therefore cater for various MoEs.

AIMSUN uses a car-following model which is founded on Gipps (1981) model. This model considers the speed of the subject vehicle to be either unconstrained or influenced by the leader. The speed of the subject vehicle during time interval [t, t+T] can be computed using Equation 2-9.

$$v_n(t+T) = \min\{v_n^a(t+T), v_n^b(t+T)\} \qquad \textbf{2-9}$$

Where:

$v_n^a(t+T)$ = maximum attainable speed of the subject vehicle [km/h],

$v_n^b(t+T)$ = maximum safe speed for the subject vehicle relative to the lead vehicle at time t [km/h].

The reaction time (T) is equal to the simulation time step; and the maximum attainable speed of the subject vehicle during a time step is expressed by Equation 2-10, while the maximum safe speed relative to the leading vehicle is calculated using Equation 2-11.

$$v_n^a(t+T) = v_n(t) + 2.5 \times a_n^{max} \times T \times \left(1 - \frac{v_n(t)}{v_n^{desired}}\right) \times \sqrt{0.025 + \frac{v_n(t)}{v_n^{desired}}} \quad \textbf{2-10}$$

$$v_n^b(t+T) = d_n^{max}.T + \sqrt{(d_n^{max}.T)^2 - d_n^{max}.\left[2\{x_{n-1}(t) - s_{n-1} - x_n(t)\} - v_n(t).T - \frac{v_{n-1}(t)^2}{\hat{d}_{n-1}}\right]} \quad \textbf{2-11}$$

Where:

a_n^{max} = maximum desired acceleration for vehicle n [m/s^2],

d_n^{max} = maximum desired deceleration for vehicle n [m/s^2],

$\hat{d}_{n-1}$ = estimate of the maximum deceleration desired by vehicle n-1 [m/s^2],

T = apparent reaction time, a constant for all vehicles [s],

s_{n-1} = effective length of vehicle [m].

AIMSUN's lane changing model was also developed using Gipps' lane-changing model (Gipps, 1986), which is a decision-based model addressing matters of need, desirability and possibility of lane changing. There are three dominant factors involved in deciding lane change necessity, that is, exit feasibility, distance to the next turn and traffic characteristics. The desirability of the lane change is dependent on whether the lane change will result in an improvement such as higher speed or shorter queue. The feasibility of the lane change is depended on there being sufficient safety distance and lane-changing possibility, otherwise it cannot be executed.

2.6.5 INTEGRATION

INTEGRATION was developed by Michel Van Aerde in 1983. It was originally established as a mesoscopic simulation model but advanced to a microsimulation model in 1995 (Rakha, n.d.). The software is called INTEGRATION because it was developed to integrate freeway and arterial roadway modelling and used the same traffic flow logic for both scenarios (Van Aerde et al., 1996). This together with the fact that the traffic simulation was integrated with the traffic assignment, and microscopic and dynamic in nature, made this software package particularly unique. This mix of qualities was accomplished by representing traffic flow as individual vehicles which were governed by macroscopic assignment and traffic flow relationships (Van Aerde et al., 1996). This combination of microscopic and macroscopic attributes led to the model being deemed mesoscopic by others. In the past couple of decades, the software has advanced considerably from these mesoscopic origins through enhancements and addition of certain features such as dynamic traffic assignment, car-following logic, lane-changing logic and weaving sections. These recent enhancements have resulted in the full conversion of INTEGRATION to a microscopic simulation model.

The model comprises in pre-trip and en-route driver decisions which are made before the driver starts the trip and can’t be revised during that same trip. These decisions include the selection of the point of origin with the purpose to reach a certain destination at a given time and using a particular transport mode (Van Aerde et al., 1996). This means that INTEGRATION does not directly model the effect of a different departure time by means of a different vehicle class or alternative destination.

INTEGRATION uses a car-following logic proposed by Van Aerde (1995) and Van Aerde & Rakha (1995). The former uses a combination of the Greenshields car-following logic and the Pipes car-following logic and seeks to overcome their shortcomings (Rakha & Crowther, 2002). The shortcoming in the Pipe model is the assumption that in the uncongested regime, vehicle speeds are not sensitive to traffic density, while the Greenshields model shortcoming is the assumption that the speed-flow relationship follows a parabolic shape (Rakha & Crowther, 2002).

2.6.6 FOSIM – Freeway Operations Simulation

FOSIM, an INTRAS derivative is a microsimulation tool developed by Bullen (1982) to simulate basic freeway traffic operations on a personal computer. It has been further adjusted, calibrated, and validated specifically for the Dutch freeways and is being used by the Dutch road authority to evaluate road capacity forecasts for infrastructure development (de Leeuw & Dijker, 2000). In FOSIM, it is possible to specify various traffic constraints and geometric configurations such as weaving sections, on and off-ramps, construction works, etc. (Heikoop & Henkens, 2016). Traffic composition is defined using different driver/ vehicle combinations and traffic operation characteristics such as speed, volume and density are calculated by detector cross sections defined in the simulation road segments.

The traffic operation in FOSIM is set up to evaluate individual driver behaviour. The behaviour of all drivers combined results in a particular traffic flow and road capacity is an output of the model (Heikoop & Henkens, 2016). The total simulation period is divided into 1 second time steps, after which the position of each vehicle on the road segment is re-calculated. With each time step, a decision process for each vehicle-driver combination is completed based on Figure 2-14. Each vehicle has a destination lane which is determined by an O-D matrix from lane to lane. In an instance that the origin lane is different from the destination lane, a lane-change action needs to be executed depending on the position of the vehicle relative to other vehicles. If the origin and destination lanes are the same, the subject vehicle can still change lanes to overtake the lead vehicle that is travelling at a lower speed (Vermijs, 1991).

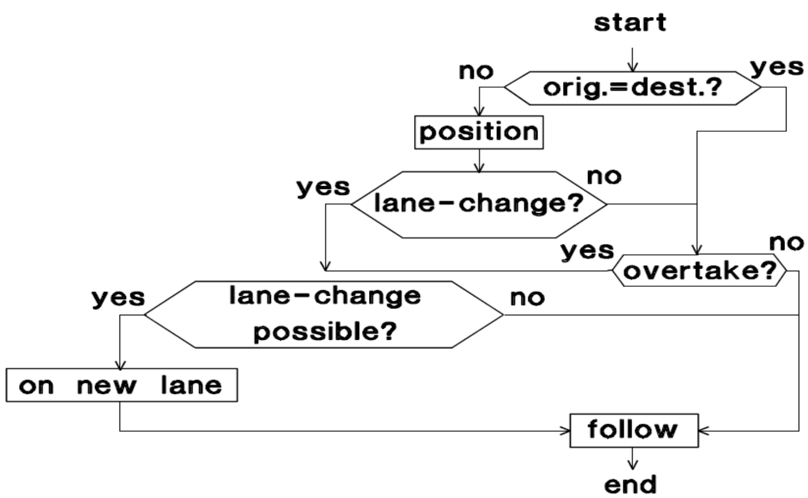

Figure 2-14: FOSIM model vehicle process flow chart

Every driver seeks to attain its individual desired speed and when it’s unable to reach this speed because of the lead vehicle, the necessary acceleration required to maintain a sufficient headway is calculated. Vehicle positions are computed in advance; this period is referred to as ‘anticipation time’ and has a default value of 4s. These calculated positions determine the acceleration needed. The subject vehicle tries to keep a headway determined by Equation 2-12.

$$d_i = L_j + z_1 + z_2 v_i + z_3 v_i^2 \qquad \textbf{2-12}$$

Where:

i, j = index vehicle i and j,

d_i = space headway for vehicle i [m]

L_j = vehicle length of the lead vehicle [m]

v_i = actual speed of the subject vehicle [m/s]

z_{1-3} = vehicle following parameters.

If the subject vehicle approaches the lead vehicle as per line q-q' shown in Figure 2-15 it will decelerate if the headway and speed differential between the two vehicles makes it necessary to avoid collision.

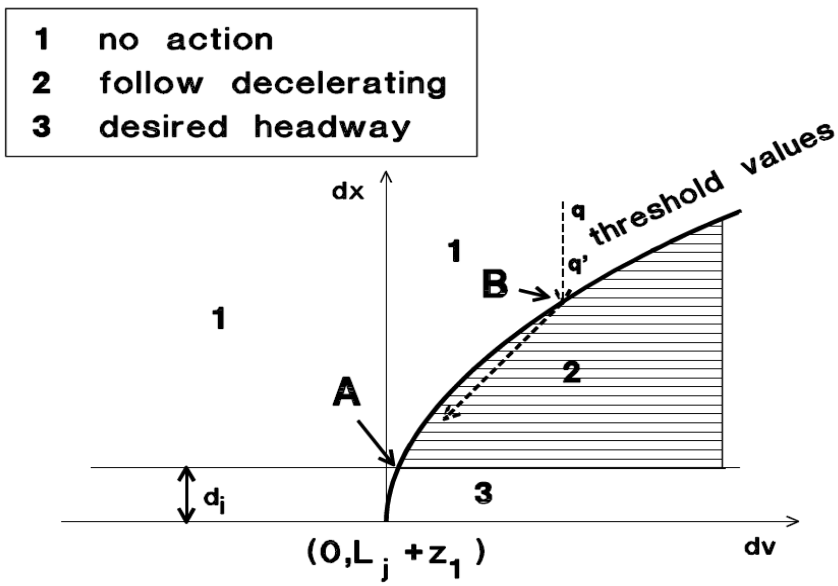

Figure 2-15: FOSIM car-following model

Like other simulation packages discussed previously, FOSIM also makes a distinction between mandatory and desired lane change as illustrated in Figure 2-16. Desired lane-change occurs between section a and b while mandatory lane-change occurs between section b and c. The risk a driver is willing to accept for the mandatory lane-change is higher than that accepted for the desired lane-change. This difference in risk acceptance is interpreted as the difference in the accepted deceleration in order to perform the lane-change. In fact, FOSIM models accepts very short headways, for example during weaving manoeuvres. In the case where a parallel driving vehicle inhibits the lane-change, the subject vehicle can take certain action such as deceleration or acceleration in the next time step to enable the lane-change. If the subject vehicle accelerates, the obstructing vehicle may decelerate to make the lane-change possible.

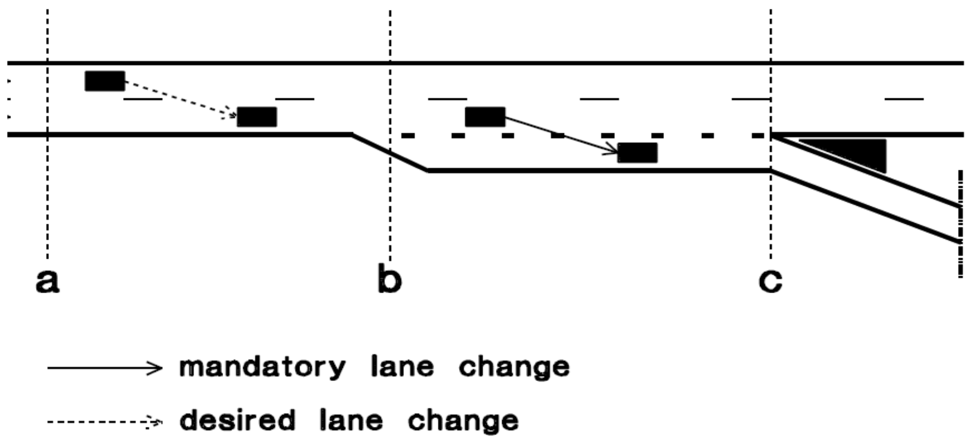

Figure 2-16: Lane change upstream of an off-ramp

2.7 Microscopic Model Calibration

Microscopic traffic simulation models have resulted in increasing comprehension of traffic flow patterns, driver behaviour and vehicle interactions. These microsimulation models differ in degree of complexity, from the basic deterministic queuing models to more complex microscopic models which are stochastic in nature. They also differ scale and level of detail, from simple single intersection analysis to larger scale freeways and traffic networks. However, no single microsimulation model should be expected to reproduce the wide-ranging local field conditions for various scenarios. In fact, previous studies have shown that geometric characteristics, traffic conditions, pavement condition and weather are some of the factors that could have a significant impact on the model output (Ali et al., 2018; Abaza et al., 2019). As such, model parameters such as those used to compute the car-following and lane-changing behaviour are necessary to fine-tune the simulation model in order to accurately represent the local traffic conditions such as speed, traffic volumes and travel time. The process of fine-tuning these parameters is called calibration and the adjusted parameters are called the calibration parameters. Hellinga (1998) defines model calibration as the process of determining the model parameters which need to be tweaked to replicate observed traffic scenarios.

2.7.1 Optimization Methods

The calibration phase one of the most crucial steps in microsimulation modelling, without which the model cannot provide accurate results. Indeed, studies have shown that the calibrated model resulted in significant improvements in the goodness-of-fit, which compares the simulated output and the observed field conditions (Arafat et al., 2020). The potential number of parameters to be tweaked vary depending on the software used. The often-large amount of unknown model parameters makes the calibration a complex and time-consuming task (Toledo et al., 2004). Given that the effects of the parameters extend beyond a single MoE, the model needs to be calibrated through and iterative and systematic process to successfully obtain an optimal solution. To this end, there is a need to automate this calibration to optimize the modelling task.

Several approaches to calibrate microsimulation models have been developed and these can be divided into manual and automated approaches (Espejel-Garcia et al., 2017). Due to difficulties associated with field data collection and a lack of readily available automated procedures and tools, traffic simulation models are often carried out using default parameter values (Chiappone et al., 2015). However, as already mentioned, default parameters are unlikely to produce reliable simulation results except for the scenario for which they were calibrated and validated. In instances where the parameters are tweaked, they are often based on educated guesses or past experience with the simulation model. Although this manual approach is broadly applied in industry because of its accuracy without the need for complex coding abilities, it is still a time-consuming task and is not always considered best practice (Park & Won, 2006). Several authors have successfully attempted to develop automated calibration procedures through the use of algorithms like genetic algorithm (GA), evolutionary algorithm (EA), Nelder-Mead algorithm (NMA), sensitivity analysis and particle swarm optimization (PSO) (Lee et al., 2001; Ma & Abdulhai, 2002; Park & Qi, 2005; Park & Schneeberger, 2003; Rrecaj & Bombol, 2015). These algorithms solve and obtain optimal parameter values by minimizing a particular objective function. Due to their inherent complexity and required number of iterations, these are also time-consuming. However, compared to the manual methods, these automated techniques require less time once the correct equations are in place.

Optimization algorithms are typically categorized into two classes: stochastic approximation (SA), which uses a probabilistic objective function and the deterministic algorithm. Methods, such as the steepest descent and Newton-Raphson utilize deterministic algorithms. The algorithms themselves can be further subdivided into two general groups: gradient and gradient-free algorithms. Nelder and Mead (1965) introduced a non-linear simplex algorithm, which is deterministic in nature and based on a gradient-free and multivariate optimization technique. The steepest descent technique is a rather simple one whereby the value of θ keeps changing to the best gradient vector up until the loss function is minimized.

The objective function of the SA algorithms (also known as the loss function) is applicable in when the gradient function $g(\theta)$ is present or absent. When there is a gradient function, the root-finding algorithm established by Robbins and Monro (1951) is usually applied on nonlinear optimization. A gradient-free approach is used where it is not possible to measure the gradient, like in simulation problems. The most commonly applied gradient approximation technique is the finite-difference approximation. However, it can only be applied when noise measurements of the objective function are known.

Some of the widely used optimization algorithms are discussed below:

2.7.1.1 Genetic Algorithm

Genetic algorithms are among the most popular types used for calibrating microsimulation models due to its good performance and relatively easy implementation (Ma et al., 2007; Kim, Kim, & Rilett, 2005; Ma & Abdulhai, 2002; Park & Qi, 2005). Genetic algorithms are a stochastic global search technique, which can solve constrained and unconstrained optimization problems. As suggested by its name, it is based on the theory that drives evolutionary biology: natural selection, to search for the global minimum solution. The GA optimization process starts with a random selection of individuals to be the initial generation (parents), like chromosomes that are assessed against the objective function. This first generation is used to produce children for the next generation through selection, crossover, and mutation. The selection process entails the retention of the best-performing parent through the various generations. Crossover is when genetic code from two parents is combined to produce a new offspring. Mutation is the process of mutating certain characteristics of the parent to create a new offspring. Over multiple successive generations, the genetic makeup of the population improves and evolves towards an optimal solution.

The basic genetic algorithm has itself evolved over the past years. Yet even with the existence of variations of the process, the following can be said to be the core characteristics that define the process (Goldberg, 1989; Mitchell, 1997):

- *Initial population:* Contrary to some optimization techniques, genetic algorithms uses a population of potential solutions as a starting point as opposed to a single estimate in the initial stages.
- *Encoding:* The different variable attributes of a particular solution are characterized by a chromosome. Typically, this is a bit string, which stores numerical data as binary digits, although other encoding methods have been developed which are more suited for continuous or categorical data.
- *Fitness function:* All solutions are tested according to their fitness, against the predetermined objective function. It is on the basis of this fitness function that the algorithm determines the solution to be produced.
- *Crossover:* Portions of the chromosomes are exchanged by the subjects of the population chosen to reproduce and thus producing new individuals who possess different combinations of genetic characteristics obtained from the parents.
- *Mutation:* In addition to exchanging portions of the chromosomes, parts of the bit string are also shifted to maintain population diversity.
- *Randomization:* There are predefined probability functions that ensure that crossover and mutation operations are performed randomly.

2.7.1.2 Simultaneous Perturbation Stochastic Approximation (SPSA)

Another optimization technique, which is commonly used, is the simultaneous perturbation stochastic approximation (SPSA). It was developed by James Spall for optimizing computationally demanding traffic simulation (Spall, 1992). The essential idea behind SPSA is to seek an optimal point in the algorithm where the objective function has a gradient of zero. It is also a type of stochastic technique, equivalent to the Newton/ Raphson algorithm (Spall, 2003) of deterministic non-linear programming and essentially extends the Kiefer and Wolfowitz version (Kiefer &

Wolfowitz, 1952) of the stochastic approximation method used to compute extrema functions when there are noisy measurements. This stochastic approximation technique performs a numerical evaluation of the function's gradient using a standard finite difference gradient estimation. SPSA on the other hand, is an improvement of the stochastic approximation technique because it evaluates the gradient based only on objective function measurements in which all the function's variables are perturbated simultaneously (as opposed to one at a time as in the stochastic approximation method). Consequently, SPSA possesses two particularly relevant features for microscopic simulation models: i) takes account of the objective function measurement errors and ii) it is normally not as expensive as other algorithms.

The SA algorithms usually focus on finding the vector value $\theta \in \Theta$, which either makes the gradient equation $g(\theta)$ equal to zero or minimizes the loss function $L(\theta)$. The SPSA has the following standard form (Spall J. C., 2003):

$$\hat{\theta}_{k+1} = \hat{\theta}_k - a_k \hat{g}_k(\hat{\theta}_k) \quad \textbf{2-13}$$

Where:

$\hat{\theta}_{k+1}$ = the variables of the function estimated at step *k+1*

a_k = a non-negative scalar gain coefficient which indicates the step size

$\hat{g}_k(\hat{\theta}_k)$ = estimation of the gradient of the function obtained by simultaneously perturbing all the variables at step k, based on the loss function.

This optimization method seeks to minimize the loss function $L(\hat{\theta}_k - a_k \hat{g}_k(\hat{\theta}_k))$ at the kth iteration. The new θ value obtained at each step is calculated by subtracting the product of the step size and the gradient at the present value from the θ value of the previous iteration. As already stated, the gradient. Stochastic Perturbation measures loss by randomly perturbing elements of $\hat{\theta}_k$. By assuming that θ is p-dimensional, the stochastic perturbation gradient can be approximated using the following form:

$$\hat{g}_k(\hat{\theta}_k) = \begin{bmatrix} \dfrac{\hat{L}(\theta + c_k\Delta_k) - \hat{L}(\theta - c_k\Delta_k)}{2c_k\Delta_k} \\ \cdot \\ \cdot \\ \cdot \\ \dfrac{\hat{L}(\theta + c_k\Delta_k) - \hat{L}(\theta - c_k\Delta_k)}{2c_k\Delta_{pk1}} \end{bmatrix} \qquad \textbf{2-14}$$

$$= \frac{\hat{L}(\theta + c_k\Delta_k) - \hat{L}(\theta - c_k\Delta_k)}{2c_k} \left[\Delta_{k1}^{-1}, \Delta_{k2}^{-1}, \dots, \Delta_{kp}^{-1}\right]^T \qquad \textbf{2-15}$$

Where:

$\left[\Delta_{k1}^{-1}, \Delta_{k2}^{-1}, \dots, \Delta_{kp}^{-1}\right]^T$ = a user-defined p-dimensional random perturbation vector.

c_k = a positive scalar.

2.7.1.3 OptQuest/Multistart Algorithm (OQMA)

Like the GA, OptQuest/Multistart algorithm (OQMA) is used to solve both the constrained and unconstrained optimization problems (Ugray et al., 2002; Ciuffo et al., 2008). This algorithm uses a Scatter Search meta-heuristic (Glover, 1997) to establish the initial values for a Generalized Reduced Gradient nonlinear programs (NLP) solver (Smith & Lasdon, 1992; Drud, 1994). In so doing, it’s inclined to merge the global optimizations faculties of a Scatter Search with the searching actions of gradient-based local NLP solvers. The Scatter Search preliminarily explores the parameter’s domain in an attempt to establish different initial values for the gradient descent (which then converges to the closest local solution). The higher the number of initial values located, the higher the probability of finding the global solution. The major disadvantage of this approach is the increased number of the required objective functions, especially when there is a high number of parameters to be calibrated.

2.7.1.4 Downhill Simplex

The downhill simplex or Nelder-Mead method or amoeba method was introduced by John Nelder and Roger Mead (Nelder & Mead, 1965). This is a gradient-free optimization technique which has been broadly used in traffic optimization analyses since 2004 (Brockfeld et al., 2005; Ossen & Hoogendoorn, 2008). It is a commonly used unconstrained nonlinear method since it is a well-defined numerical technique for second order differentiable functions. However, it is only a heuristic method since it is able to converge to non-stationary points (Lagarias et al., 1998).

2.7.2 Goodness-of-fit Measures

As already mentioned, at the core of traffic simulation model calibration is a comparison of observed data measurements to the simulation outputs. Irrespective of the employed calibration procedure, the success and accuracy of the calibration parameters must be evaluated using a goodness-of-fit test. The goodness-of-fit test is therefore performed to evaluate the difference in distributions between the empirical data and simulation results of the respective MoEs.

Table 2-2 presents various goodness-of-fit measures that are found in the literature. For all the expressions shown in the table, x and y represent the model output and the empirical traffic data measurements, respectively. N represents the number of measurements or sample size (taking into account the applicable dimensions, temporal, spatial, etc.), and i represents the single generic observation index. $\bar{x}, \sigma_x, \bar{y}, \sigma_y$ represent the mean and standard deviation of the output and the field measurements, respectively. F_x and F_y represent the cumulative probability density function for x and y, while X and Y are the area over the speed-flow diagram which is covered by the output and the field measurements, respectively.

Table 2-2: Goodness of Fit Measures

Name	Measure	Used by	Comments
Percent Error (*PE*)	$\frac{x_i - y_i}{y_i}$	Shaaban & Radwan (2005), (Park & Qi, 2005), (Merritt, 2004)	Employed either to a single pair of simulated-field measurements or aggregate network measurements.
Squared Error (*SE*)	$\sum_{i=1}^{N}(x_i - y_i)^2$	(Ben-Akiva, Darda, Jha, Koutsopoulos, & Toledo, 2004), (Chu, Liu, Oh, & Recker, 2004)	Most used GoF measure which heavily penalizes large errors. It forms the base of the famous Least Square Method. Low values of SE indicate a good fit.
Mean Error (*ME*)	$\frac{1}{N}\sum_{i=1}^{N}(x_i - y_i)$	(Toledo & Koutsopoulos, Statistical validation of traffic simulation models, 2004)	Useful in indicating the existence of systematic bias. Not suitable for calibration since low values do not guarantee a good fit.

Name	Measure	Used by	Comments
Mean normalized error (*MNE*)	$\frac{1}{N}\sum_{i=1}^{N}\frac{x_i-y_i}{y_i}$	(Toledo, et al., 2003), (Toledo & Koutsopoulos, 2004), (Chu, Liu, Oh, & Recker, 2004)	Like ME, MNE also highlights the presence of systematic bias. Beneficial when applied individually to measurements at each location.
Mean absolute error (*MAE*)	$\frac{1}{N}\sum_{i=1}^{N}\lvert x_i-y_i\rvert$	(Ma & Abdulhai, 2002)	Not specifically sensitive to large errors.
Mean absolute normalized error (*MANE*)	$\frac{1}{N}\sum_{i=1}^{N}\frac{\lvert x_i-y_i\rvert}{y_i}$	(Ma & Abdulhai, 2002), (Kim & Rilett, 2003), (Merritt, 2004), (Kim, Kim, & Rilett, 2005)	Not specifically sensitive to large errors.
Exponential mean absolute normalized error (*EMANE*)	$A.\exp\left(-B.MANE\right)$ (A and B are parameters)	(Kim & Rilett, 2004)	Applied in genetic algorithm as a fitness function.
Root mean squared error (*RMSE*)	$\sqrt{\frac{1}{N}\sum_{i=1}^{N}(x_i-y_i)^2}$	(Ciuffo, Punzo, & Torrieri, 2008), (Ciuffo & Punzo, 2010), (Punzo & Tripodi, 2007), (Punzo & Simonelli, 2005), (Dowling R. , Skabardonis, Halkias, McHale, & Zammit, 2004)	Allows model calibration through the use of different MoEs. Heavily penalizes large errors.
Root mean squared normalized error (*RMSNE*)	$\sqrt{\frac{1}{N}\sum_{i=1}^{N}\left(\frac{x_i-y_i}{y_i}\right)^2}$	(Ma & Abdulhai, 2002), (Brockfeld, Kuhne, & Wagner, 2005), (Hourdakis, Michalopoulos, & Kottommannil, 2003), (Toledo, et al., 2003)	Heavily penalizes large errors. Low values in the fraction’s denominator due to instabilities make it undesirable.
GEH statistic	$\sqrt{\frac{2(x_i-y_i)^2}{x_i+y_i}}$	(Chu, Liu, Oh, & Recker, 2004), (Ma, Dong, & Zhang, 2007), (Ciuffo & Punzo, 2010)	Unlike other measures which are evaluated over a series of data, GEH statistic is usually evaluated over a single pair of field and output measurements. *GEH*<5 for 75% of the pairs indicate a good fit.
Correlation coefficient (*r*)	$\frac{1}{N-1}.\sum_{i=1}^{N}\frac{(x_i-\bar{x})(y_i-\bar{y})}{\sigma_x\sigma_y}$	(Hourdakis, Michalopoulos, & Kottommannil, 2003)	Measures the strength of linear association between field traffic data and output results. It does not provide additional information about the nature of the error (difference)

Name	Measure	Used by	Comments
Theil's bias proportion (*Um*)	$\frac{N(\bar{y}-\bar{x})^2}{\sum_{i=1}^{N}(y_i-x_i)^2}$	(Barcelo & Casas, 2004), (Brockfeld, Kuhne, & Wagner, 2005)	High values indicate the presence of systematic bias. *Um*=0 implies a perfect fit while *Um*=1 indicates the worst fit.
Theil's variance proportion (*Us*)	$\frac{N\left(\sigma_y-\sigma_x\right)^2}{\sum_{i=1}^{N}(y_i-x_i)^2}$	(Hourdakis, Michalopoulos, & Kottommannil, 2003), (Barcelo & Casas, 2004), (Brockfeld, Kuhne, & Wagner, 2005)	High values imply significantly different distribution of output measurements for the field data. *Us*=0 implies a perfect fit while *Us*=1 indicates the worst.
Theil's covariance proportion (*Uc*)	$\frac{2(1-r)\cdot N\cdot\sigma_x\sigma_y}{\sum_{i=1}^{N}(y_i-x_i)^2}$	(Hourdakis, Michalopoulos, & Kottommannil, 2003), (Barcelo & Casas, 2004)	Low values indicate the presence of unsystematic error. *Uc*=1 implies a perfect fit while *Uc*=0 indicates the worst.
Theil's inequality coefficient (*U*)	$\frac{\sqrt{\frac{1}{N}\sum_{i=1}^{N}(y_i-x_i)^2}}{\sqrt{\frac{1}{N}\sum_{i=1}^{N}y_i^2}+\sqrt{\frac{1}{N}\sum_{i=1}^{N}x_i^2}}$	(Punzo & Simonelli, 2005), (Ossen & Hoogendoorn, 2008), (Ma & Abdulhai, 2002), (Barcelo & Casas, 2004), (Brockfeld, Kuhne, & Wagner, 2005), (Hourdakis, Michalopoulos, & Kottommannil, 2003)	Combines the effects of all three error proportions (*Um*, *Us*, *Uc*). *U*=0 implies a perfect fit while *U*=1 indicates the worst.
Kolmogorov-Smirnov test	$max\left(\left\|F_x-F_y\right\|\right)$	(Kim, Kim, & Rilett, 2005)	*F* is the cumulative probability density function of *x* and *y*. Requires more detailed traffic measurements which is not always feasible to collect.

Most of the measures listed in Table 2-2 can indicate poor model fit between the simulated and field measures compared samples, however, not many of them are sensitive to the variance and covariance. In order for a calibration procedure to produce efficient and robust results, the goodness of fit employed should not just provide indicators describing the fit but should also include insight pertaining to the nature of the difference between the field and output measurements to enable the user to target specific model calibration parameters.

Some of the measures such as PE, ME and MNE allow errors that are similar in magnitude but have opposite signs to cancel out. These measures are good when it comes to the detection of systematic bias but are generally not recommended for calibration studies. Other measures such as MAE and MANE assign equal weights to all errors by taking the absolute value of the difference between the field and output measurements. SE, RMSE and RMSNE tend to heavily penalize large errors since they take the squared difference.

2.7.3 Review of Previous Calibration Studies

Cheu et al. (1998) built a FOSIM model of a 6 km long section of the Ayer Rajar Expressway in Singapore. He used surveillance video recording to collect the necessary data wherein two data sets were collected. The set consisted of two weekdays of data collected over a period of two weeks. The data from one of the days was used for model calibration while the second set for model validation. Genetic algorithms were used to optimize the parameter calibration process. They encoded the model parameters into chromosomes made of 40 decimal digits. To avoid overestimating the model accuracy, the data used for determining simulation inputs was not included in the fitness calculation. The MoEs used were traffic volumes and speed, and the fitness function employed is shown in Equation 2-16.

$$F = e^{\frac{-AAE(u_1)}{s_1}} + e^{\frac{-AAE(u_2)}{s_2}} + e^{\frac{-AAE(u_3)}{s_3}} + e^{\frac{-AAE(q_2)}{s_4}} + e^{\frac{-AAE(q_3)}{s_5}} \qquad \textbf{2-16}$$

Where:

F = fitness value
u_i = average speed at detector station i [km/h]
q_i = average flowrate at detector station i [vhe/h]
s_i = scale factor i and
$AAE(x)$ = Average absolute error, given by Equation 2-17.

$$AAE(x) = \frac{\sum_{t=1}^{T}\left|x^{field}(t) - x^{FRESIM}(t)\right|}{T} \qquad \textbf{2-17}$$

Where:

T = number of time steps
$x^{field}(t)$ = field observation at timestep t, and
$x^{FRESIM}(t)$ = FRESIM calculation at timestep t.

This algorithm maximized the fitness value by minimizing average absolute error. The sensitivity analysis revealed that a population size of 4 converged to a much higher fitness value than with larger populations sizes, such as 10 and 40, even though it was lower than what is typically recommended in genetic algorithms. Further sensitivity analyses also showed that minimum car-following distance, free flow speed and car-following portrayed high sensitivity and thus had the most influence in the model accuracy. Interestingly, this study showed that there are different driver characteristics and behaviour during different peak periods. As a result, a different set of parameters was deemed to be appropriate for each peak period (e.g., morning, midday and evening).

Park and Qi (2005) used Paramics, CORSIM and VISSIM to propose a thorough microscopic calibration procedure using genetic algorithm on a five-mile highway section near Covington, Virginia. The procedure placed large emphasis on preprocessing to establish the necessity of genetic algorithm and to ensure the even distribution of the initial population over the search space. The model was initially performed using default parameters and if an adequate model fit was obtained, then further calibration was deemed unnecessary. Because CORSIM is stochastic in nature, multiple runs had to be performed for each parameter set. To verify how well the selected search range covered the possible solutions, they conducted a feasibility test on each of the adjusted parameters. If the field data fell within the middle 90% of the output data, then search ranges were accepted. The fitness function which measured the error was used as illustrated by Equation 2-18.

$$e = \frac{|x_o - x_s|}{x_o} \qquad \textbf{2-18}$$

Where:

e = error,

x_o = observation data, and

x_s = model output calculation.

Instead of transforming the error into an exponential maximization problem, the genetic algorithm can minimize it directly. Once the calibration was successfully completed and an optimum set of parameters obtained using the genetic algorithm, the model was validated using a data set from a different day. Many of the parameters in CORSIM can be defined by distributions, such as free-flow speed for each driver type or discharge headway. In this study, the factors within the parameters which could be described through distributions were not individually fine-tuned. Instead, the analyst defined three to five possible parameter distribution and used the algorithm to choose the best one. This technique simplified the process of calibration since it resulted in a substantial reduction of the number of parameters. However, this approach also implies that the algorithm does not search all possible solutions.

Jobanputra & Vanderschuren (2014) used PARAMICS software to conduct a calibration procedure for an agent-based microsimulation model for vehicle and pedestrian interaction. This study was done on a 600m long corridor in Cape Town, which was notorious for poor levels of safety, characterized by high pedestrian fatalities and injuries. The study found that the default values produced a good fit between observed and simulated travel time values, but the GEH statistic was unacceptable in some cases. Several key parameter values were thus adjusted through a calibration process. For vehicles, these significant parameters were Mean Target Headway, Mean Driver Reaction Time and the assignment matrix type, while for pedestrians, blocking compliance levels, scan area angle and the allowable base speed deviation were key parameters. While the calibration led to outputs that matched observed data for travel time and volumes, pedestrian and driver behaviour and interactions did not match reality. This was mainly due to the fact that the model at the time could not sufficiently account for pedestrian behaviour.

In another study, Vanderschuren (2007), again, used PARAMICS for a calibration exercise. This time, on two major corridors – the Ben Schoeman Highway (BSH) in Gauteng and the N2 near Cape Town. The seed value, target headway, reaction time, aggression and awareness were established to be the significant parameters for investigation. The calibration showed that a normal distribution for aggression and a squared distribution for awareness were appropriate for BSH. Whereas, for the N2, a squared distribution was appropriate for both the aggression and awareness parameters. The squared distribution for aggression signifies a large variation in driver behaviour and experience, as well as vehicle quality. Furthermore, the model found that the simulated volumes mimicked the observed measurements quite well in the first two hours, before alternating slightly thereafter. A travel time analysis, however, showed that the model traffic build up was slower than the actual build up on the N2. The Modelled travel times were also about 10 minutes less than observed, while at the tail of the peak period, the model showed higher travel times than measured, with a maximum difference of five minutes, which was deemed acceptable. Inaccurate lane change behaviour and the abuse of on and off ramps by minibus taxis were some of the issues raised with regards to travel time discrepancies.

Gardes et al. (2002) calibrated a traffic model of Interstate 680 in Francisco Bay Area using PARAMICS. To perform the calibration, a number of significant checks were made for four major model categories. The first being network (network geometry, link speed and signage), the second was on demand (vehicle volumes, mean top speed), the third was the overall simulation configuration (speed memory, time steps per second) and lastly, the driver behaviour factors (mean reaction time, mean target headways). A range of other of other applicable operational strategies were included in the model network such as ramp metering, auxiliary and HOV lanes.

Other authors who calibrated a PARAMICS model include Lee et al. (2001), who used the GA to model a Southern California network. The key parameters in the study were mean reaction time and target headway. Mean target headway influences the vehicle's deceleration and acceleration time within the traffic stream, while mean reaction time influences gap acceptance for a lane change. Using the GA, model parameters were adjusted through an iterative process until the values converged to reach an optimized model. The first test compared the volume and occupancy obtained from the field data to that of the simulation output. Like Lee et al. (2001), Ding (2003) also performed a PARAMICS model using the same parameters (i.e., mean reaction time and mean target headway). However, instead of a GA algorithm, Ding (2003) employed the SPSA optimization technique, and the objective function was the relative error of density and flow. The selection of the calibration parameters was in fact based on an earlier study by Sanwal et al (1996).

Schultz and Rilette (2004) calibrated a microsimulation model using CORSIM. They used car-following sensitivity as the main calibration parameters.   These car-following sensitivity factors incorporated certain driver behaviour attributes that depend on the leading vehicle. They identified ten classes of car-following sensitivity factors to explain the variability among different drives. The parameters were calibrated using the GA optimization approach and simulated distribution was evaluated against the observed data. The authors outlined two alternative sensitivity analyses: lognormal and normal, and these were compared with the initial distribution.

Hourdakis et al. (2003) presented a systematic technique for the calibration of a microsimulation model using a 20-km section of the freeway in Minneapolis. He divided the parameters into global and local categories. The global category included road width, desired speed, section length, minimum headways and maximum deceleration and acceleration. Local parameters, on the other hand, included the speed limit along individual freeway sections. Global parameters are those strongly associated with the model performance in its entirety, while local parameters are concerned with isolated portions of the road. The calibration was also divided into speed-based and volume-based calibrations. The objective of the study was to obtain simulation speeds and volumes that matched the real-world data as closely and possible. The objective function thus sought to minimize the sum of squared errors for both the speed and volume MoEs.

Park and Qi (2005) calibrated a stochastic microsimulation model for an intersection in the U.S in Virginia using VISSIM. The simulation study included a lane-changing logic, a car-following logic and a signal state generator which determines the signal control logic model. This study used the GA optimization technique and used the average travel time as the main MoE. The acceptable range of eight parameters were first determined to acquire an accurate simulation result. To account for the stochastic variance of the model, multiple simulation runs were performed. Furthermore, a t-test and visualization checks were performed to verify the statistical significance of the calibrated parameters.

A model calibration guideline recommended by Miliam & Choa (2000) required a modification of traffic control operations, driver behaviour and traffic flow attributes. Like Park and Qi (2005), they summarized the default parameter values to be included in the calibration as well as their effective range. The study was conducted in CORSIM and the selected measures of effectiveness were traffic volume, average speed, average travel time, density, average and maximum queue lengths. For each of these MoEs, the author recommended the acceptable error range between the model result and the field data. Table 2-3 shows the validation guidelines adopted for each of the MoEs. To obtain more accurate result, multiple runs were performed with many different random seed values and the average simulation result was used.

Table 2-3: MoEs & Evaluation Criteria

MoEs	Validation Guidelines Description	Validation Criteria
Traffic Volume	Difference between field volume and simulated volume in CORSIM.	95% to 105% of observed value.
Average Travel Time	Standard Deviation between the observed average travel times and the simulated travel time.	1 Standard Deviation
Average Speed	Standard Deviation between the observed speed and the model output.	1 Standard Deviation
Density	Difference between observed freeway density and simulated output density.	90 to 110% of observed value
Average and maximum Queue Length	Difference between field queue lengths and simulated output queue lengths.	80 to 120% of observed value

Dowling et al. (2004) recommended three steps in which microsimulation models could be calibrated. They suggested that the model firstly be calibrated for capacity, and thereafter for traffic volume, and that in both cases the model be done at a section with a bottleneck. Lastly, the model should be calibrated for system performance at a wider network level. To calibrate for capacity, the maximum possible flow rate of the target section was determined so that the capacity of the model could be estimated, and the parameters observed to be directly influencing capacity were chosen. Like with many other studies, the optimal set of parameters was established through a minimization of an objective function. In this case, the author used the mean square error (MSE) as the objective function. In order to replicate the field-observed traffic flow, route-choice parameters were changed until the model estimated volumes matched the observed data. Finally, the overall traffic performance calibration was done by comparing a variety of field data such as queue lengths, queue duration and travel time.

3. Modelling Environment

3.1 Background of the model

As discussed in section 2.1, the traffic simulation for this study was conducted using a micro-simulation software called FOSIM. The FOSIM model, owned by the Ministry of Infrastructure and the Environment Public Works and Water Management of Rijkswaterstaat, is being developed at the Laboratory of Traffic Engineering at Delft University of Technology. The software is originally of American origin but has been so radically modified to model the Netherlands traffic scenario that it can now be regarded as a Dutch software. FOSIM is therefore specifically calibrated and validated for Dutch motorways and is used by the Dutch and some UK government authorities with the intention of testing interventions prior to implementation. It was primarily developed to measure the real capacity of a freeway configuration through the analysis of traffic volumes, lateral and longitudinal behaviours, speed adaptation and testing of traffic management rules.

3.2 Principles of road geometry and driver behaviour

The software can handle road section types that typically occur in The Netherlands, such as insertions, merges, splits, symmetrical and asymmetrical weaving, construction zones or the combination of these elements. The road section can have up to a maximum of twelve lanes, with a maximum of ninety-nine origins and ninety-nine destinations. The total length of the road to be modelled is only limited to the capabilities of the computer used. FOSIM makes certain assumptions regarding the geometric features of the model, which generally apply on the Netherlands freeways. For example, horizontal and vertical curves are usually large and their effect on speed is thus considered negligible. Similarly, since The Netherlands is mostly a flat country, the slopes are generally short and therefore deemed not to have a major impact on the speed. As a result, FOSIM does not explicitly take account of the restrictive effect of tight horizontal and vertical curves or steep grades. However, it is possible to specify local speed limitations in the input by applying a speed suppression factor where the abovementioned geometric features deviate from those mentioned above.

Since it’s a microscopic simulation model, FOSIM mimics the individual driving behaviour, and the combined behaviour of all drivers results in a certain traffic state. Driver behaviour in this model is primarily governed by the following:

- Drivers have a desired speed they wish to maintain;
- When drivers come across slower traffic and can no longer maintain their desired speed, they will try to change lanes to pass the slow traffic;
- When passing a slower vehicle is not possible, the driver adjusts his speed and follows the leading vehicle with his desired following distance;
- Drivers also make lane changes necessary to reach their destination, such as at a weaving section.

3.3 Simulation process

In the simulation model, time is divided into time steps of fixed duration - with the assumption that all the motion variables (e.g., acceleration) are constant during each time step. At the end of each time step, the position of all vehicles present on the road section are re-determined. The new position depends not only on the old position, but also on the characteristics of the vehicle, the driver, interaction with other road users as well as road geometry.

The simulation results partly depend on the values drawn during the simulation. These in turn depend on a start value specified in the input for the random generator. With the same start value, the results are always the same. Therefore, in order to make accurate conclusions about the results, several simulations must be performed - each with a different starting value for the random seed number.

3.4 Vehicle generator operation

At the beginning of each lane is a vehicle generator (also called origin or source). This generator determines whether a new vehicle should be placed based on the specified volumes and distribution of different vehicle-driver combinations. The input contains the traffic data per roadway, while the source places vehicles per lane. Therefore, the source converts the roadway data into lane data, namely the volumes per vehicle-driver combination per lane. To this end, the source moves down the lanes from left to right, and the vehicle-driver pairs from the slowest to the fastest, and each time divides the volumes per lane according to whether there is enough space to accommodate them. On the one hand, if the demand for vehicle placement is more than the roadway can accommodate, an error message will appear. On the other hand, if the requested volume is small, the model ensures that not only the right-hand lanes are completely field, but that the traffic is distributed to other lanes as well.

The source keeps track of time per lane since the previous vehicle was placed. Based on the current density, the source then determines after how long the next vehicle must be placed. The model assumes that at a constant density, all vehicles follow each other at the same interval from the generator. This is obviously not the case downstream as driver behaviour causes the follow-up time distribution to change. When it is time to place a new vehicle, the source calculates the exact coordinates at which the vehicle needs to be placed. This is not simply at the beginning of the road section because vehicle placing can only occur at the end of a time step, while the moment at which a vehicle has to be generated can be at any time. Vehicles have therefore usually already travelled some distance downstream from the source when the source places them.

Once the position of the vehicle to be placed has been determined, FOSIM checks whether the distance to the next vehicle downstream is sufficient so that the new vehicle does not need to brake immediately before it. This implies that the distance must at least be equal to the distance that the driver experiences as sufficiently comfortable, according to a function defined by FOSIM. If the distance happens to be too small, the placement of the vehicle will be postponed until after the next time step.

3.5 Vehicle following behaviour

When following, vehicles are concerned with two principles: maintaining a desired following distance and preventing accidents. In FOSIM, drivers do the former by changing the position of the accelerator pedal (from engine braking to maximum acceleration), while for the collision avoidance the brake pedal is used. A more detailed description of the following behaviour is discussed below.

3.5.1 Maintaining desired following distance

The following distance that drivers seek to maintain is dependent on the current speed. The relationship assumed in FOSIM is outlined in Figure 3-1 and can be expressed using Equation 3-1.

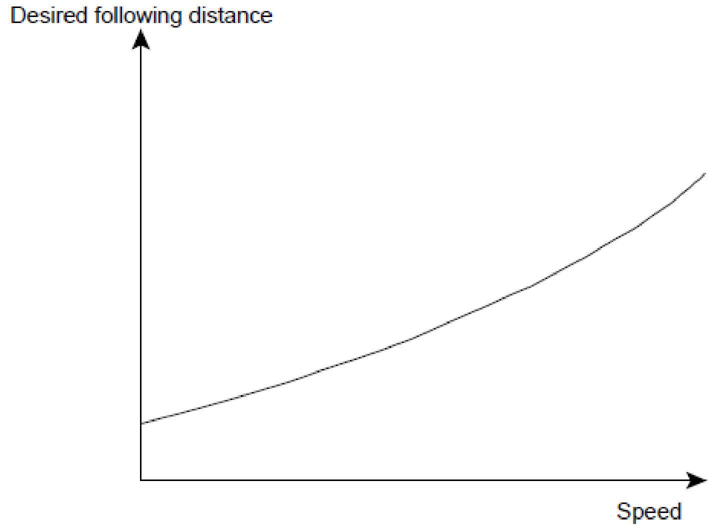

Figure 3-1: Speed - Desired following distance relationship

$$d_i = z_{1,i} + z_{2,i}.v + z_{3,i}.v^2 \quad \textbf{3-1}$$

Where:

d_i = desired net following distance of vehicle type i [m]

$z_{1,i}, z_{2,i}, z_{3,i}$ = calibration parameters for vehicle type i

v = the speed of the vehicle concerned [m/s]

Figure 3-1 shows that at lower speeds, the headways distance and headway time are smaller than at higher speeds. The choice of gear that a driver must use to achieve the desired following distance can be executed in two ways:

1. When approaching a slower vehicle at a greater distance, the (limited) human perception plays a vital role. The greater the distance between two vehicles, the more difficult it is to estimate the speed difference between the vehicles. In FOSIM, this means that a vehicle only adjusts its speed when a certain perception threshold has been exceeded, this theory is modelled Wiedemann (1974). Figure 3-2 shows the perception threshold applied: the

horizontal axis shows the speed difference between the vehicles (the relative speed dv), while the vertical axis shows the distance between the vehicles (dx).

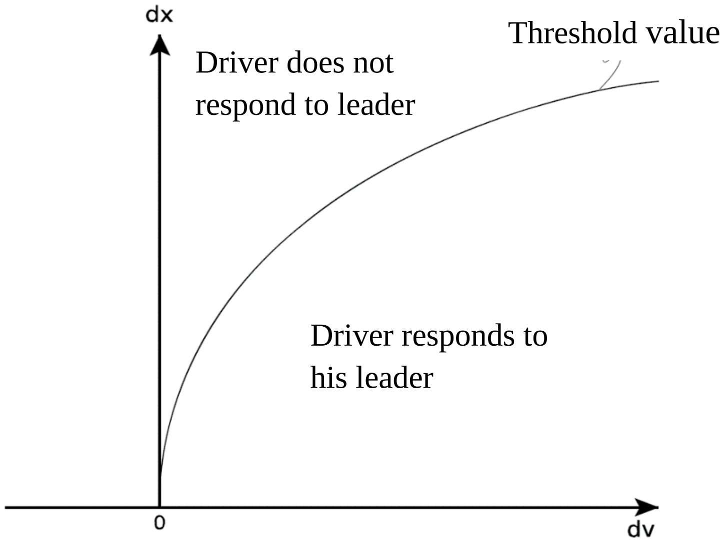

Figure 3-2: Perception threshold principle model ***(Wiedemann, 1974)***

2. When vehicles are closer to each other, a different behavioural model determines the applied accelerations. This model assumes that if the condition deviates from the desired condition (following distance too small or too large), this must be corrected after certain period of time - the so-called 'anticipation time'. The required acceleration required for this is calculated.

3.5.2 Collision avoidance

The car-following behaviour described above is limited to the driver keeping their distance using the accelerator pedal, so that it never results in decelerations greater than engine braking (a calibration parameter named 'maximum following acceleration'). A separate calculation is used where braking is necessary, i.e., where the brake pedal is applied. The principle is similar to the 'anticipation time model' described above, in that the precise implementation is such that drivers now want to ensure they do not collide with their leader after the anticipation time. The result of this is not limited to engine braking but to maximum deceleration, which is again a calibration parameter.

In reality, drivers never react to a situation immediately, but only after a certain reaction time. This has been included, to a limited extent, in FOSIM by accounting for the response time. This is the time taken between making a decision to brake or accelerate and actually executing that action, and this is part of the total reaction time which has an influence on both collision avoidance and maintaining desired following distance. The response time for braking is slightly shorter than that of acceleration.

3.6 Geometric changes requiring lane changes

Assume a road section with two consecutive exits (see Figure 3-3). The names A, B and C for the destination were chosen at random. In reality, the following can be expected for this situation: drivers with destination C will feel pressure to sort to the right at some distance from the start of the exit in question. The moment at which drives do this, depends on the traffic conditions and the 'type' of driver. Some drivers are cautious and want to be pre-sorted in advance, while other drivers take more risks and sometimes only turn right at the exit. Drivers with destination B will of course only pre-sort near the exit that corresponds to their destination, but the expected behaviour is the same.

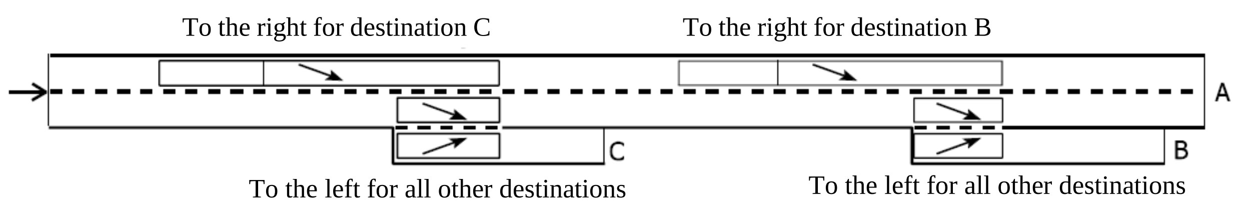

Figure 3-3: Lane change areas on a road section with two exits

In reality, drivers are aware of the scenario in which they want to carry out the necessary lane changes. Road users can have this knowledge based on experience at the location in question, the existing signage, a route description, etc. In FOSIM however, drivers do not have this knowledge by themselves; they can only see the vehicles immediately surrounding them. As a result, there must be data linked to the road that informs drivers where lane changes are necessary due to the geometry. This is done through the so-called "lane-change areas".

FOSIM has two types of lane-change areas: desired lane change and mandatory lane change areas. These two lane-change types are linked to each other in a sense that desired lane changes precede mandatory lane changes. Figure 3-4 shows how the areas are typically placed for the considered road section.

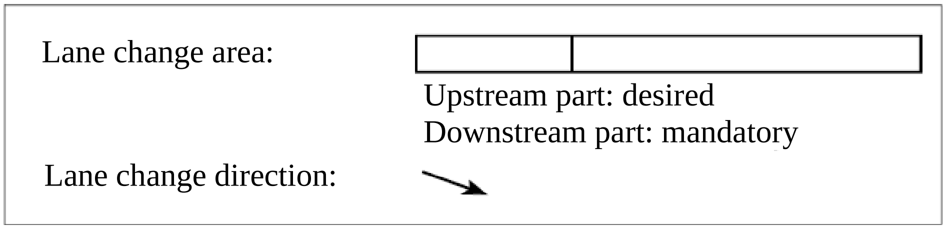

Figure 3-4: Lane change area components

The driver first checks whether the desire to change lanes exist and then whether it can be performed with acceptable acceleration/ deceleration (without braking too hard) for both the lane changing vehicle and its new follower. Now consider vehicles on the left lane in Figure 3-3: Lane change areas on a road section with two exits shown in Figure 3-3, with exit C as their destination. In the upstream part of the lane change area, the desired lane change applies. At the beginning of this area, no driver wishes to change lanes, while at the end of the area all drivers going to destination C wish to change lanes. In other words, the proportion of vehicles that want to change lanes increases linearly from 0% to 100% at the end of the desired lane change area. If the driver does not get a chance to change lanes in upstream portion, they proceed to the downstream portion in which the mandatory lane-change applies. In this area, all vehicles to destination C always have the desire to change lanes. The maximum accepted deceleration depends on the distance travelled in the lane-change area and starts from zero to maximum lane change deceleration at the end of the mandatory lane change area as shown in Figure 3-5.

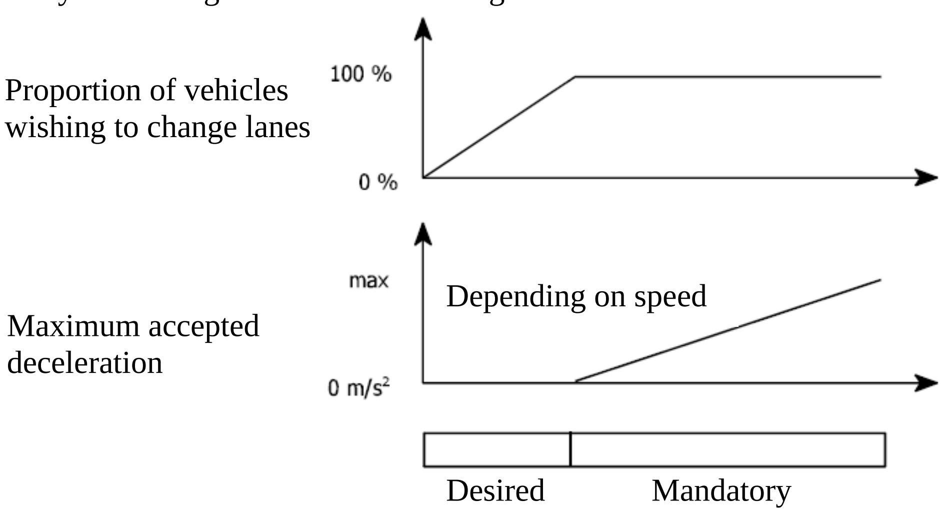

Figure 3-5: Overview of mandatory and desired lane change

In instances where the accepted deceleration is not satisfied, thus rendering the lane change impossible, the vehicle checks whether it wants to brake to get a better chance for lane change in the next time step. Another possibility is to have other vehicles anticipate the lane change. These anticipating vehicles can choose to either brake in order to create a larger gap or to make a lane change to the right, as often happens at ramps, for example, to give traffic from the ramp room to enter the freeway.

3.7 Desired speed and speed limit relationship

As previously discussed, every driver in FOSIM strives for his desired speed. However, this desired speed is not the same in all circumstances, and one of the influencing factors is the speed limit. The influence of the speed limit can be explicitly specified in FOSIM. FOSIM assumes a maximum speed of 120km/h and the calibration parameters determine which desired speeds belong to this speed limit. If a lower speed limit applies to the road section, the model will calculate the desired speeds belonging to this speed limit.

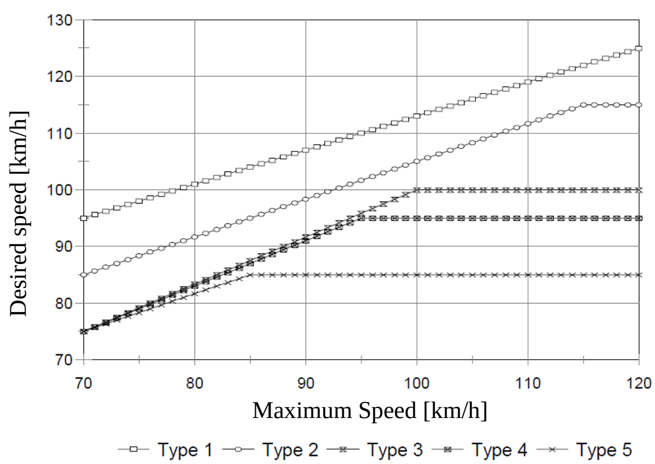

Figure 3-6: Maximum speed vs desired speed per vehicle-driver type

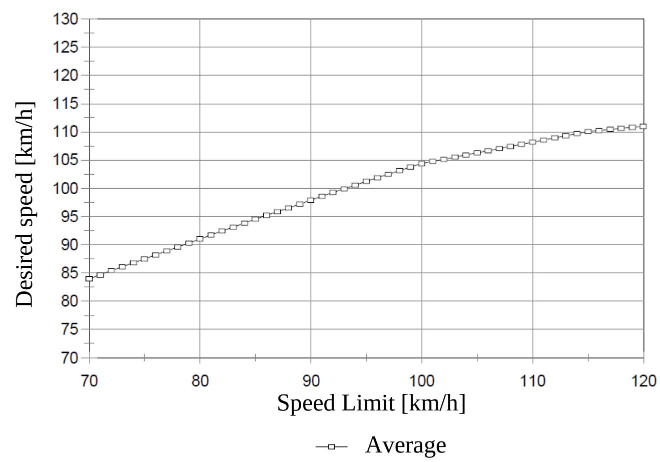

Figure 3-7: Speed limit vs desired speed-average vehicle-driver type with 10% freight vehicles

In reality, the desired speed can depend on many factors and will therefore differ considerably over time and per location. It is therefore problematic to establish the relationship between the speed limit and the desired speed in one general model. The model that FOSIM uses is, therefore, only an approximation and relies on assumptions. Figure 3-6 shows the assumed relationship between the speed limit and the desired speed for each vehicle-driver combination, while Figure 3-7 shows the average with 10% freight traffic. The model is based on the desired speeds that apply at a limit of 120km/h and these desired speeds decrease linearly with the speed limit to the desired speed that applies at a maximum speed of 70km/h (a calibration parameter). When the vehicle exits the lower speed limit zone, it will calculate its new target speed and use the available acceleration to reach that new speed.

3.8 Geometric influence on speed

The maximum speed model is intended for scenarios where only the speed limit determines the desired speeds and is therefore not suitable for cases where characteristics, such as road geometry (e.g., curves, construction) also play a role. In such cases, FOSIM does not explicitly account for geometric influence on speed or traffic flow. This, is because FOSIM has been developed for traffic simulation in The Netherlands' freeways, and as already state, the following usually apply:

- The horizontal curves are generally large, and the effect of these curves on the speed is deemed negligible. As a result, all lanes are straight and curved road sections cannot be explicitly modelled.
- The Netherlands is for the most part a flat country and the slopes that nevertheless occur are generally short. The effect of vertical grades on speed thus cannot be explicitly modelled.
- The vertical alignment of the freeways also consists in wide curves.

In the case of the road geometry which deviates from the above, the model is not yet able to explicitly account for those effects, rather, the application of speed suppression to globally mimic reality may offer some solution. Speed suppression reduces the desired speed associated with the speed limit of 120km/h by a certain percentage. This percentage must have a value between 0% and 100%, where a 100% implies no speed reduction.

4. Study Area Context

This chapter presents and overview of the study area by providing a description of the locality, road network infrastructure and general traffic operations.

Figure 4-1: Study Area

The corridor of study falls within the first section of the National Road N2 (Settlers Way) in Cape Town, Western Cape Province. This is a 560m section running between the M4 off-ramp and Hospital Bend in the in-bound direction as shown in Figure 4-1. The road consists of three lanes going towards Cape Town CBD and an off-ramp going towards the University of Cape Town along the M3 metropolitan expressway.

The road forms part of the Hospital Bend major freeway junction which underwent major roadworks upgrade to address the traffic capacity issues between 2008 and 2010. Four highways approach Hospital Bend from the following directions:

- N2 - City Bow known as Nelson Mandela Boulevard, from the Foreshore.
- M3 – Phillip Kgosana Drive, from Gardens.
- M3 – Roads Drive, from the Southern Suburbs.
- N2 – Settlers Way from the Cape Town International Airport.

This section of the freeway was selected due to its unique freeway operation features. The road is characterized by a variety of vehicle compositions, from smaller passenger vehicles to minibus taxis and then large articulated buses, each possessing different performance parameters and exhibiting varying driving behaviour. Minibus taxis, for example, are generally known for aggressive driving, which often includes erratic lane changing and acceptance of small gaps, causing various disturbances to the flow of traffic and sending shockwaves downstream, which affect the capacity of the freeway.

Furthermore, before the start of the analysis section (downstream), a substantial amount of weaving is observed between the M5 interchange and the M4 (Main Road) off-ramp. This weaving can be attributed to buses and minibus taxis exiting the median lane of the three-lane carriageway after the termination of the reserved BMT lane and moving to the outer lanes in order to take the off-ramps onto the M57 (Liesbeek Parkway) and the Main Road. In addition, the high traffic volumes on the M5 and Liesbeek Parkway connecting the southern suburbs traffic also merges from their respective on-ramps to join the N2 towards the CBD. The weaving section between the Liesbeek Parkway off-ramp and the M4 on-ramp is particularly short, which causes capacity constraints in that section. In addition, the upstream portion of the analysis section at Hospital Bend exhibits a high longitudinal grade combined with a tight horizontal curve, both of which contribute to capacity constraints.

In general, Settlers Way forms one of the backbones of Cape Town's freeway system and is a major public transport corridor, connecting all of the south eastern areas of the Metropol with the Central Business District (CBD). Settlers Way is characterized by high morning peak traffic volumes and heavy congestion levels starting all the way from the M32-Spine Road near Khayelitsha, approximately 30km from the CBD. To this end, a bus and minibus taxi (BMT) lane was initiated by the Western Cape Government and the City of Cape Town in 1995 between the M7 and the M5 to reduce the externalities of congestion on public transport users and has since been extended to cover a larger portion of the corridor. The BMT lane currently begins 1.5km from the R300 and terminates just after the M5 interchange (Tichauer & Watters, 2008). The study area for this research begins shortly after the termination of this BMT lane. The lane is only reserved in the morning peak between 05:30am and 09:00am on weekdays.

5. Methodology

As discussed in the preceding chapters, calibration inputs are essential for producing a reliable simulation model. While inputs, such as traffic volumes, heavy vehicle percentage and road geometry may be relatively easy to observe in the field, other inputs explaining driving behaviour or characteristics of the vehicle, such as individual drivers' aggressiveness in lane changing and propensity for risk, or individual vehicle acceleration and deceleration power are not easy to collect directly. As a result, the traffic engineer must adjust the parameters related to driving behaviour and vehicle characteristics by comparing the simulated MoEs to those observed in the field. This chapter discusses the necessary steps followed in fine-tuning the model parameters in this research.

5.1 Overview of Model Development and Calibration Process

The overall calibration process in this research consisted of four major phases, with several component steps within each phase of the modelling as illustrated in Figure 5-1.

Phase 1 comprised in those activities which are conducted before initiating the modelling process. These activities included formulating the study objectives and goals; identifying the required and available data; the selection of measures of effectiveness (MoEs) that are consistent with the study objectives; examining the availability of data and the required effort for collection and simulation model capabilities. Since calibration is the repeated comparison of simulated model output and empirical data, each of the selected MoEs requires that its associated field data be collected. E.g., if average speed is chosen as an MoE, then the average speed data from both the field and simulation output are necessary for calibration. The collection and preparation of data involves assembling the following information:

- Road geometry – Lengths, number of lanes, curvature.
- Controls – Signage and road markings.
- Existing demands – Link volumes, ramp volumes.
- Calibration data – Flows, travel time and speed.
- Modal share – Buses, trucks, passenger vehicle.

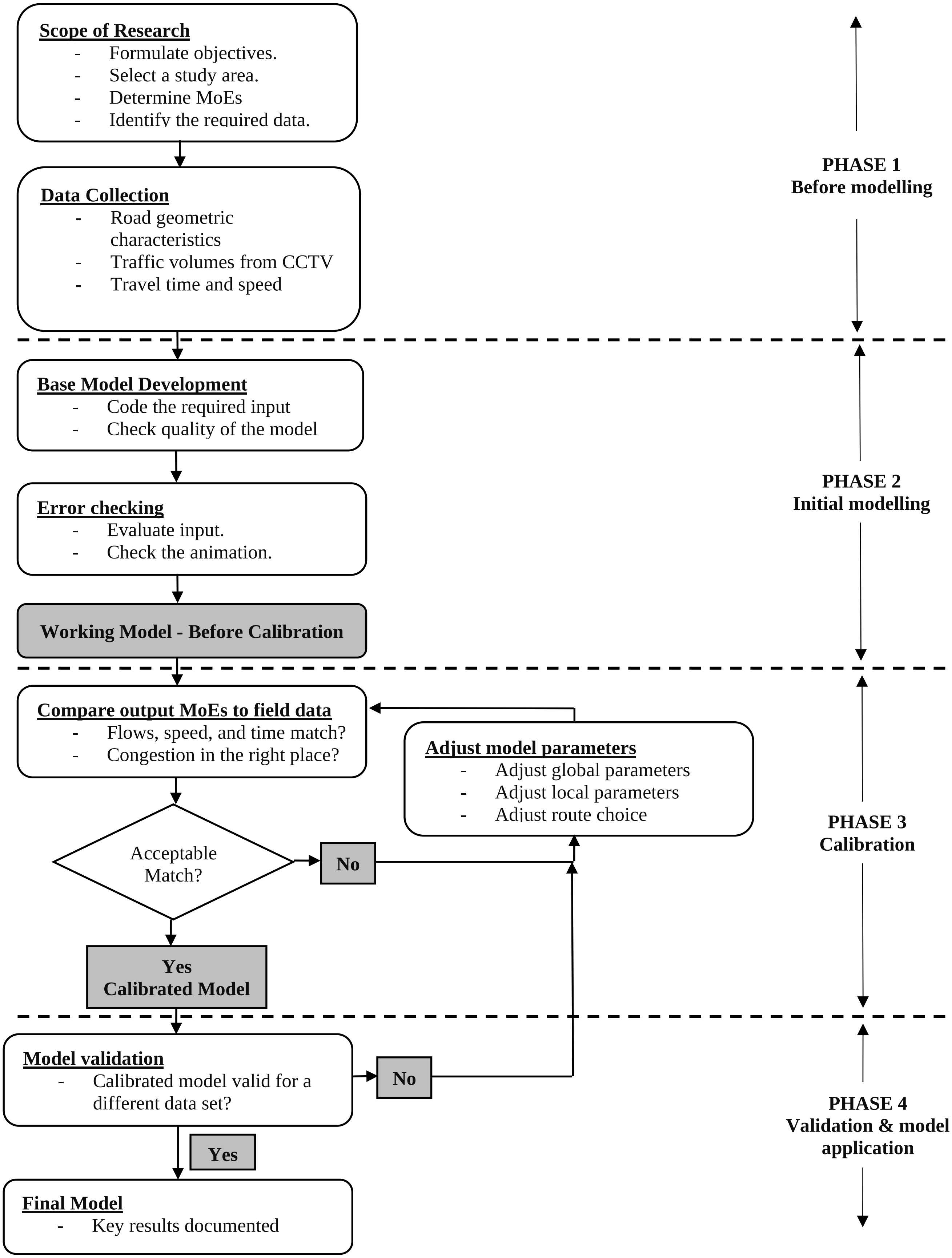

Figure 5-1: Calibration model process

Phase 2 was concerned with developing a base model, which is reproducible, verifiable, and accurate, prior to the fine-tuning of any model parameters. This can be a complicated and time-consuming activity depending on the software used, the optimization technique and the chosen goodness-of-fit measure. The details of the model development for this study are traversed comprehensively in the FOSIM's user's guide, and some aspects have been discussed in the previous chapters of this document. Generally, the model development process involves building multiple layers (one at a time) of the model until all the component of the model are successfully coded. The first layer (the road infrastructure - links, nodes, etc.) set the foundation upon which all the other components would be built. More data, such as lane operations and traffic control mechanisms were added on top of the model foundation. Thereafter, traffic flow data were added to the model. Finally, simulation run set-up and controls were specified to conclude the development of the initial model.

Error-checking was essential for identifying and correcting errors in the model input to avoid interference with the model calibration task. It is obvious that a model with input errors could distort the output of the calibration and result in the adoption of inaccurate calibration parameter values. This error checking process involved various checks of the coded road network and travel demand data.

Phase 3 consisted in the calibration of the model by the fine-tuning the parameter values through an iterative process. Like many other microsimulation models, FOSIM contains a set of adjustable parameter values which enable the analyst to calibrate the model to replicate field conditions. These parameter modifications are essential since it is not practical for FOSIM to account for all possible factors, which might influence traffic volumes and operations on freeways across the globe. The calibration process thus caters to the effects of these "un-modelled" site-specific factors by adjusting the parameter values included in FOSIM for this specific purpose.

Typically, the parameters that require calibration include network coding; identification of nodes and link locations; link characteristics such as speed and traffic regulation measures; lane change areas; driver behaviour such as gap acceptance, maximum acceleration and deceleration accepted; and origin-destination data. Therefore, this step of the model involved the selection of parameters which ought to be calibrated and through an iterative process, identified the best values for those parameters.

5.2 Data Requirement and Collection

Most of the studies in which microsimulation models are used, very limited resources exist for the collection of field data, and this study was no exception. Even when adequate resources are available, some data is difficult to measure directly from the field (e.g., lane change behaviour, vehicle engine power, accepted gaps for individual drivers). Thus, it was important to establish a priority list of the required data as shown in Table 5-1. This list identified the type of data (e.g., link volumes), the temporal resolution (e.g., aggregated to 1 – minute average flows), the spatial resolution (e.g., counts over a particular length of road), the temporal coverage (e.g., 7 AM to 8 AM), and the spatial coverage (e.g., only one direction of traffic – inbound).

Table 5-1: Data Requirements

Category	Data Required	Source	Comments	Status	Obtained?
O-D Demands	Link flows	Loop detector/ Manual counts/ CCTV	1-minute aggregated classified flows from 7AM to 8AM.	Required	Yes
	Turning movements	Manual counts/ CCTV	Turning movement at on and off ramps.	Required	Yes
	Existing O-D data	SANRAL/ WCG	Obtain any existing data	Desired	Yes
Emergent behavior & Traffic state	Average speed	Loop detector/ INRIX/ TomTom/ Google APIs	5 - 15-minute aggregated speed	Required	No
	Travel time	Manual collection/ TomTom/ Google APIs	Obtain any existing travel time data	Desired	No
	Queue lengths	Manual collection/ TomTom/ Google APIs	Existing queuing data or observe from CCTV.	Desired	No
Network coding	Link length	Google Earth/ Maps	Length of lanes and ramps	Required	Yes
	Number of lanes	Google Earth/ Maps	No. of lanes for the section of interest	Required	Yes
	Lane connectivity	Google Earth/ Maps	Connectivity of lanes & ramps	Required	Yes
	Lane use restrictions	Google Earth/ Maps	Barrier lines and merging lanes	Required	Yes

Each item on the list was given a relative priority to indicate its relative importance in the modelling process. The development of the list enabled a more streamlined decision-making process regarding the resources that should be allocated to the collection of data. Furthermore, where decisions were made not to collect certain data, due to resource limitations, the consequences of such decisions on the calibration process could be realistically defined. It also made it easier to identify which MoEs could and could not be explored.

Given the fact that this study formed part of a minor dissertation, the limited time and financial resources played a major role in determining the type of data that could realistically be obtained. Rather than manual data collection methods such as conducting physical counts on the roadside to acquire traffic volumes, the analyst relied on readily available data sources such as closed-circuit television (CCTV) footage. Not only did this limit the types of MoEs, which could be investigated in the study, but it also imposed a limitation on the breadth of the analysis, i.e., the geographical boundaries, size and complexity of the model. After establishing a list of required data, the required resources for the collection of that data were compared to the resources available. Where the available resources were insufficient, the lowest priority data were eliminated from the list and the list of possible MoEs was revised accordingly.

5.2.1 Cape Town Freeway Management System

The video footage used for traffic counts in this study was obtained from the Cape Town Freeway Management System (FSM) CCTV camera. Traffic count data was then obtained by playing back the videos and counting vehicles per class for each destination (exit). FMS is located at the Cape Town Transport Management Centre (TMC) in Goodwood. The FMS is a project jointly funded by the City of Cape Town (CoCT), the Provincial Government of the Western Cape (PGWC) and the South African National Roads Agency Limited (SANRAL). The project has been operation since May 2010 and was the first integrated public transport, safety and security and traffic management centre in South Africa, and one of the first of its kind in the world.

The negative effects of severe traffic congestion on productivity, the environment and running costs of vehicles are widely acknowledged. The implementation of the FMS was, therefore, the CoCT's attempt at establishing an efficient way of dealing with accidents and incidents that impact on traffic flow using CCTV cameras mounted at various locations along the freeway network. Not only does the FMS co-ordinate law enforcement on public roads, but also enables improved incident management and traffic flow, faster response times, delivery of real time information to the public, which enables better route selection as well as improved travel time.

The effectiveness of this system is dependent on timeous detection of incidents. Therefore, the extent of visual coverage of the network and strategic placement of cameras is paramount to informing the travelling the public on what's to be expected on various sections of the freeway via Variable Message Signs (VMS). Figure 5-2 and Table 5-2 show the extent of the network covered by FMS operations per road authority. There are currently 240 CCTV cameras, 50 VMSes, 82 VDSes and 10 weather stations monitoring approximately 163 kilometres of the busiest freeways in the Cape Town Metropolitan area. These are monitored by operators on a 24-hour basis. The operators in turn, provide reliable information to the public, road users, law enforcement and emergency services.

Figure 5-2: Extent of network covered by CT FMS Operations

Table 5-2: Extent of FMS network (km): Summarized by road authority

ROAD	SECTION	COCT	WCG	SANRAL
M5	M5		4.3	
NR0001	Foreshore Freeway	1.2		
NR0001	N1			41.5
NR0001	FW de Klerk Boulevard	4.15		
NR0001	TR0901		18.9	
NR0002	Airport Approach		1.5	
NR0002	Nelson Mandela Boulevard	6.6		
NR0002	N2			22.8
NR0002	TR00201		15.3	
NR0002	TR00202		7.7	
NR0002	Sir Lowry's Pass			8.7
M3	De Waal Dr	1.8		
NR0007	TR01101		11.3	
R300	R300		1.6	16.1
Totals (km)		**13.8**	**60.6**	**89.1**
			163.5	
Percentage Split		**8.4%**	**37.1%**	**54.5%**

5.2.2 Traffic Count Data

CCTV footage was used to conduct traffic counts along the freeway mainline and the off-ramp. Since the entry and exit volumes could be determined from the counts, no origin-destination estimation process was necessary. The counts were collected over three different days (Tuesday, 24 January 2023 to Thursday, 26 January 2023), for a 1-hour period during the morning peak period (7:00 to 8:00 a.m.) and aggregated to 1-minute intervals. The data from Tuesday the 24th was used for calibration, while the data collected on Wednesday and Thursday was used for model validation.

The volumes from the three days were compared to check for any irregularities in the demand patterns that could result from counting errors or unusual traffic scenarios. The volumes across the different days were found to be similar with differences less than 4%, thus no further investigation or reconciliation was necessary. It is essential to go through these checks in the data collection process since inconsistent counts make error checking and model calibration more complicated.

5.2.3 Road Geometry Data

The basic geometric data collected in this study consisted in the number of lanes, section length, location of the M3 off-ramp, horizontal curvature, vertical alignment, and longitudinal grade. The number of lanes and section lengths were obtained from site observation and through the use of Google Earth. Since no geometric design as-built drawings were available, Cape Farm Mapper and Google Earth were used to trace the approximate vertical profile and determine the longitudinal grade, this is shown in Figure 5-4 below. The horizontal curvature was determined using aerial imagery and a geometric design software named OpenRoads by Bentley where a horizontal alignment was drawn to determine the curve radius (see Figure 5-3) – this enabled the analyst to determine the approximate design speed for the curve at hospital bend in order to determine a more realistic speed suppression factor.

The longitudinal grade was found to be in the lower region, ranging between 0.5% and 3.6%. Because the grade is relatively low and is not sustained over a long section length, the effects of grade on speed was disregarded. The radius for the horizontal curve joining the N2 and the M3 was found to be in the region of 110m, which typically corresponds to a design speed of 60-70km/h. This is significantly lower than the 120km/h speed assumed by FOSIM and thus required that speed suppression be applied.

Figure 5-3: Horizontal alignment indicating curve radii.

The road itself, is posted at 80km/h prior to the analysis section and an advisory speed of 70km/h is shown (see Figure 5-5), warning the drivers of the sharp curve ahead. The speed indicated aligns with the curve radius determined above.

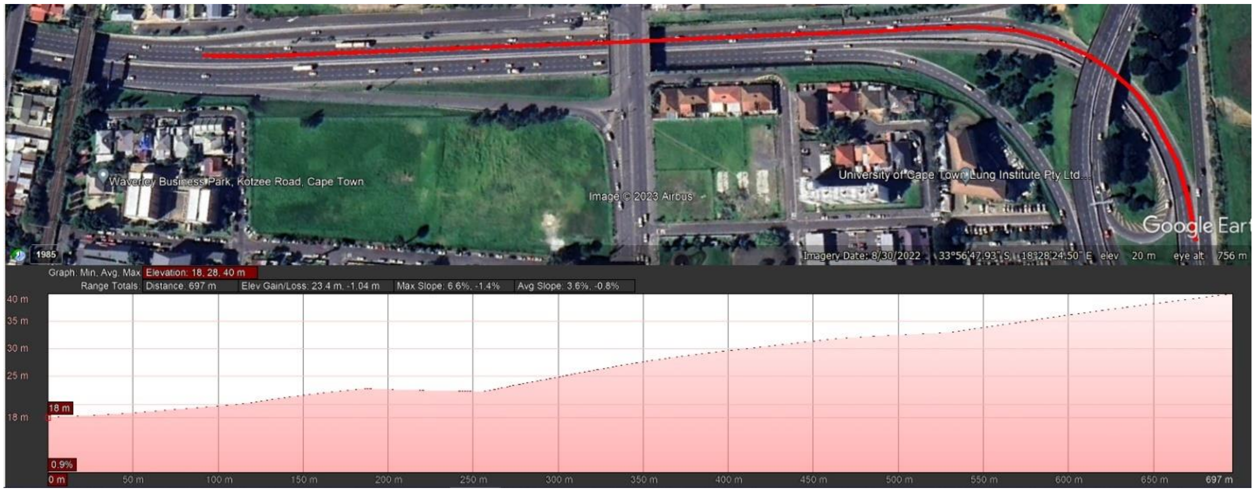

Figure 5-4: Vertical profile

Figure 5-5: Posted speed & advance warning sign.

5.2.4 Traffic Regulation Data

Regulation data consists in taking inventory of the locations where road elements that regulate traffic are found. This included speed limit signage and barrier lines at the off-ramp approach. These areas were noted by driving through the site and through the use of Google Earth.

5.2.5 Vehicle characteristics

FOSIM allows for five vehicle-driver combination types. Type 1 to 3 concerns passenger cars, while type 4 and 5 account for heavy vehicles. The classification of vehicle types is usually based on the distinction between freight traffic and passenger traffic. This is because FOSIM essentially regards all vehicles with the length of less than 6 m as passenger traffic and the other as freight traffic. If several types are defined within freight traffic, the total share of freight traffic is divided equally between type 4 and 5. The same applies for passenger traffic.

For example, suppose an origin has 10% freight traffic; this implies that 5% of the traffic on the roadway belongs to type 4 and another 5% belongs to type 5. Types 1 to 3, which represent passenger vehicles must also be presented in equal proportions. Therefore, in the case of 10% freight, 90% passenger traffic remains, or 30% for each type. Compared to reality, this distinction results in a limited number of types and is, of course, a simplification. However, it is still sufficient to represent reality while maintaining reasonable model complexity. It is, however, possible to change the vehicle parameters, as well as to increase the number of classes distinguished (up to a maximum of eight classes).

In this study, the freight vehicle classes were split equally between type 4 and 5 as FOSIM suggests; this would not have a major impact on the model since the modal share for freight traffic was low (not more than 2%). However, the passenger vehicles could not be split in equal parts since there is a sizeable modal share of minibus taxis. Due to their particularly distinct driver behaviour characteristics compared to other passenger vehicles, they were coded according to their exact modal share. Thus, type 1 and type 2 were split equally, and type 3 was assigned the actual percentage share of counted minibus taxis. The vehicle dimensions used in the model were extracted from the SANRAL Geometric Design Manual shown in Table 5-3 below.

Table 5-3: Model vehicle dimensions

	Dimensions (m)			
Vehicle	**Wheelbase**	**Front overhang**	**Rear overhang**	**Width**
Passenger car	3,1	0,7	1,0	1,8
Single unit	6,1	1,2	1,8	2,5
Single unit + trailer	6,7 + 3,4 + 6,1	1,2	1,8	2,5
Single unit bus	7,6	2,1	2,6	2,6
Semi-trailer	6,1 + 9,4	0,9	0,6	2,5

5.2.6 Travel time data

Trave time data was collected by driving a vehicle along the length of the road section a few times during the analysis period, and then computing the average travel time and speed. This collection method is typically referred to as "floating car runs" and is one of the best sources for point-to-point travel time data. The data was also supplemented and verified by CCTV footage observations. The minimum number of vehicle runs necessary to obtain a mean travel time at a 95% confidence interval is dependent on the ravel time variability measured on the road. For example, on the one hand, under free-flow conditions, the travel time from multiple runs is likely to be more similar and thus may require as few as three runs. On the other hand, congested conditions would result in greater variability and may require more runs (10 or more) to establish a reliable mean travel time.

The minimum number of floating car runs required to determine the mean travel time within a 95% confidence level was calculated using the Equation 5-1.

$$N = \left(2 \times t_{0.025,N-1}\frac{s}{R}\right)^2 \qquad \textbf{5-1}$$

Where:

R = 95% confidence interval for the true mean

$t_{0.025,N-1}$ = t-statistic for two-sided error of 2.5% (totals 5%) with N-1 degrees of freedom

s = standard deviation of floating car runs

N = number of floating car runs required

The initial sample collected on the first day was 12 floating car readings for travel time and average speed. The travel time statistics were then used to determine the required minimum number of floating car runs. Using Equation 5-1, the t-value - read from the t-distribution table for 11 degrees of freedom and 5% significance level was 2.201; the standard deviation was calculated from the data set for each day as shown in Table 5-4, R was determined by subtracting the confidence interval from 100% (100% - 95% = 5%). Substituting these values into Equation 5-1, the minimum number of floating car runs was 4.9, 4.3 and 4.7 respectively. Thus, indicating that the initial 12-samples collected were more than sufficient for determining the mean travel time within a 95% confidence level.

Table 5-4: Field Travel Time

	Travel Time (sec)				
Date	**Mean**	**Median**	**St. dev**	**Min.**	**Max.**
Tuesday	33.68	34.00	2.52	28	38
Wednesday	34.84	35.00	2.37	30	40
Thursday	36.12	36.00	2.49	31	41
Ave.	**34.88**	**35.00**			

5.3 Measures of Effectiveness & Evaluation Criteria

As discussed previously, simulation models can, generally, provide various measures of effectiveness (MoEs). Potential MoEs include link volume, link speed, link travel time, queue size and location, average fuel consumption, and average accident risk. The choice of appropriate MoEs is influenced by the available field data, study objectives, and capabilities of the model. Conversely, the type of field data collected is also influenced by the choice of MoEs to be used in the evaluation process.

The selected MoEs for this research were link volumes, average speed, and link travel time. While the primary objective is to establish the best possible fit between the simulated output and field data for the selected MoEs, there is a limited amount of time and effort with which one can minimize errors in the calibration model. There comes a point of diminishing improvement, whereby considerable efforts put into calibration yields minor improvements in model accuracy. The modeler needs to know when further calibration is no longer practical or productive. This is the reason for establishing evaluation criteria or setting calibration targets.

These calibration targets are developed based on the minimum model performance requirements with due consideration of the available data. The adopted calibration targets were developed by Wisconsin DOT for their Milwaukee freeway system simulation model, based on the United Kingdom guidelines.

Table 5-5: Model Calibration Targets

Calibration Item	Calibration Measures	Calibration Targets
Traffic Volume	Individual Link Flows	
	Within 100 veh/h for volumes less than 700 veh/h	> 85% of cases
	Within 15% for volumes between 700 veh/h and 2700 veh/h	> 85% of cases
	Within 400 veh/h for volumes greater than 2700 veh/h	> 85% of cases
	Sum of All Link Volumes	Within 5% of sum of all link counts
	GEH Statistic < 5 for individual link volumes*	> 85% of cases
	GEH Statistic for sum of all link volumes	GEH < 4
Travel Time	Within 15%	> 85% of cases
Average Speed	Within 10km/h of field measured speed	> 85% of cases
Visual Audits	Individual link speeds	To analyst's satisfaction
	Visually acceptable speed-flow relationship	To analyst's satisfaction
	Visually acceptable speed-density relationship	To analyst's satisfaction
	Visually acceptable flow-density relationship	To analyst's satisfaction
	Lane utilization/ choice consistent with field conditions	To analyst's satisfaction
	Weaving manoeuvres consistent with field conditions	To analyst's satisfaction
	Vehicles reaching the correct destination	To analyst's satisfaction

*The GEH statistic is expressed as follows:

$$GEH = \sqrt{\frac{(E-V)^2}{(E+V)/2}} \qquad \textbf{5-2}$$

Where:

E = model estimated volume [veh/h]

V = field counted volume [veh/h]

The GEH statistic, named after its inventor Geoffrey E. Havers is used to represent the goodness-of-fit for traffic volumes in a model. It takes account of both the absolute difference and the percentage difference between the simulated and empirical flows. GEH is not a unitless measure, but has the units of (vehicles/hour)$^{0.5}$ and the acceptability thresholds are as follows:

- GEH < 5: Good fit.
- 5 < GEH < 10: Requires investigation.
- GEH > 10: Unacceptable.

5.4 Base Model Development

There are many software programs available for performing the modelling task, and each has a unique model coding methodology. This section discusses the procedure followed in coding the base model using FOSIM.

Coding a simulation model is in many respects, analogous to building a house. One starts with a blueprint and then builds each element of the structure in sequence – from the foundation to the frame; roof; utilities; until the interior details are finalized. Similarly, the developing of the simulation model in this study began the blueprint (link-node diagram) and then the model was built in sequence, coding one particular element at a time until the model was fully developed. This included specifying lane widths, traffic control features, O-D name, lane change behaviour, traffic composition and O-D matrix. Thereafter, driver behaviour data was added, and the model run control parameters were determined.

5.4.1 Road Design

5.4.1.1 Physical Road Layout

A schematic of the physical road layout determined from arial photography and site inspection was coded into FOSIM as shown in Figure 5-6, the section length, segments and lane widths were coded accordingly.

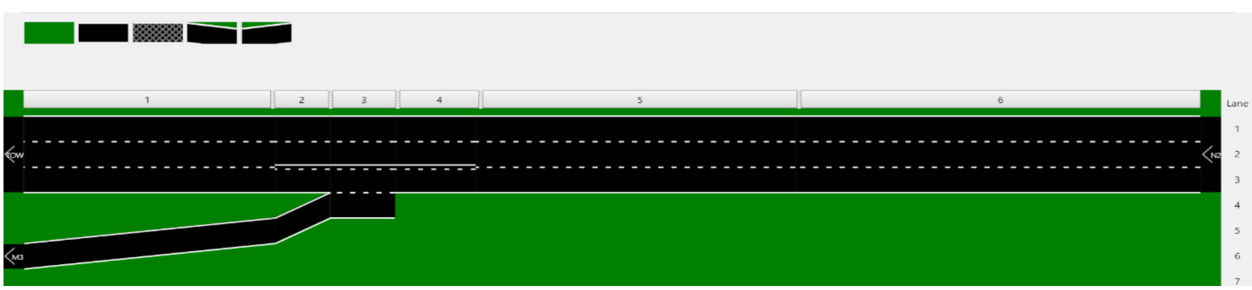

Figure 5-6: Road schematization layout

5.4.1.2 Origin-Destination Names

The section of study consists of one origin and two destinations. The Origin was assigned a name: N2 Inbound, while the destinations were assigned the names: Town and M3 for the traffic continuing along the N2 towards the city centre and that taking the off-ramp to join the M3, respectively as shown in Figure 5-7.

Origin location	Name
Section 6, Lane 1 - 3	N2 INBOUND

Destination location	Name
Section 1, Lane 1 - 3	Town
Section 1, Lane 6 - 6	M3

Figure 5-7: O-D Names

5.4.1.3 Local Details – Speed Limit

As discussed, the posted speed limit along this length of road is 80km/h. The speed limit was coded consistently along the different segments and across the lanes as shown in Figure 5-8.

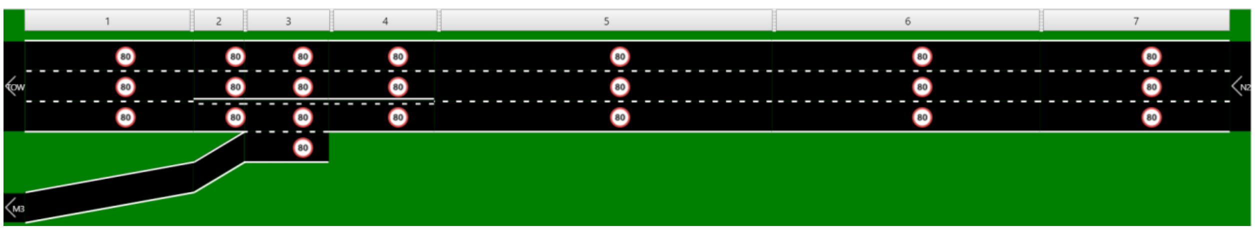

Figure 5-8: Local details - speed limit

5.4.1.4 Lane-Change Areas

The lane change areas and lengths recommended by the model were used for the developing the base model as shown in Figure 5-9. These would later be changed once the initial model run was performed and assessed as to whether it conforms to field conditions.

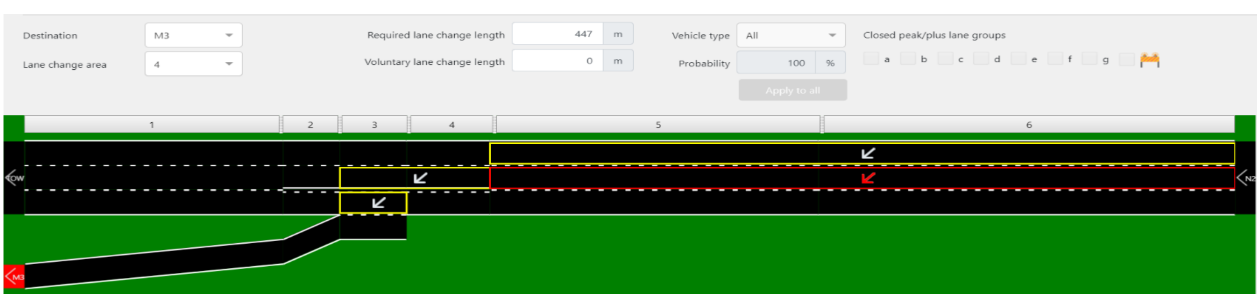

Figure 5-9: Lane change areas

5.4.1.5 Loop Detectors

Loop detectors were initially placed along various critical sections of the roadway for the purposes of measurement. Some of these detectors would later be moved or removed depending on the significance of the location in term of traffic flow behaviour. Figure 5-10 illustrates volume measurement positions.

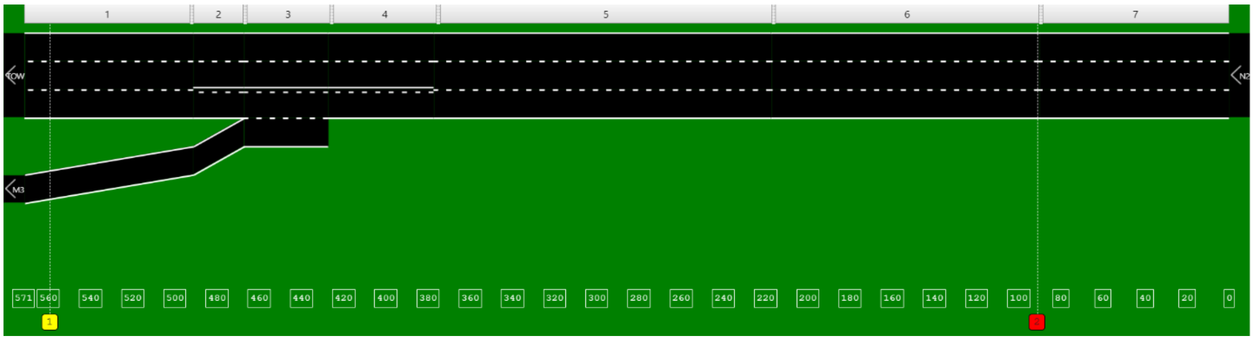

Figure 5-10: Example of loop detector positions for volume measurements

5.4.2 Traffic Coding

5.4.2.1 Traffic Composition

FOSIM automatically allows for 5 vehicle-driver combination to be specified and these are labelled Type 1 through to Type 5. This research considered four vehicle-driver combinations, namely: Type 1 (Passenger cars); Type 2 (Minibus taxis); Type 3 (Buses) and Type 4 (Heavy vehicles). The modal split was coded in FOSIM as shown in Figure 5-11.

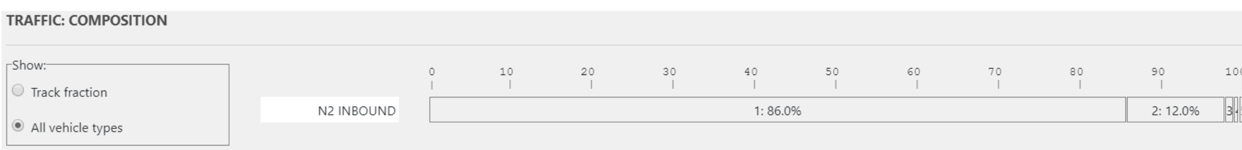

Figure 5-11: Modal split

5.4.2.2 Flow per Origin

FOSIM requires that traffic counts be converted and specified as hourly-equivalent volumes. Thus, the 1-minute aggregated volumes at the origin were multiplied by 60 and coded in FOSIM as shown in Figure 5-12. The destination fractions were also specified for each vehicle-driver type.

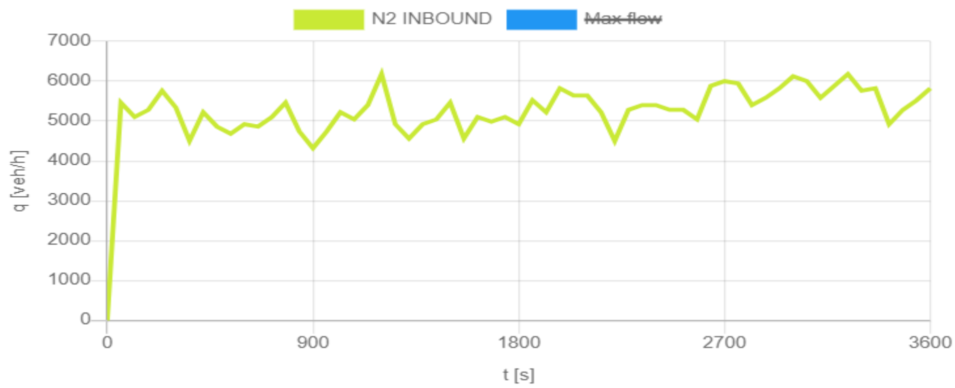

Figure 5-12: Traffic volumes at the origin

5.4.2.3 Vehicle-driver properties

FOSIM consists in two types of vehicle driver properties – the general properties shown in Table 5-6, which apply to all modes and drivers; and the vehicle-driver type-specific properties shown in Table 5-7.

Table 5-6: General Vehicle-Driver Properties

Parameter	Unit	Low Limit	High Limit	Value
Lane-change time	s	1	5	3
Acceleration reaction time	s	0	2	0.3
Deceleration reaction time	s	0	2	0.2

Table 5-7: Vehicle-Driver Type-Specific Properties

Parameter	Unit	Low Limit	High Limit	Type 1	Type 2	Type 3	Type 4	Type 5
Max. positive jump in acceleration per second	m/s^3	0.1	10	1	0.6	0.6	0.5	0.4
Linear following factor	s	0.1	10	0.56	0.72	1.25	2.08	2.23
Max. acc	m/s^2	0.1	8	4	2.4	2.4	1	0.4
Max. following dec	m/s^2	-2	0	-0.5	-0.5	-0.5	-0.5	-0.5
Max. lane change dec	m/s^2	-8	0	-3	-2.4	-2.4	-2	-1.6
Max. dec	m/s^2	-8	-3	-7	-7	-7	-6	-6
Desired speed @ 120km/h speed limit	km/h	75	200	125	115	100	95	85
Vehicle length	m	3	26	4.5	4	4	8	14
Static following factor	m	0.1	8	3	3	3	3	3
Quadratic following factor	s^2/m	0	0.02	0.005	0.005	0.005	0.005	0.005
Desired speed @ 70km/h speed limit	km/h	70	100	95	85	75	75	75
Avg. of the probability distribution of the specific power	kW/ton	5	100	80	50	35	12	9

Parameter	Unit	Low Limit	High Limit	Type 1	Type 2	Type 3	Type 4	Type 5
Std. deviation of the probability distribution of the specific power	kW/ton	0	10	0	0	0	5	5
Drag coefficient	1/km	0.1	1	0.6	0.5	0.4	0.2	0.1
Max. dec for traffic light	m/s^2	-5	-1	-3.5	-3.5	-3	-3	-2.5
Narrow lanes: distance from vehicle to centre of lane marking	m	0	1	0.2	0.2	0.2	0.2	0.2
Narrow lanes: distance from vehicle to barrier	m	0	1	0.6	0.6	0.6	0.6	0.6
Narrow lanes: sensitivity parameter		0	10	1.4	1.4	1.4	1.4	1.4
Narrow lanes: sensitivity parameter		0	10	0.2	0.2	0.2	0.2	0.2
Narrow lanes: phi-factor		0.5	5	1	1	1	1	1
Narrow lanes: alpha factor for overtaking		0	10	1	1	1	1	1
Narrow lanes: theta-factor	1/s	0	50	0.8	0.8	0.8	0.8	0.8
Narrow lanes: limit value for csmax	m	0.5	1.5	0.5	0.5	0.5	0.5	0.5
Narrow lanes: Fcmax	m	0	4	0.7	0.7	0.7	0.7	0.7
Narrow lanes: limit value for w	m	1.9	3.6	3	3	3	3	3
Narrow lanes: vehicle width	m	1.5	2.6	1.67	1.67	1.84	2.53	2.53
Chance peak lane		0	1	0.9	0.5	0.1	0.9	1
Chance plus lane		0	1	0.5	0.8	1	0.5	0
Narrow lanes: alpha factor for passing		0	10	1	1	1	1	1
Narrow lanes: trajectory control overtaking threshold		0	10	3.6	3.6	3.6	3.6	3.6

5.5 Model Calibration Procedure

Once the base model had been established and checked against any errors, the calibration process commenced. The calibration process followed in this study consisted in three steps. First, a sensitivity analysis was conducted to determine which parameters have a relative influence in the model output and should thus be included in the calibration. Secondly, the calibration was performed using the single-parameter search algorithm to obtain the optimal parameter value based on the list of parameters determined in the sensitivity analysis. Finally, the set of optimal parameter values was validated using the data collected on a day separate from that used in the calibration process.

5.5.1 Sensitivity Analysis

As indicated in Table 5-7 above, FOSIM consists of up to 30 calibration parameters, with each parameter varying in value for each of the 5 vehicle-driver types. This results in a combination of 150 potential parameters to be calibrated. Calibrating such a large number of parameters would result in a complex model, which would require extensive computational techniques and large amounts of processing time. It was, therefore, essential for the analyst to determine which parameters have a significant influence on the outcome of the model so they could be the focus of the calibration process. This was done by conducting a sensitivity analysis. Parameters which were found to have insignificant effect on the model accuracy were omitted from the calibration process and their default values were maintained. The sensitivity analysis was carried out in three steps which are discussed below.

From the three MoEs, which formed part of this study, only traffic volumes and travel time are shown and discussed in this chapter. These two MoEs were chosen as representative MoEs for two reasons. First, average speed and average travel time are directly and proportionally related to each other since the section length is constant. Second, the parameters that failed the test based on travel time also failed for speed.

5.5.1.1 Random Seed Sensitivity

The first step of the sensitivity analysis entailed conducting 10 simulation runs using default values for all model parameters. Each model run was conducted using different random seed numbers in order to check the variability of the simulation output solely as a result of random generation and arrival of vehicles. The results of the default test runs are shown in Table 5-8 and Figure 5-13.

Table 5-8: Random Seed Number Sensitivity

Run Number	Random Seed Number	Avg Volume (veh/h)	Avg Travel Time (s)
1	1	5302	35.94
2	3	5283	36.57
3	5	5281	37.03
4	7	5324	37.33
5	9	5340	36.27
6	11	5312	36.26
7	13	5273	37.65
8	15	5312	36.39
9	17	5305	37.24
10	19	5298	35.78
Mean		5303	36.65
Median		5303.5	36.48
Std Dev.		20.51	0.63
Min		5273	35.78
Max		5340	37.65
Range		**67**	**1.87**

5.5.1.2 Parameter Value Sensitivity

Secondly, to examine the impact of different vehicle characteristics and driving behaviour parameters, the simulation was performed with the minimum and maximum parameter values recommended by FOSIM software. For each of these runs, the values of all other parameters which were not being tested were kept constant at their default values while the subject parameter was being varied. In addition, the random seed number was also kept the same for all model runs in this step. Since the random seed number was held constant during these model runs, any variability in the simulation output as a result of using the minimum and maximum parameter value could only be attributed to the effects of those parameter values. It is important to note that the primary focus of this analysis was not to examine whether the parameter value produced accurate results, but rather to test whether significant changes in the value of the parameter might have consequentially significant effects on the model output. The results of these test runs are provided in Table 5-9.

Table 5-9 consist in four columns; where the first column indicates the parameter being examined. The second column shows the minimum and maximum parameter values used to run the simulation model as well as the range - which is simply the difference between the maximum and minimum value. The third and fourth columns show the average volume and average travel time corresponding to the minimum and maximum parameter values in the second column and similarly, their range – which is again the difference between the maximum and minimum value. The remainder of the parameters are not shown in the table since they mostly relate to unusual scenarios in the roadway such as narrow lanes and traffic lights, which are not applicable in this study. When tested, these parameters exhibited no difference in the model output when simulated with their minimum and maximum values (similar to the effect of drag shown in the table) – which implies that the model is not sensitive to these parameters. These parameters were thus not included in the calibration process.

The last step of the sensitivity analysis involved comparing the computed ranges resulting from varying a single parameter value while holding the random seed number constant (Table 5-9), to the observed range resulting from changing the random seed number while holding the parameter values constant (Table 5-8). This comparison is illustrated in Table 5-10.

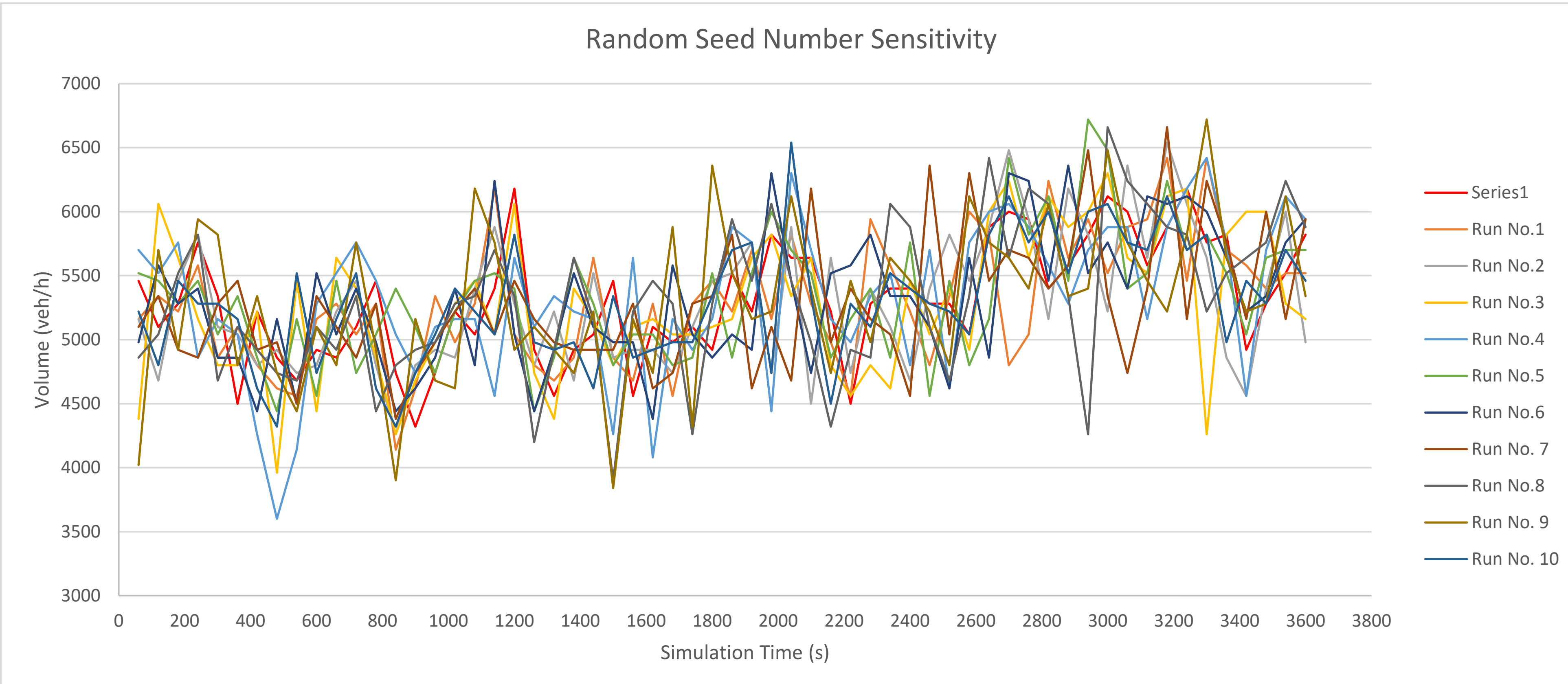

Figure 5-13: Volumes for different random seed numbers

Table 5-9: Parameter Value Sensitivity

		Network MoEs	
Parameter	**Parameter Values**	**Volume (veh/h)**	**Travel Time (s)**
Maximum Positive Jump in Acceleration	0.1	2218	37.65
	10	5307	35.71
Range	***9.9***	***3089***	***-1.94***
Linear Following Factor	0.1	4995	34.53
	1.2	4797	41.32
Range	***1.1***	***-198***	***6.79***
Maximum Acceleration	0.1	2079	95.96
	8	5287	37.43
Range	***7.9***	***3208***	***-58.53***
Maximum Following Deceleration	-2	4783	35.44
	0	5299	35.92
Range	***2***	***516***	***0.49***
Maximum Lane Change Deceleration	-8	4887	41.37
	0	5304	34.51
Range	***8***	***417***	***-6.86***
Maximum Deceleration	-8	5298	36.13
	-3	5301	36.34
Range	***5***	***3***	***0.21***
Static Following Factor	0.1	5314	34.40
	8	4979	38.13
Range	***7.9***	***-335***	***3.73***
Quadratic Following Factor	0	5314	35.99
	0.02	5263	39.32
Range	***0.02***	***-51***	***3.33***
Avg. of the probability distribution of the specific power	5	5311	35.92
	100	5281	37.03
Range	***95***	***-30***	***1.103***
Std. dev. of the probability distribution of the specific power	0	5281	36.53
	10	5308	36.24
Range	***10***	***27***	***-0.2975***
Drag coefficient	0.1	5281	36.53
	1	5281	36.53
Range	***0.9***	***0***	***0***

Table 5-10: Default ranges and Parameter Sensitivity Analysis

Parameter	Volume (veh/h)	Travel Time (s)
Default Range (From Table 5-8)	***67***	***1.87***
Maximum Positive Jump in Acceleration	3089	-1.94
Linear Following Factor	-198	6.79
Maximum Acceleration	3208	-58.53
Maximum Following Deceleration	516	**0.49**
Maximum Lane Change Deceleration	417	-6.86
Maximum Deceleration	**3**	**0.21**
Static Following Factor	-335	3.73
Quadratic Following Factor	**-51**	3.33
Avg. of the probability distribution of the specific power	**-30**	**1.10**
Std. dev. of the probability distribution of the specific power	**27**	**-0.30**
Drag coefficient	**0**	**0.00**

Based on the results shown in Table 5-10, maximum deceleration, average of the probability distribution of the specific power, standard deviation of the probability of the specific power, drag coefficient were all omitted from the calibration process, as illustrated by the bold and red values. This is because the variation in the model output as a result of setting these parameters to their minimum and maximum values was no greater than the variation which resulted from simply changing the random seed number (Default range). Furthermore, this test showed whether the parameter is sensitive for only one or all MoEs. This was particularly the case with maximum following deceleration and the quadratic following factor; where on the one hand, it was observed that the maximum following deceleration showed significant influence in the average volume results, while on the other hand, no influence in the average travel time was evident. Conversely, the quadratic following factor exhibited significant influence in the travel time, while insignificant influence was observed in the average volume. As mentioned previously, although only average volume and average travel time are shown and discussed in this section, the parameters that failed based on average travel time also failed based on average travel speed.

5.5.2 Simulation Repetitions

Simulation models, typically, produce different results for repeated simulation runs. This is due to the stochastic nature of microsimulation models caused by randomly generated seed for each simulation. The random seed number determines simulation time step characteristics such as the time at which a particular vehicle is loaded, the vehicle type and the path for each generated vehicle. It also determines the characteristics of a driver, such as level of aggressiveness and propensity for risk. Each random seed will produce a different model output, and if the output data from multiple runs is aggregated, they will follow a certain distribution of values with minimum and maximum values. The result of a particular simulation model will therefore not be one specific value but will be a distribution of values. The more times the simulation is repeated – the larger the sample size, and the more representative the model distribution will be.

The minimum number of repetitions required to obtain a representative sample was determine using the same procedure used to estimate the minimum number of floating car runs required for travel time data collection in Section 5.2.6. Figure 5-14 shows the flow chat indicating the sample size determination process.

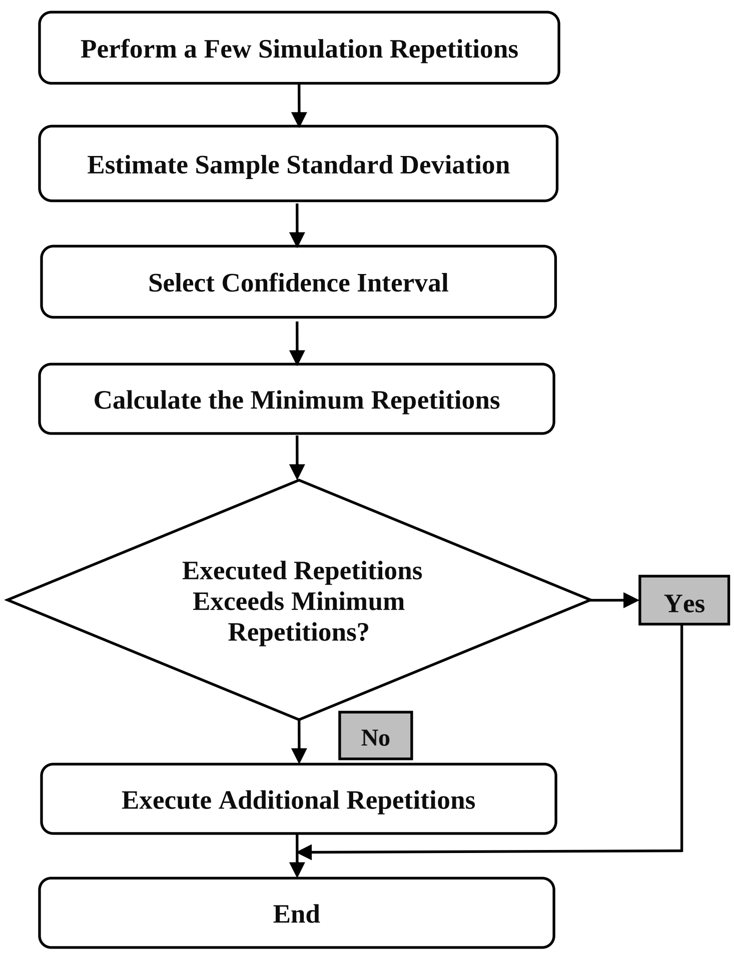

Figure 5-14: Sample size determination process

The 10 simulation repetitions executed in Table 5-8 were used as the initial sample size. With a 95% confidence interval and a degree of freedom of 9, the t-critical value was determined to be 2.262. With a standard deviation of 20.51, the minimum number of repetitions calculated using Equation 5-1 was 345.

5.5.3 Parameter Search

As discussed earlier in this study, there are several methods available for obtaining the optimal parameter values to produce the simulation results that align with the field data. These can either be automated algorithms which minimize the specified objective function or manual techniques which rely on trial and error as well as the experience of the analyst. For the purpose of this study, the use of fully automated searches could not be achieved, instead a systematic manual search algorithm was employed. This is a single-parameter search algorithm, which is also referred to as the Golden Selection Method and recommended by Dowling et al. (2004). It is called a single-parameter search because it is concerned with the optimization of a single parameter at a time. There exists other search algorithms such as the Simple Two-Parameter Search Algorithm and Dual-Objective Parameter Search Algorithms where more than one parameter can be optimized at the a time. The below steps describe the adopted parameter optimization technique.

Step 1: Compute the MoE results using the minimum and maximum parameter values

In this step, the model was performed with the recommended minimum and maximum parameter ranges. The resulting traffic volumes, travel time and speeds were then recorded. It is important to keep in mind that the larger the range covered between the minimum and maximum value, the more robust the search. However, finding the optimum value over a large range requires more processing time. On the other hand, a smaller range increases the likelihood of the optimum solution lying outside the range and thus producing an inaccurate model.

Step 2: Selection and calculation of the objective function

This analysis sought to minimize the square error (SE) between the model output and the field measurements of traffic volumes. In Table 2-2 above, it was stated that SE is the most commonly used goodness-of-fit measure which strongly penalizes large errors, and that low values of SE indicate a good fit.

The analysis thus involved selecting a set of parameters ***p*** to minimize:

$$SE = \sum_{i=1}^{N} (x_i - y_i)^2 \quad \textbf{5-3}$$

Subject to: $p_m^{min} \leq p_m \leq p_m^{max}$ for all adjustable model parameters p_m

Where:

SE = Square error

x_i = model estimated flows [veh/h]

y_i = field measured flows [veh/h]

p_m = model parameter value number m

p_m^{min} , p_m^{max} = user-specified limits to the allowable range of parameter values p_m

Once the simulation run was conducted using the maximum and minimum parameter values and the resulting volumes determined as discussed in step 1, the squared error for each of the models was computed using Equation 5-3.

Step 3: Identify two interior parameter values

The two interior parameter values (x_1 and x_2) were computed based on the specific ratios of the total range which preserves these rations as the search range is narrowed in the subsequent iterations. The formulae for computing the two interior parameter values are as follows:

$$\boldsymbol{x_1 = min + 0.382 \times (max - min)} \quad \textbf{5-4}$$

$$\boldsymbol{x_2 = min + 0.618 \times (max - min)} \quad \textbf{5-5}$$

Where:

x_1 = lower interior point value

x_2 = upper interior point value

min = minimum parameter value (lower end of the search range)

max = maximum parameter value (upper end of the search range)

The initial minimum and maximum parameter search range values are those which are recommended by the model as the two extreme values, however, the search range was gradually narrowed as each iteration was conducted until the optimum values were found.

Step 4: Compute the squared error for interior points

Once the two interior parameter values were computed, the model was run to determine the flows corresponding to these new parameter values. Thereafter, like it was computed for the minimum and maximum parameter values, the squared error was also calculated for the two interior values.

Step 5: Identify parameter values that appear to bracket the optimum

During this step, the parameter search range was narrowed further. The parameter values (x_1 or x_2) which produced the lowest squared errors were identified. Where the square error function mimicked the third order polynomial such as the one shown in Figure 5-15, the parameter values to the left (lower) and right (higher) of the point, with the least error became the minimum and maximum values for the new search range. For example, in Figure 5-15, parameter value x_2 produces the least square error. Thus, x_1 and 'max' would be the new extreme values and new x_1 and x_2 values would need to be computed for this reduced range.

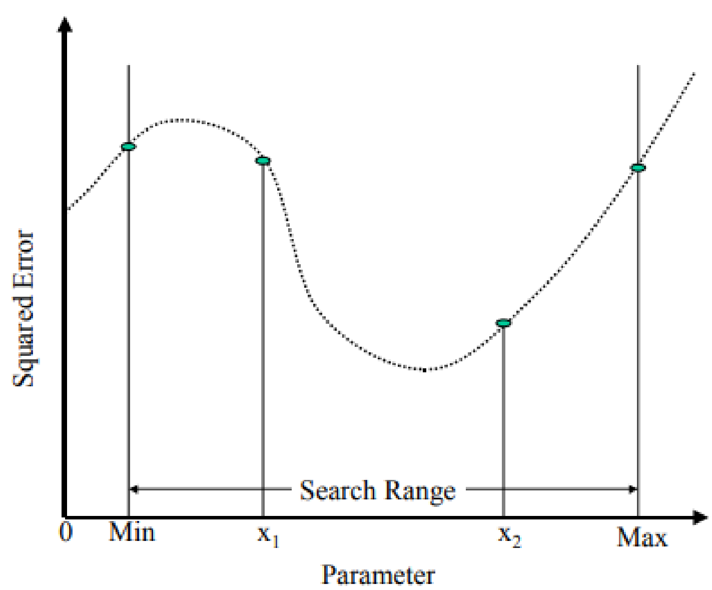

Figure 5-15: Single-Parameter Search Illustration

In instances where either the minimum or the maximum parameter values produce the least error, then the search range was reconsidered. However, where the squared error function did not mimic a third order polynomial, but rather exhibited a power function, for example, then a minimum or maximum parameter value could produce the least error.

For illustration, Figure 5-16, Figure 5-17 and Figure 5-18 show the single-parameter search functions from this study for the maximum jump in acceleration, linear following factor and maximum acceleration respectively. On the one hand, the analysis showed that the acceleration functions mimicked a power function where the model accuracy increased with an increase in the maximum jump in acceleration and maximum acceleration. This implies that there are no local minima and local maxima for these parameters. Therefore, increasing the parameter values beyond the point at which the curve begins to plateau, that is, where the point tangent approaches zero, will have minimal to no effect in the model accuracy. On the other hand, other parameters, such as the liner following factor mimicked a third order polynomial function. In this case, there exists local minima and maxima. The steps required to narrow the search range until the optimum parameter value was obtained were thus employed as described previously.

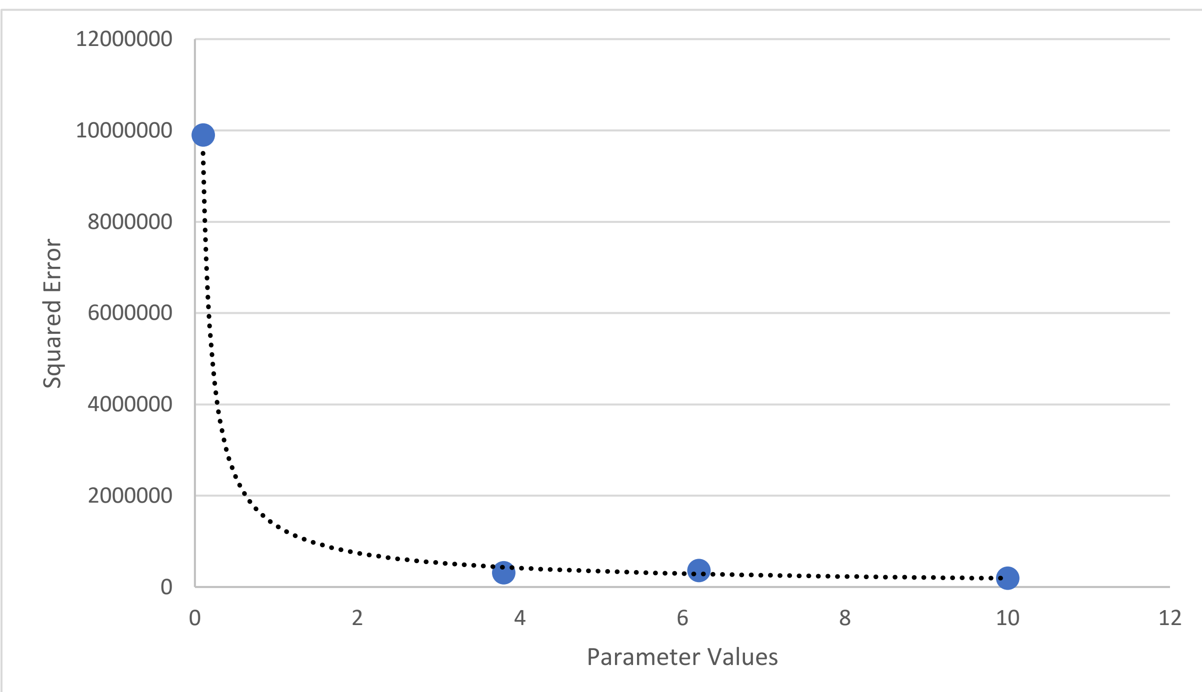

Figure 5-16: Rate of change of vehicle's acceleration squared error

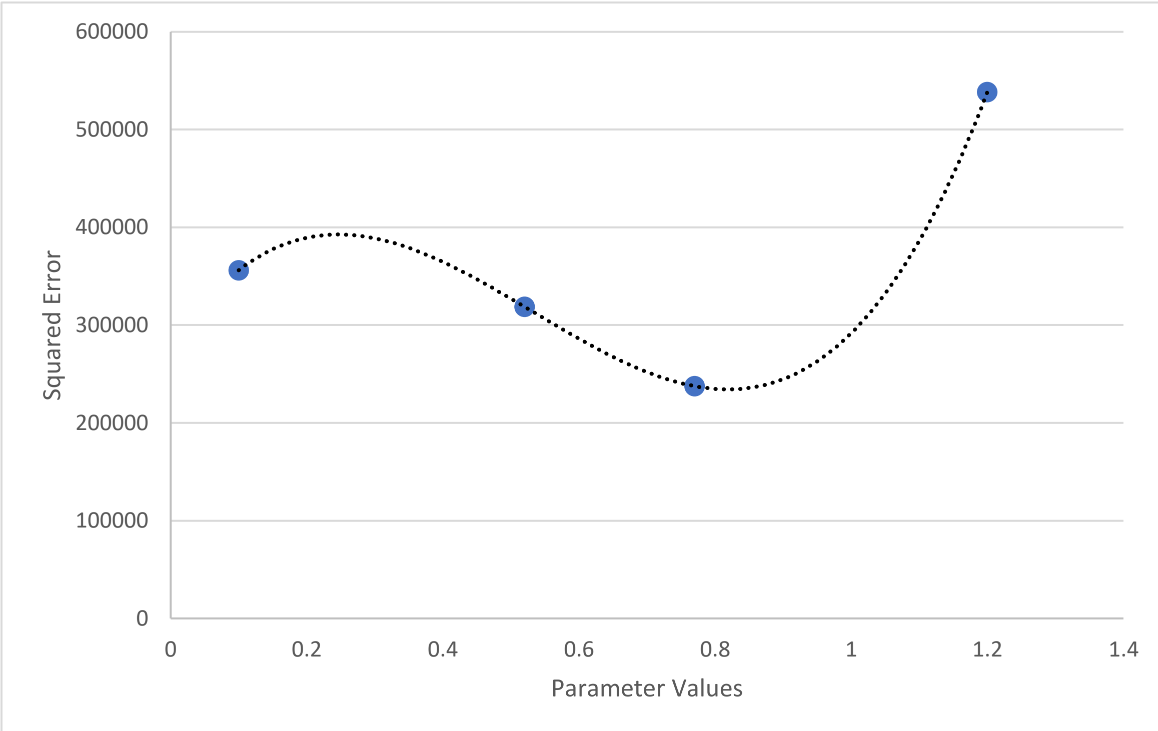

Figure 5-17: Linear following factor squared error

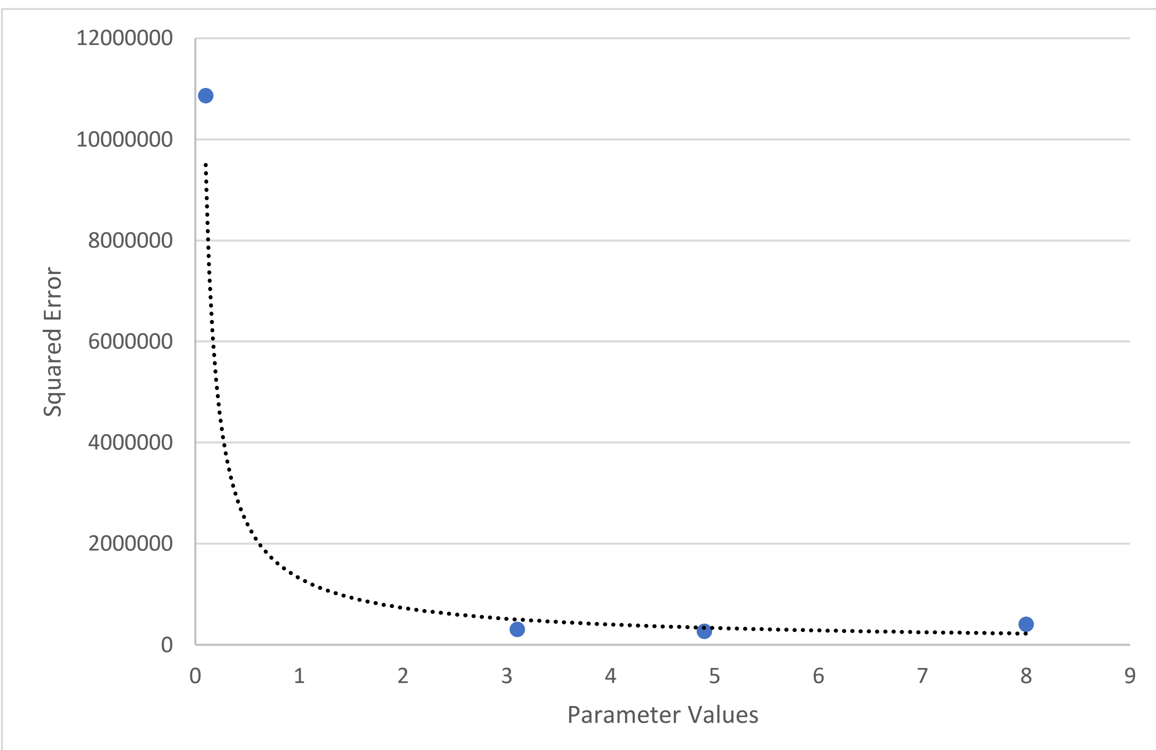

Figure 5-18: Maximum acceleration squared error

Step 6: Return to step 3 and repeat until optimal parameter value is obtained

The single-parameter search was repeated multiple times until the range of values in which the optimum parameter value lies was small enough to provide a satisfactory model in line with the specified model calibration targets.

5.6 Model Validation

The optimum parameter set obtained from the calibration process was applied to a model with traffic demand data from a different day along the same section of road. Whereas the calibration was done using data collected on the 24th of January 2023, the data used for the validation was that collected on the 25th of January 2023. The model was simply conducted by coding the respective traffic demand data from the 25th of January and running the simulation with the parameter values obtained in the calibration process. The obtained simulation results were thereafter compared to the empirical data to check if they fell within the acceptable range as specified.

6. Results and Discussions

This chapter discusses the calibration and validation results of the analysis conducted in this study. The text first deals with the results of the model before any calibration took places and draws a contrast to those obtain in the different stages of the calibration process up to a point that the model output conformed to the established acceptance criteria. The calibration process was carried out using the empirical data and methodology discussed in Chapter 5. Furthermore, to test the applicability of the model on a different data set, a validation model was produced using a dataset from a day separate to that used in the calibration.

6.1 Model Output Before Calibration

Following the base model development discussed in Section 5.4, a simulation run was performed to determine whether the default parameters and local road design features could produce the output which matched the empirical data. These default parameters are listed in Table 6-1. Section 5.3 highlighted the MoEs with which the validity of the model was tested – these are traffic volumes, average travel time and travel speed.

Table 6-1: Parameters before calibration

Parameter	Unit	Low Limit	High Limit	Type 1	Type 2	Type 3	Type 4
Max. positive jump in acceleration per second	m/s3	0.1	10	1	0.6	0.6	0.5
Linear following factor	s	0.1	10	0.56	0.72	1.25	2.08
Max. acc	m/s^2	0.1	8	4	2.4	2.4	1
Max. following dec	m/s^2	-2	0	-0.5	-0.5	-0.5	-0.5
Max. lane change deceleration	m/s^2	-8	0	-3	-2.4	-2.4	-2
Vehicle length	m	3	26	4.4	4	4	8
Static following factor	m	0.1	8	3	3	3	3
Quadratic following factor	s^2/m	0	0.02	0.005	0.005	0.005	0.005

On the one hand, the results of the model performed using default parameters showed that the model could closely mimic the traffic volumes; with a GEH statistic of less than 5 for 97% of the cases (well above the 85% target) and an average GEH statistic of 2.

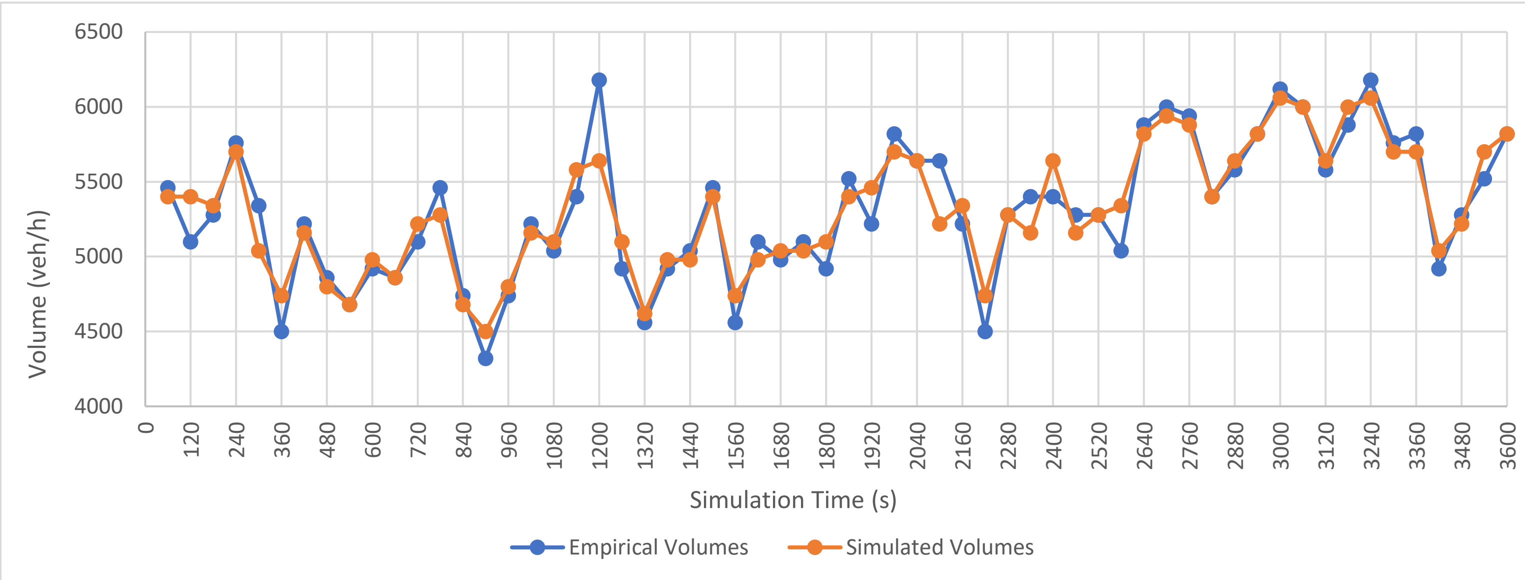

Figure 6-1: Observed and simulated traffic volumes before calibration

Figure 6-1 shows the traffic volumes in vehicles per hour for each minute of the simulation period. Both the observed field volumes and simulated volumes are depicted. Figure 6-2 shows the corresponding traffic volume regression model, where the diagonal line is a 45-degree line representing a perfect fit between field volumes and simulated volumes and the red crosses representing the actual model-fit. Since the GEH statistic measure is low, as mentioned above, it's not surprising that the red crosses are scattered closely along the diagonal line with a high R-squared value of 0.88, which implies that the simulated volumes largely coincide with the field volumes.

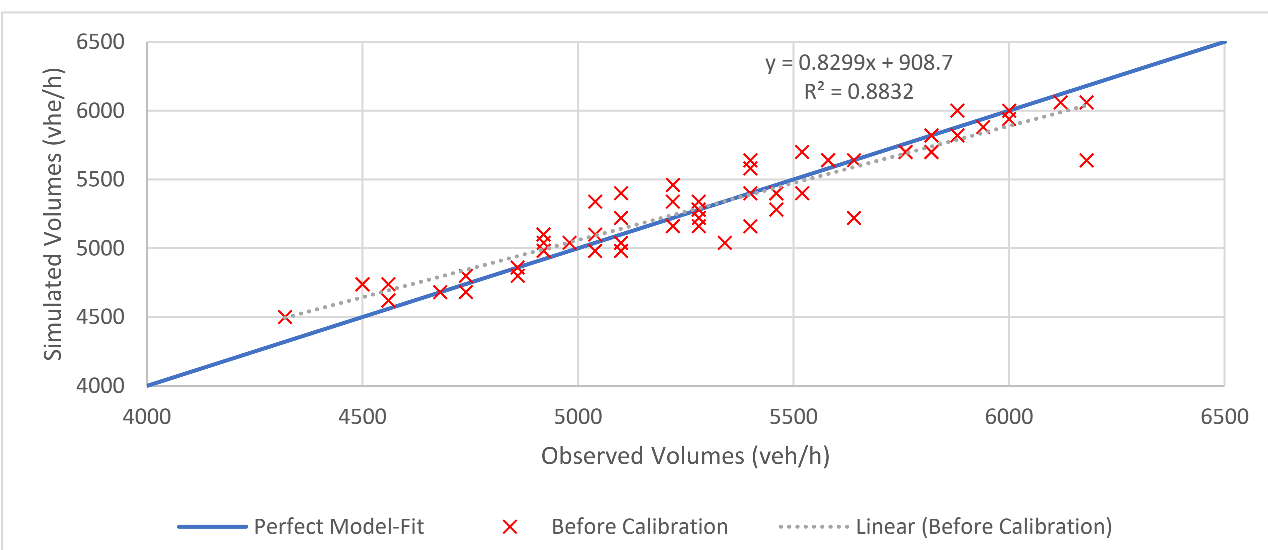

Figure 6-2: Traffic volume regression model before calibration

The simulated average travel time and speeds were significantly different from the observed averages. As shown in Figure 6-3 and Figure 6-5, the observed average travel time and average speed are 33.68 seconds and 60.20 km/h respectively. However, the simulated average travel time and average speed are 20.33 seconds and 99.76 km/h respectively. This discrepancy is also evident in the speed profiles per lane as shown in Figure 6-4, where the observed average speeds are 67.30km/h, 62.34km/h and 52.64km/h for the middle, inner and outer lanes respectively.

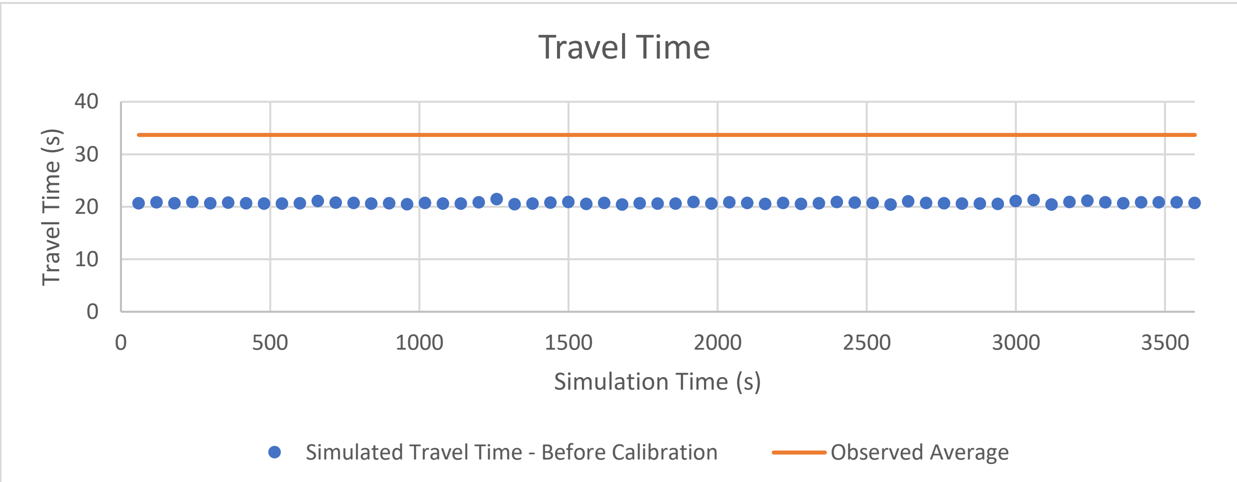

Figure 6-3: Travel time before calibration

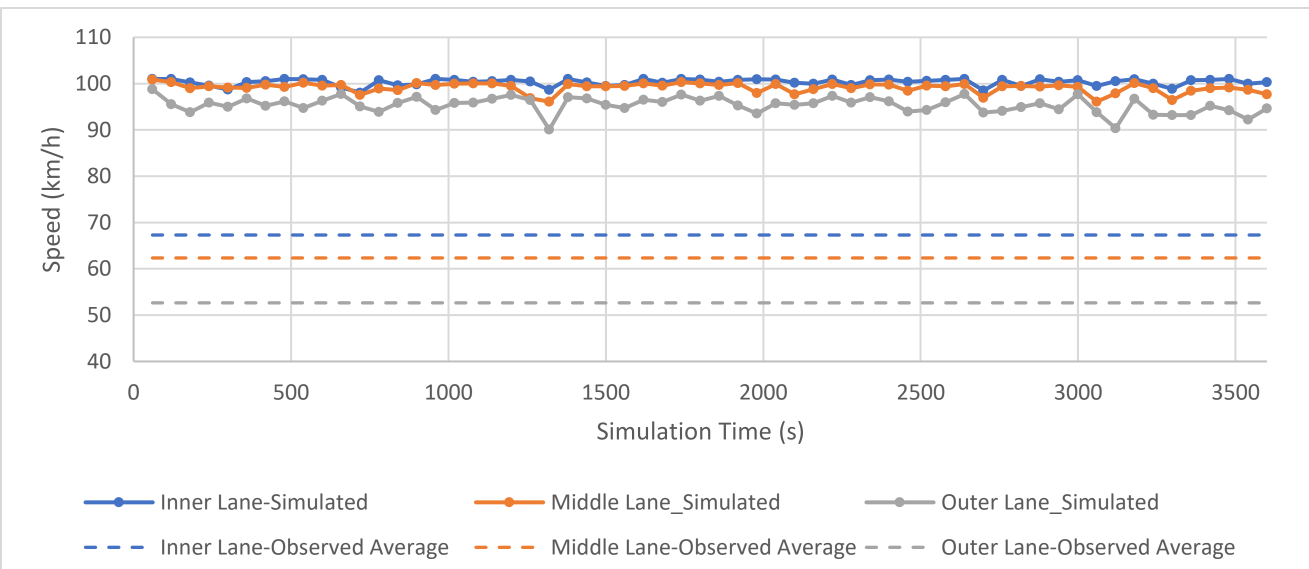

Figure 6-4: Lane speed before calibration

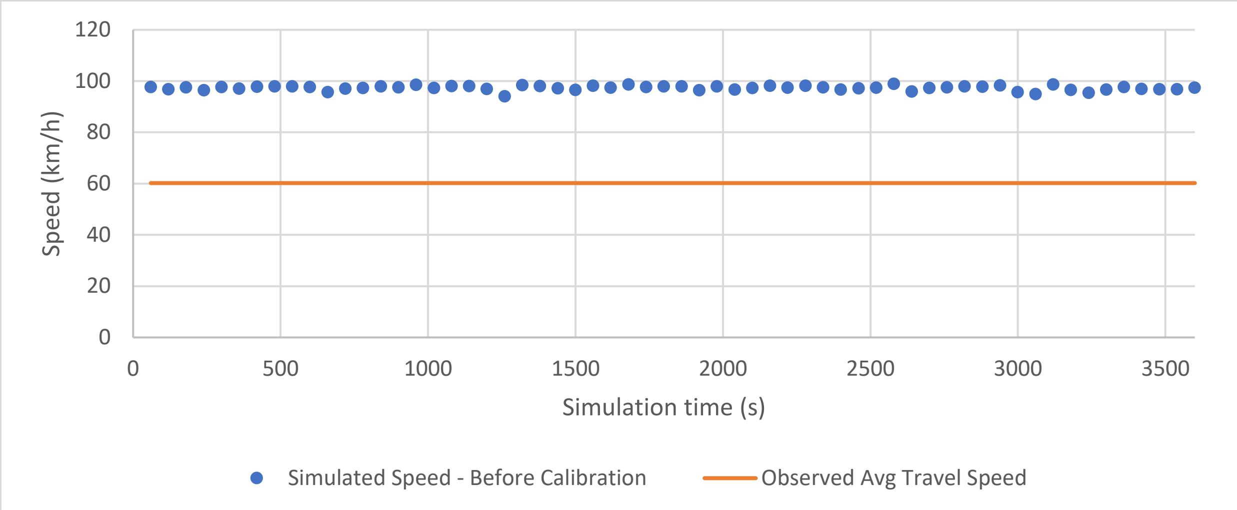

Figure 6-5: Average speed before calibration

The simulated speed and travel time are largely influenced by the desired speed corresponding to the specified speed limit. As discussed in Section 5.2.3, the posted speed limit on this section of road is 80km/h. This was therefore specified in the base model as shown in Figure 5-8 of Section 5.4.1.3. According to FOSIM, the desired speed corresponding to this speed limit ranges from 85km/h for heavy vehicles up to 100km/h for passenger vehicles. The simulated average speed of 99.77km/h thus attests to the fact that the speed in this model is governed purely by the desired speed. However, the significant disparity between the observed and simulated values indicates that notwithstanding the fact that the model parameters have not been calibrated, the existing model may not be taking cognizance of other local traffic operational elements which have a major effect on the speeds beyond just the desired speed alone.

A number of floating car runs performed over a period of three days also revealed that it is impossible for a vehicle to attain its desired speed over this section of road during the morning peak hour for at least three reasons. Firstly, the starting point of the analysis section follows shortly after the Liesbeek Parkway (M57) on-ramp and the Main Road (M4) off ramp. The high traffic volumes coming from the Liesbeek parkway joining the N2 combined with the high volumes (especially minibus taxi and buses) taking the Main Road off-ramp from the N2 causes major capacity problems along this road. This capacity constraint is exacerbated by the short weaving length (approximately 150 meters) available between the two ramps. Vehicles entering the analysis section are thus driving at a speed significantly lower than the desired speed as they are recovering from the bottleneck and shockwaves caused by the weaving section. The model is, however, unaware of the effects of these preceding sections since they are outside the limit of the analysis. Secondly, once the vehicles have entered the analysis section, in addition to recovery from the congested weaving section, drivers also need to sort by weaving to the appropriate lane, depending on their desired destination. The drivers whose destination is the M3 need to sort to the outer left lane while those proceeding to Cape Town mostly sort to the right and centre lanes. Finally, vehicles continuing to Cape Town must prepare to navigate a sharp curve, with reduced sight distance due to the bridge abutments and retaining structures as well as an uphill climb at Hospital Bend.

All these are factors which influence driver's perceptions and behaviour as well as vehicle performance. For the model to take account of these factors, some local calibration was necessary to ensure a more realistic base model prior to the calibration of vehicle and driver parameters. To this end, the speed suppression function - introduced and discussed in detail in Sections 3.2 and 3.8 was explored. This enabled the incorporation of local effects, which the model could not, otherwise, explicitly model. The results of these adjustments are discussed in the section below.

6.2 Local Calibration

Figure 6-7 below shows the observed and simulated traffic volumes following the speed suppression application. The adjustment of local conditions changed the simulated volumes, such that they no longer mimicked the observed volumes as closely as they did in the initial model. In comparison to Figure 6-1, many of the simulated data points no longer coincide with those observed in the field. Consequently, the GEH statistic increased from an average of 2 in the previous model to 4.56. Furthermore, the GEH statistic was less than 5 for only 63% of the cases, which is much lower than the 85% target – indicating that the model is therefore not acceptable when assessed against the established calibration acceptance criteria detailed in Table 5-5. Therefore, further calibration was necessary in order to reduce the average GEH statistic and standard error between the observed and simulated volumes.

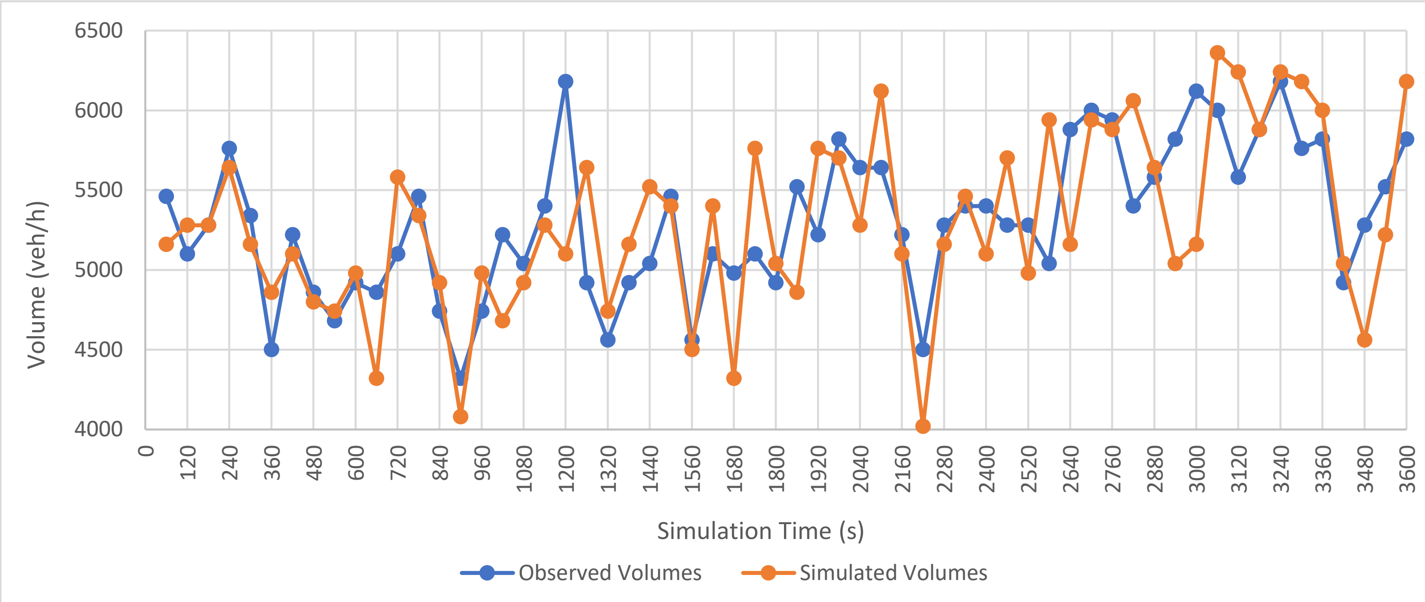

Figure 6-7: Observed and simulated volumes after local calibration

Given the above, it comes as no surprise that the regression model would have also deteriorated; with traffic volume data points moving further away from the line of perfect fit (diagonal line), thus exhibiting a low correlation between the two datasets. As illustrated in Figure 6-8 the R-squared value decreased from 0.88 in the previous model to 0.42 - a reduction by more than half.

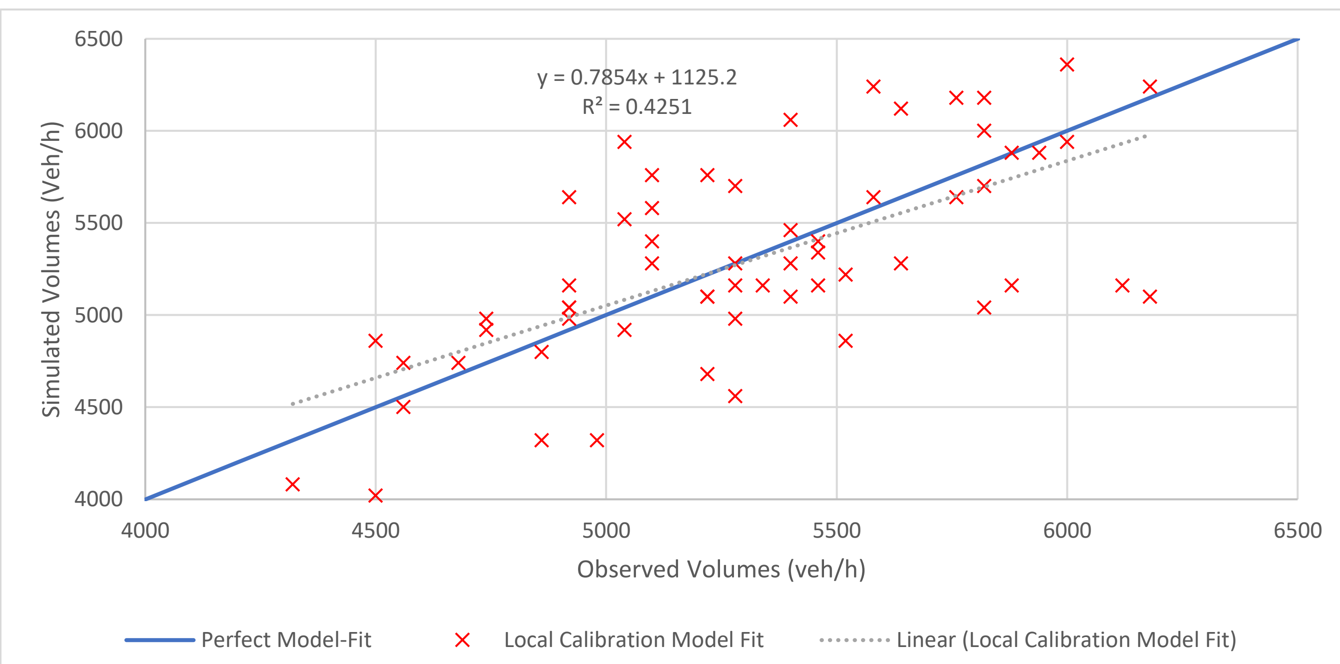

Figure 6-8: Traffic volume regression model after local calibration

While the initial model exhibited a significant disparity between the observed average and simulated measurements for both travel time and speed, the updated model showed an improvement, with the simulated average travel time increasing from 22.23 to 33.68 seconds, and the simulated speed decreasing from 99.77 to 60.2km/h. Figure 6-9 and Figure 6-11 illustrate average travel time and speed for the local calibration model and makes a distinction between the observed average and simulated data points.

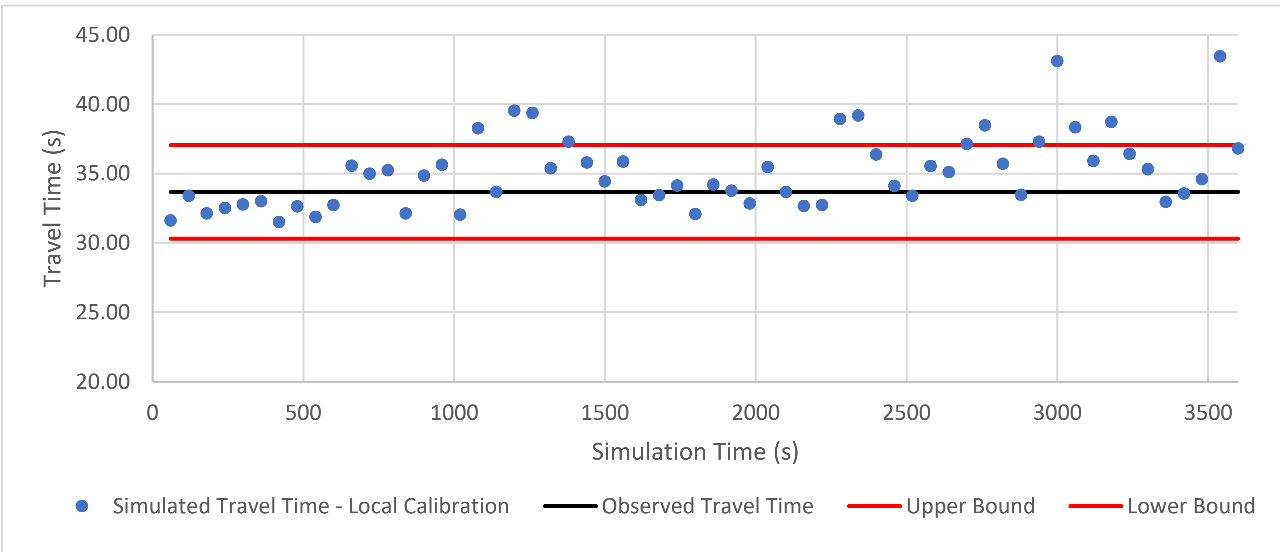

Figure 6-9: Average travel time after local calibration

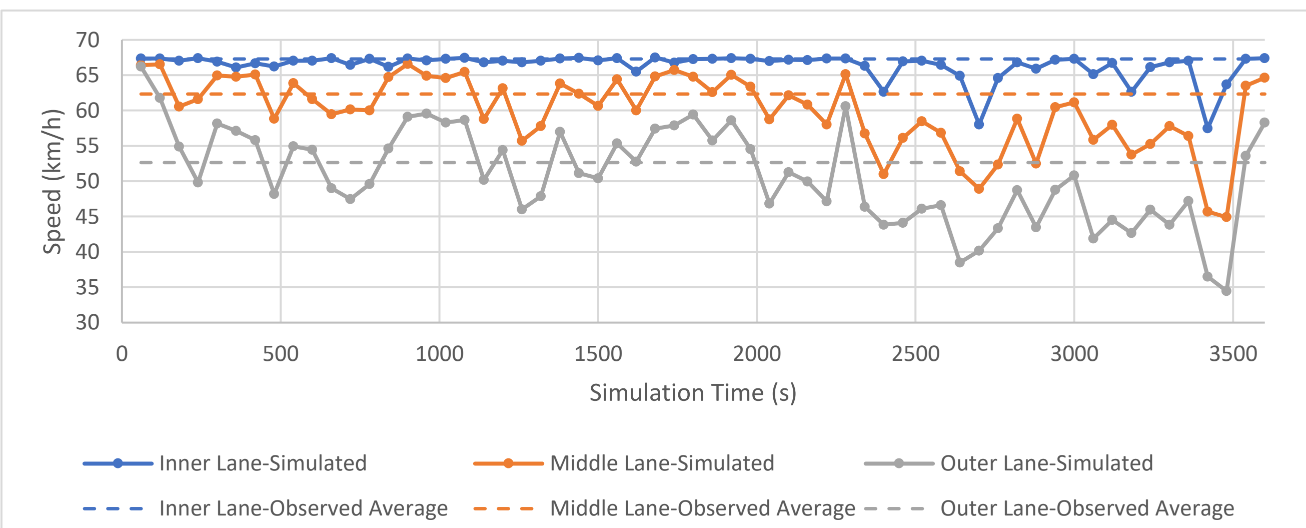

Figure 6-10: Lane speed after local calibration

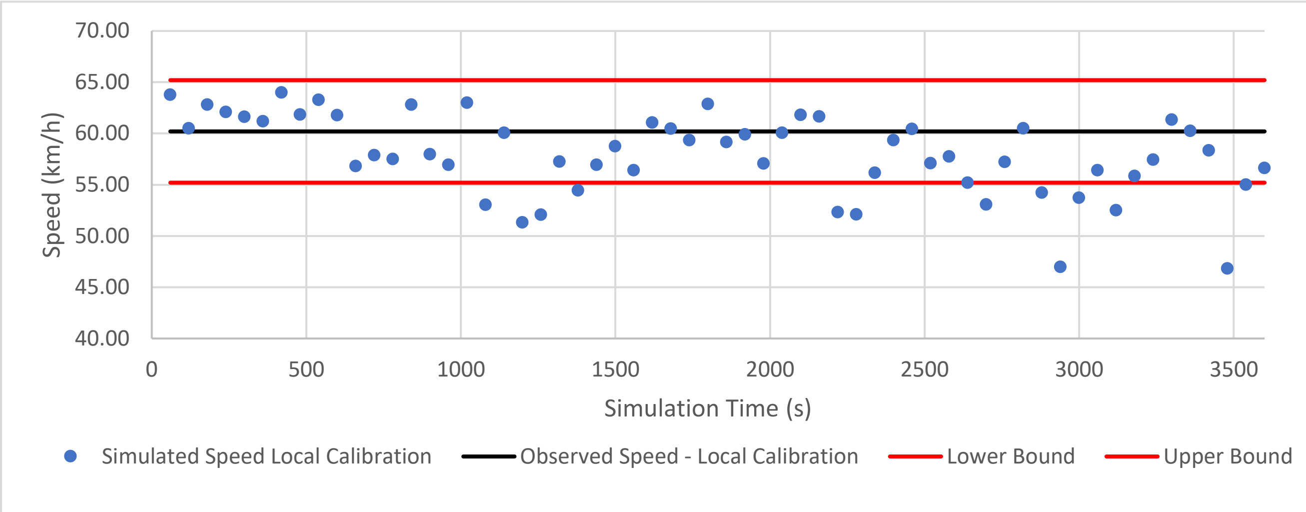

Figure 6-11: Average speed after local calibration

Figure 6-10 shows the simulated speed per lane, and the speed profiles are closer to the observed lane average in comparison to the uncalibrated model. Even though the travel time and speed results had improved compared to the previous model, some data point fell far from the observed average and did not meet the acceptance criteria set out in Table 5-5. The established acceptance criteria specifies that all simulated travel time data points must be within 10% of the observed average, while the speed needs to be within 5km/h of the observed average speed. These boundary vales are indicated with the red lines in Figure 6-11 and Figure 6-9. Since all three MoEs (volume, travel time and speed) did not meet the acceptance criteria, the model was advanced further by calibrating the default vehicle-driver parameters.

6.3 Parameter Calibration

The model parameters were adjusted through an iterative process discussed in Section 5.5.2. By repeatedly narrowing the parameter value search range, until it was small enough to yield an optimum value, many models were developed as a result. For illustration, this section discusses the best calibration model (prior to validation) resulting from the optimization process. The parameter values for this model are shown in Table 6-2. The values in red are those that have been fine-tuned and are thus different from the models presented previously.

As illustrated in Figure 6-12, the calibration model (referred to as Calibration-1) showed a significant improvement when compared to the local calibration model discussed above. The average GEH statistic for traffic volumes decreased from 4.56 to 2.2. Furthermore, the GEH statistic was less than 5 for 97% of the cases, which is well above the set acceptance criteria of 85% - indicating a good model-fit. The regression model in Figure 6-13 further confirmed this through an improved R-squared value of 0.82 compared to 0.42 on the model discussed previously.

Table 6-2: Calibrated parameter values before validation

Parameter	Unit	Low Limit	High Limit	Parameter Values	Type 1	Type 2	Type 3	Type 4
Max. positive jump in acceleration per second	m/s^3	0.1	10	Default	1	0.6	0.6	0.5
				Calibrated	4	3	2	2
Linear following factor	s	0.1	10	Default	0.56	0.72	1.25	2.08
				Calibrated	0.7	0.9	1.28	1.2
Max. acceleration	m/s^2	0.1	8	Default	4	2.4	2.4	1
				Calibrated	4	3.5	3	2
Max. following deceleration	m/s^2	-2	0	Default	-0.5	-0.5	-0.5	-0.5
				Calibrated	-0.2	-0.4	-0.2	-0.2
Max. lane change deceleration	m/s^2	-8	0	Default	-3	-2.4	-2.4	-2
				Calibrated	-1	-1.2	-1	-1
Vehicle length	m	3	26	Default	4.4	4	4	8
				Calibrated	4.8	5.2	6	12
Static following factor	m	0.1	8	Default	3	3	3	3
				Calibrated	1.2	1.2	1.2	1.2
Quadratic following factor	s^2/m	0	0.02	Default	0.005	0.005	0.005	0.005
				Calibrated	0.018	0.018	0.018	0.018

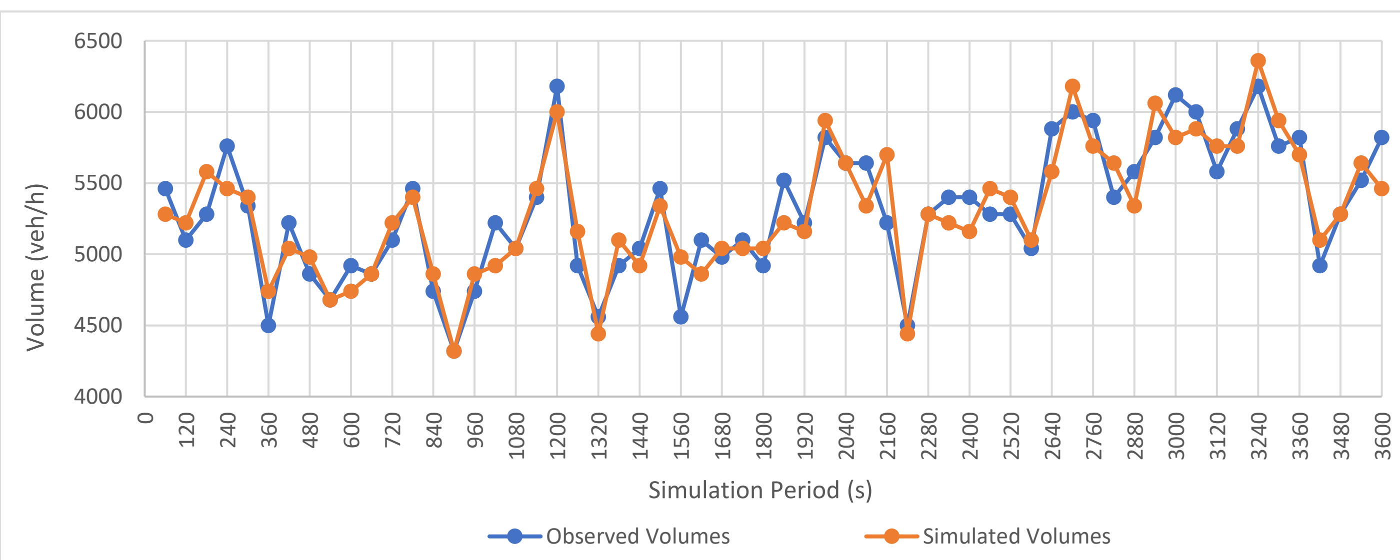

Figure 6-12: Observed and simulated volumes – Calibration-1

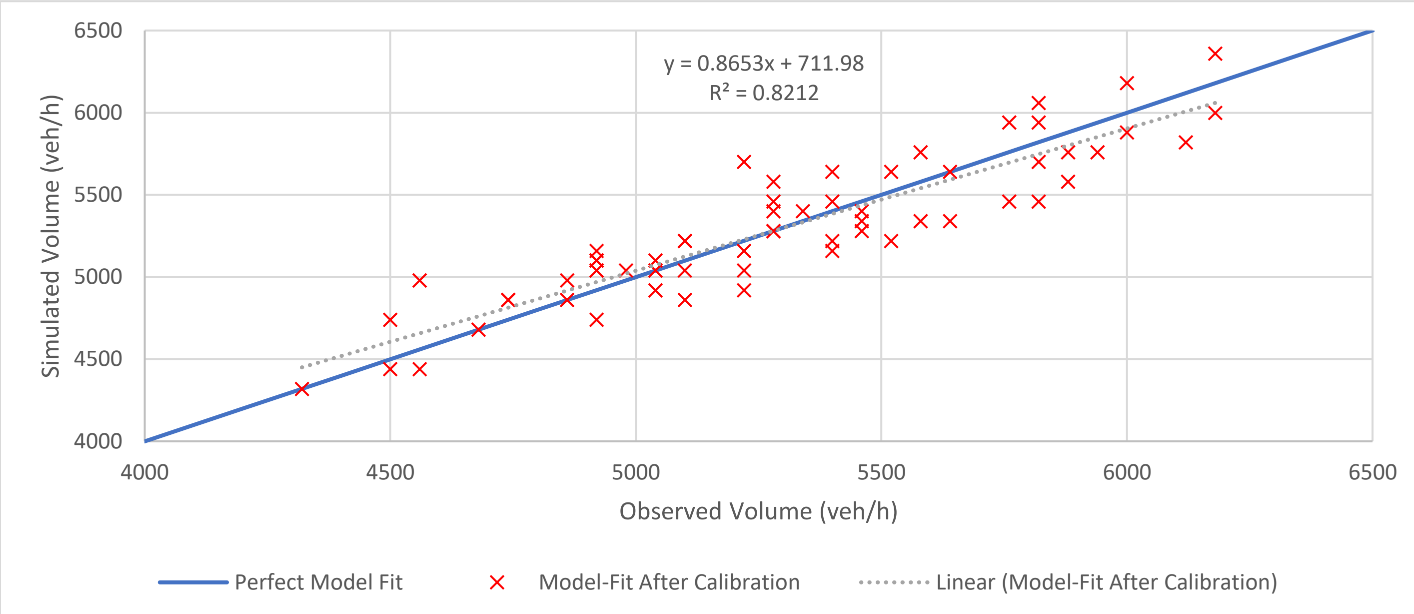

Figure 6-13: Traffic volume regression model – Calibration-1

Travel time and speed also showed improvement compared to the previous models. 98% of both the simulated travel time and speed measurements fell within the acceptance criteria, which is well above the 85% target. In the previous model, more than 20% of the data point fell beyond the acceptance criteria. Figure 6-14 and Figure 6-16 show the average travel time and speed results for the calibration model respectively, and Figure 6-15 shows the speed per lane. The average simulated travel time and speed are 33.89 seconds and 59.91 km/h respectively, while the average observed travel time and speed are 33.68 seconds and 60.2km/h respectively. Seeing that all three MoEs conformed to the acceptance criteria, the validation could commence.

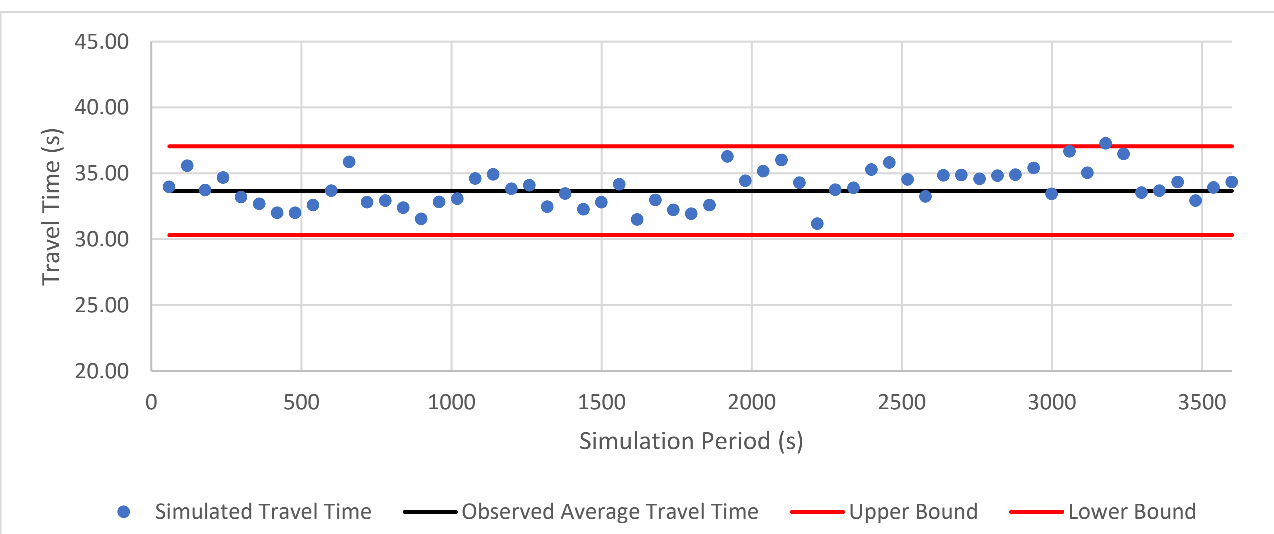

Figure 6-14: Average travel time – Calibration-1

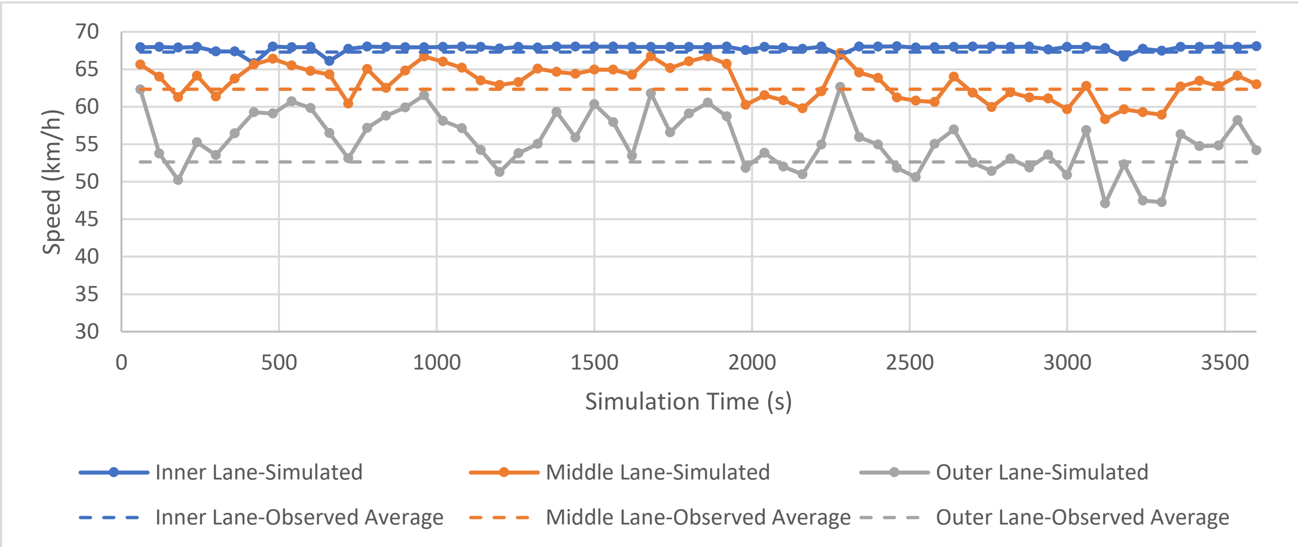

Figure 6-15: Lane speed - Calibration-1

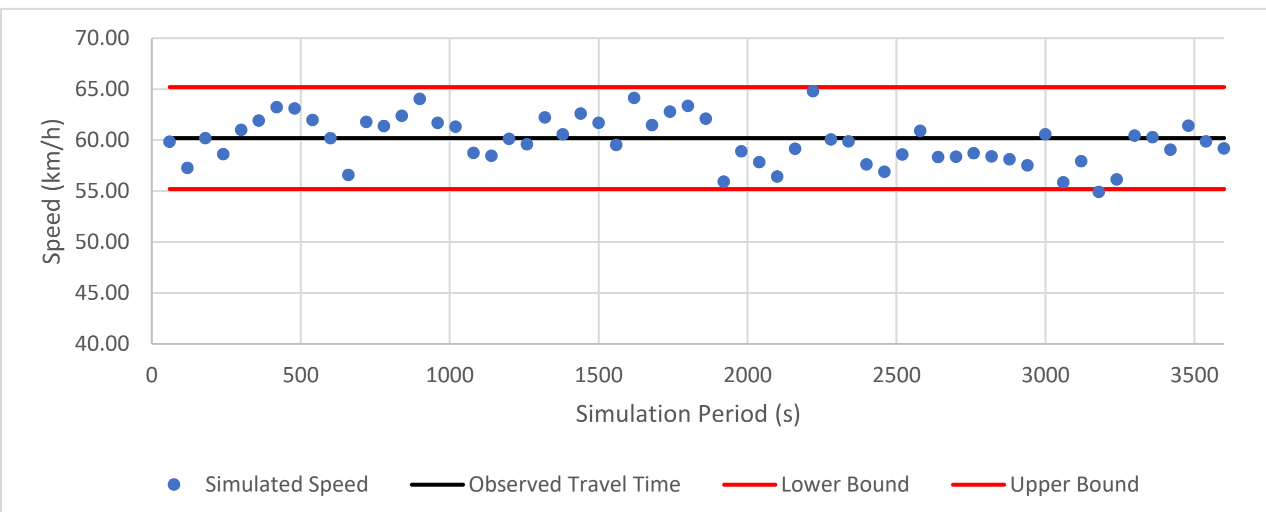

Figure 6-16: Average speed – Calibration-1

6.4 Validation

Even though the calibration process produced low GEH statistic values – thereby mimicking the field volumes quite closely, the true test would be to check if the same results could be maintained on a new set of field data. The optimum parameters obtained from the calibration model were thus applied on a different data set. This process would ultimately result in the validation of the model and justify its application in other scenarios. The results of the first validation model (Validation-1) are shown in Figure 6-17, Figure 6-18 and Figure 6-19.

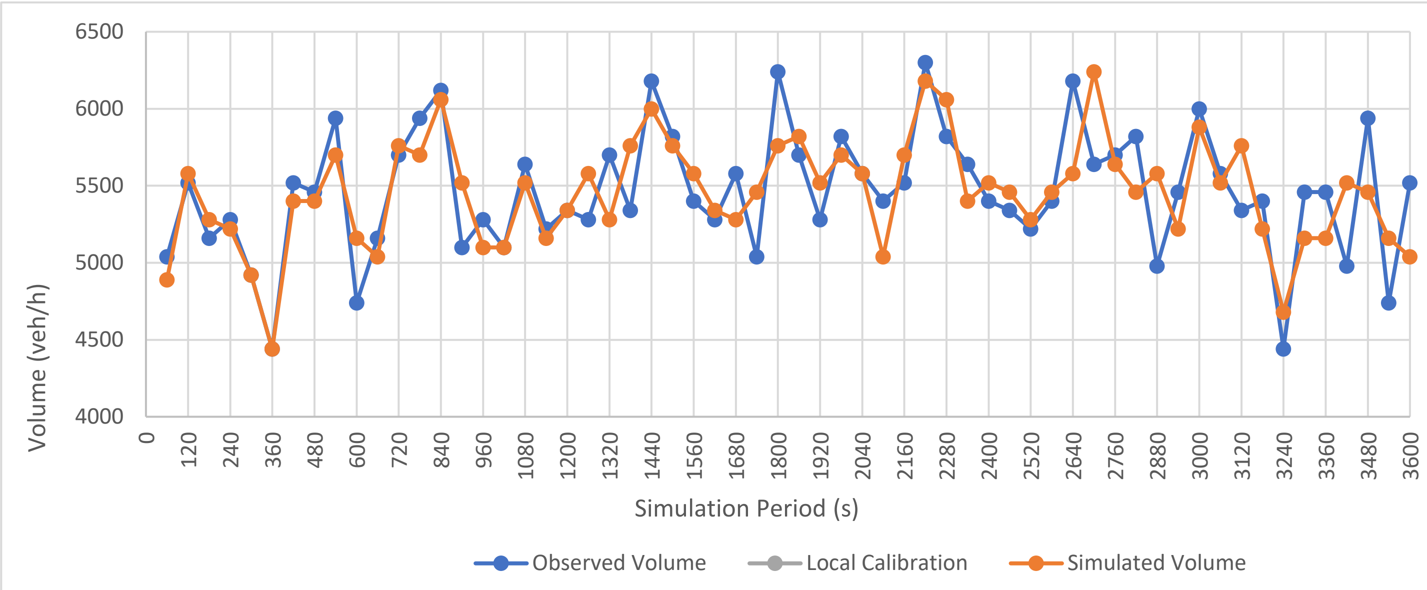

Figure 6-17: Observed and simulated volume - Validation-1

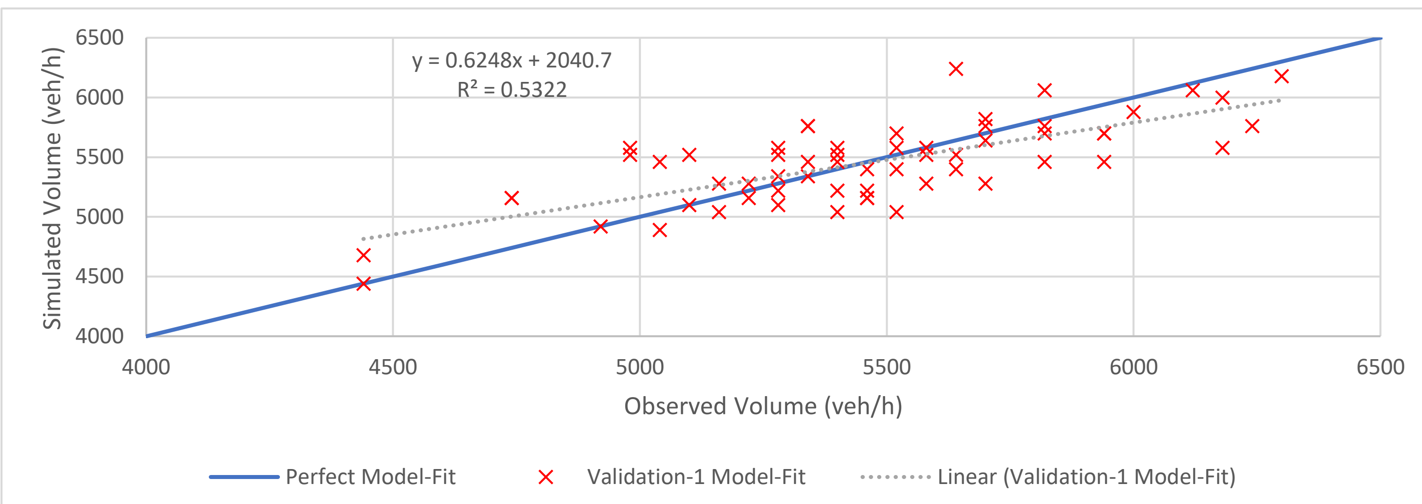

Figure 6-18: Traffic volume regression model - Validation-1

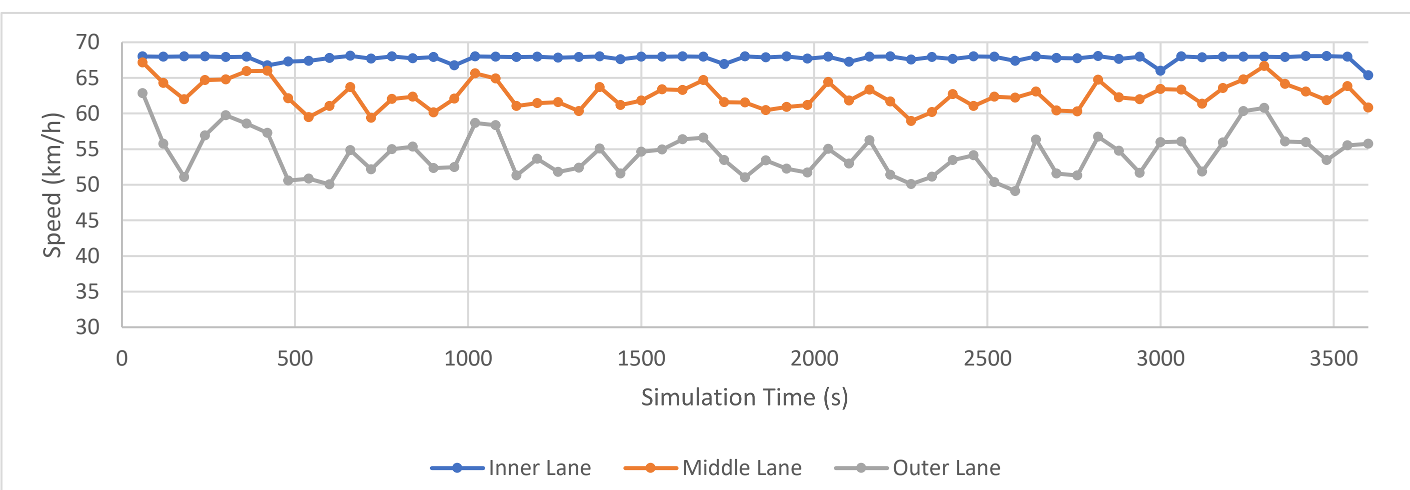

Figure 6-19: Lane speed - Validation-1

The first validation model produced acceptable travel time and speed results. However, it showed less explanatory power for traffic volumes compared to the calibration model. The average GEH statistic for the peak hour was 3 – which is still relatively low. However, it was less than 5 for only 77% of the cases – less than the 85% acceptance criteria. This implied that even though the model parameters produced a good model during calibration, they were not good enough to be applied on a different data set. A possible explanation for this is that the calibration parameters may have been overfitted. Which would imply that the parameters were adjusted to fit the calibration model too closely to the extent that it negatively impacted the model performance on a different set of data. In an attempt to model all variation and noise in the model, it masked any possible inaccuracies in the calibration data.

Since the first validation model did not sufficiently meet the acceptance criteria, the parameters in the calibration model were adjusted further until another optimal set of parameters was obtained. The new set of parameters was once again applied on the validation model and the output was compared with the empirical data to test the validity of the model. This was done until the set of parameters which produced acceptable calibration results also yielded acceptable validation results. Figure 6-20 and Figure 6-21 below indicate the results of the final validation model (Validation-2). This model did not only produce a good fit in terms of travel time and speed, but it also showed an improvement in reproducing the observed volumes. The average GEH reduced to 2.8 and the GEH was less than 5 for 85% of the cases, which meets the acceptance criteria. As shown in Figure 6-22 and Figure 6-24, the simulated travel time and speed were within the acceptance envelope. The lane speeds in Figure 6-23 also compare well with the average.

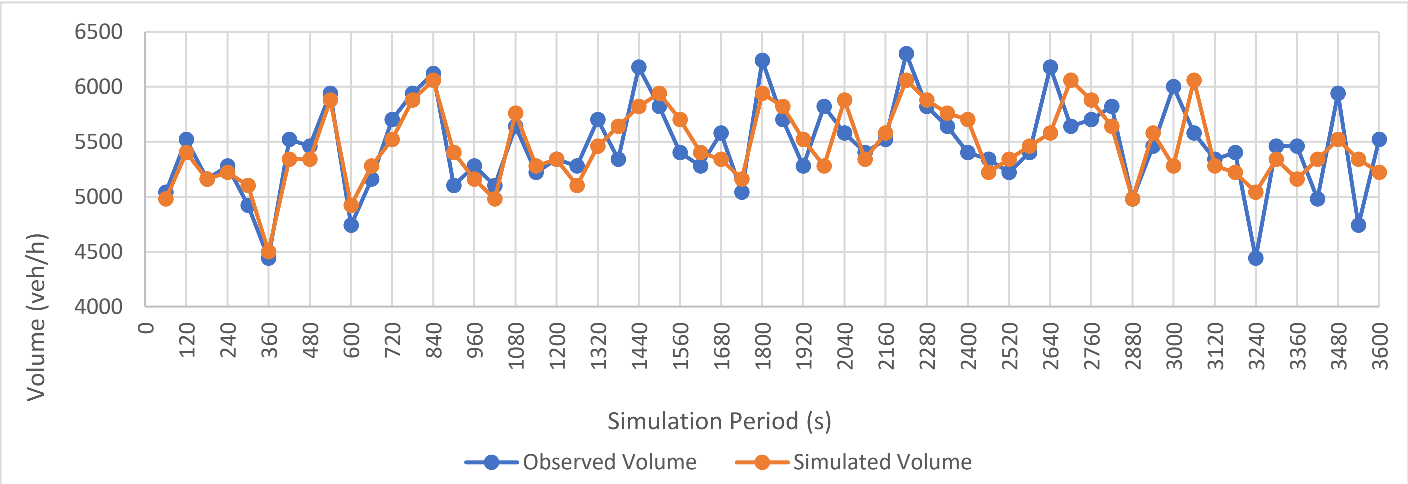

Figure 6-20: Observed and simulated volume - Validation-2

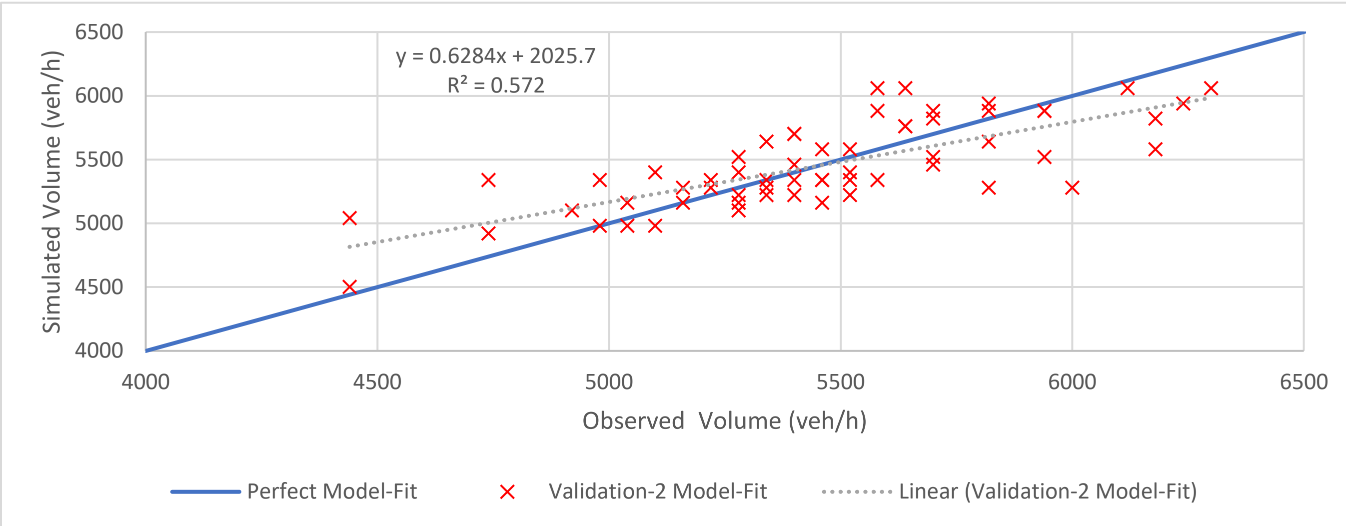

Figure 6-21: Traffic volume regression model - Validation-2

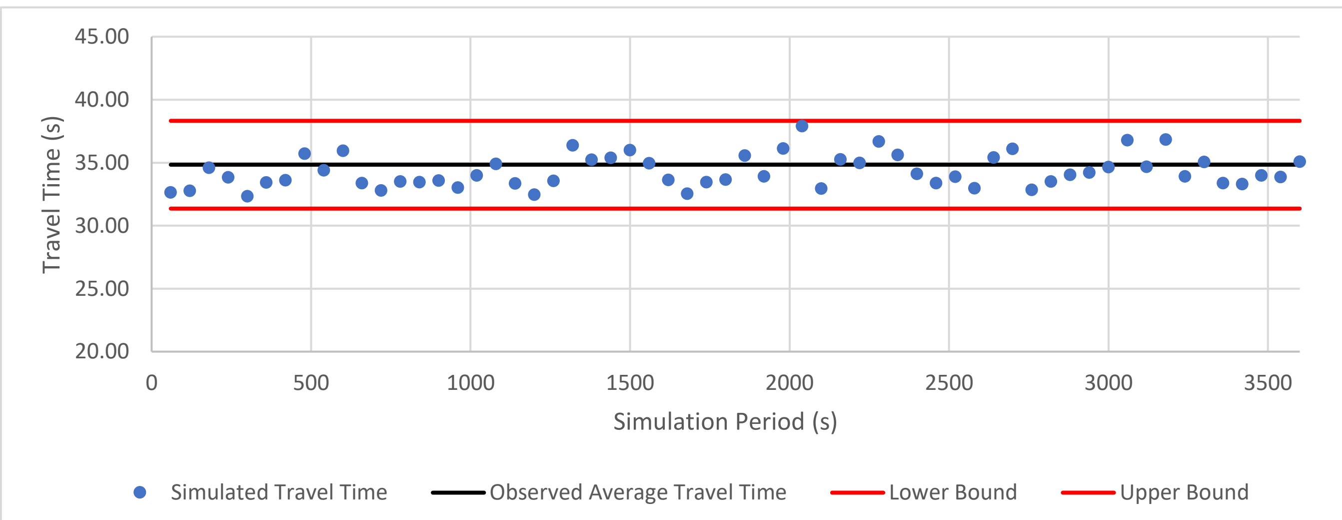

Figure 6-22: Average travel time - Validation-2

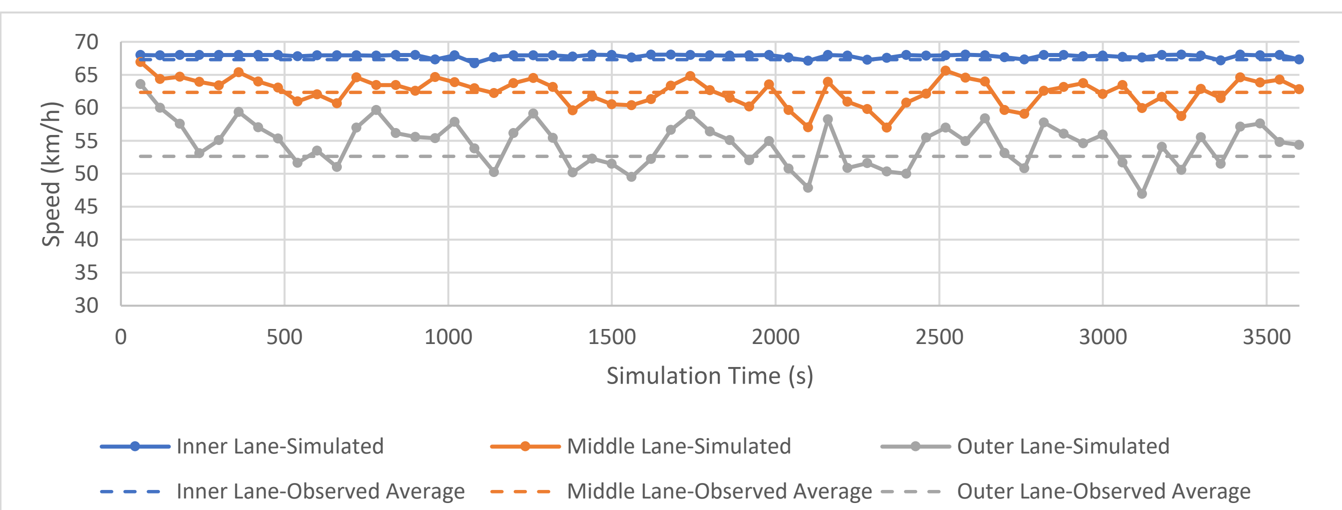

Figure 6-23: Lane speed - Validation-2

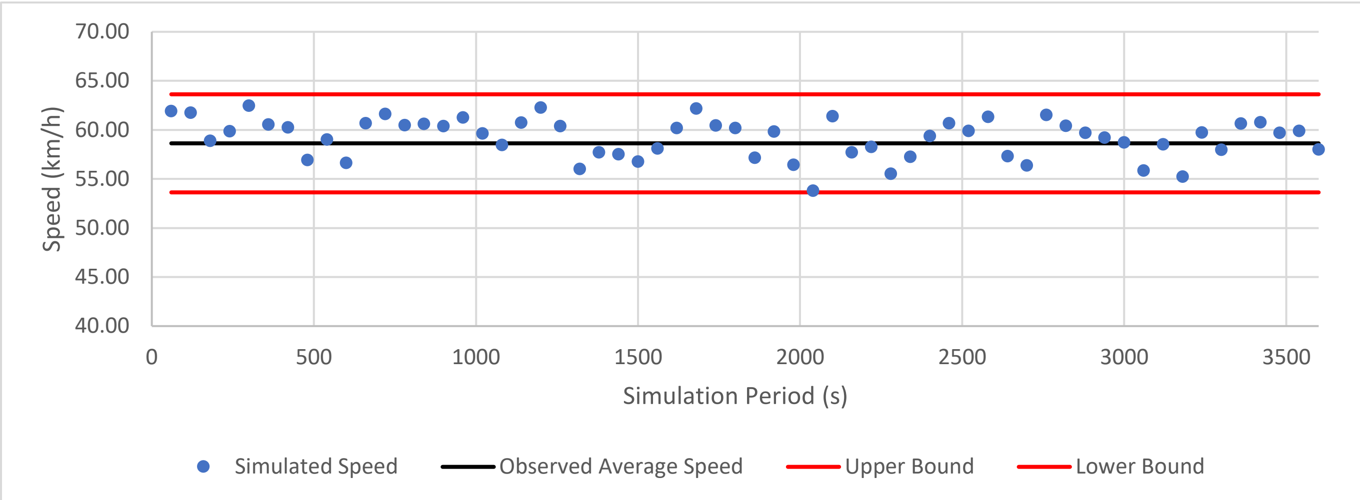

Figure 6-24: Average speed - Validation-2

6.5 Final Calibration Results

As mentioned previously, the failure of the initial calibrated model in producing an acceptable validation model implied that the obtained set of parameters in the Calibration-1 model needed to be optimized further. The calibration re-optimization produced a new set of parameters and MoE results for the updated model. These are illustrated in Figure 6-25 and Figure 6-26.

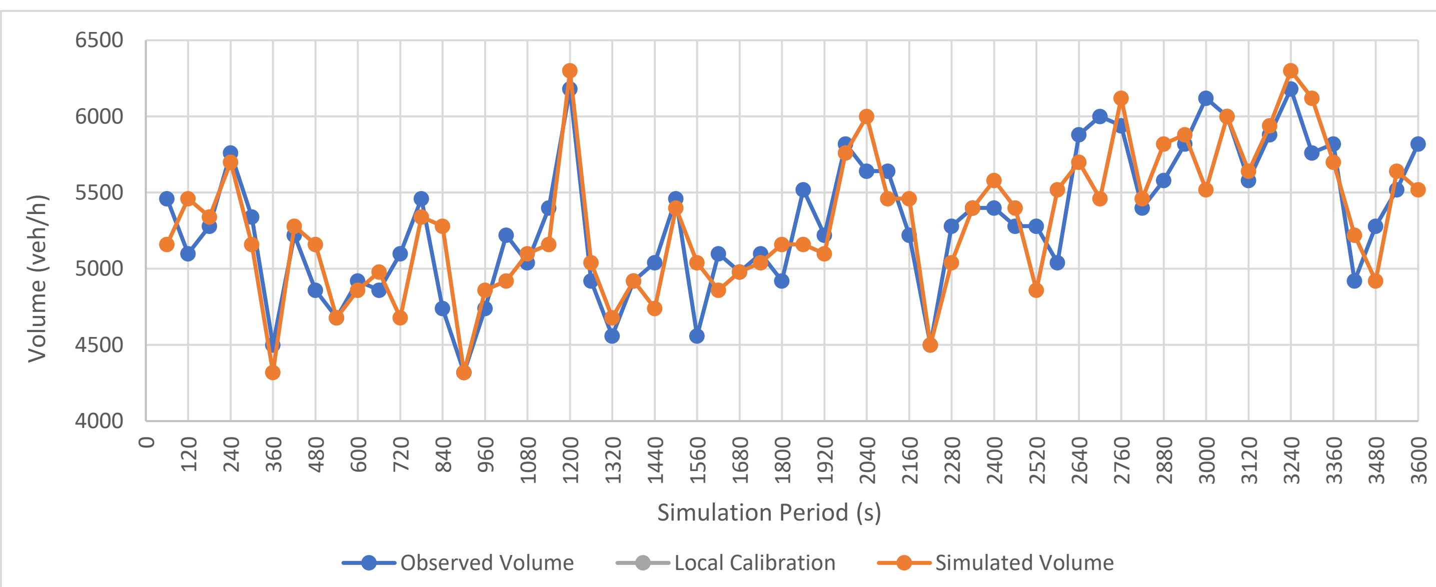

Figure 6-25: Observed and simulated volume - Calibration-2

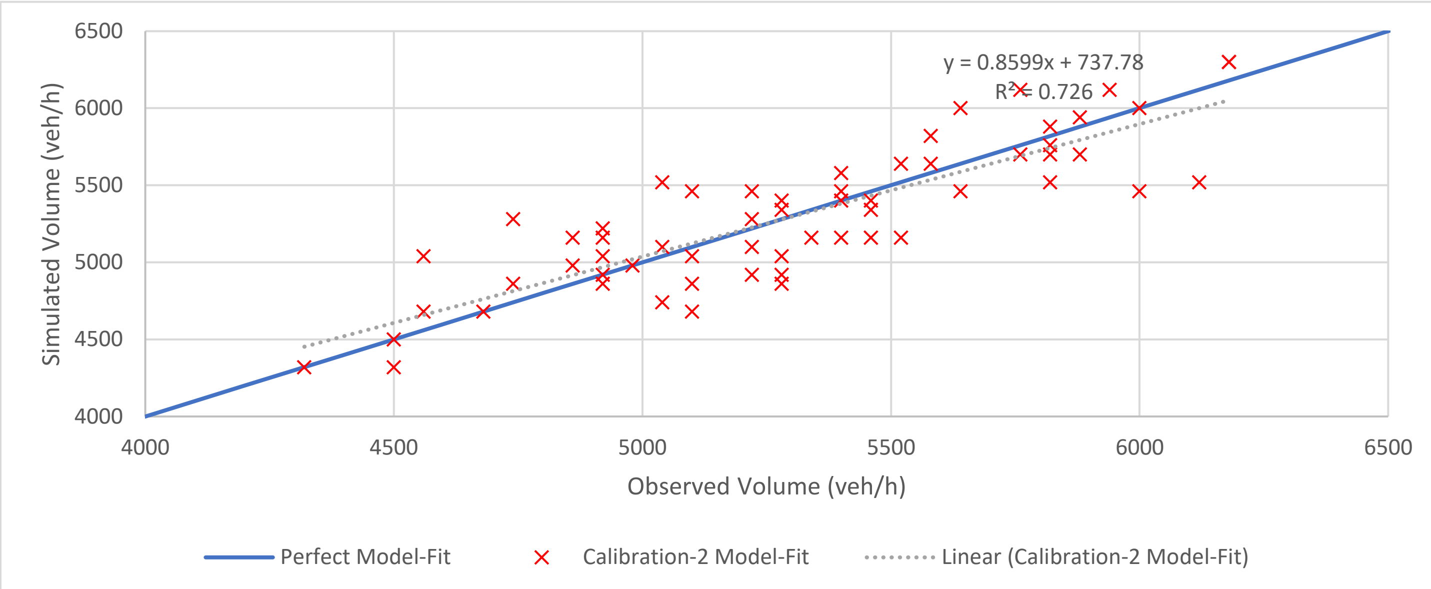

Figure 6-26: Traffic volume regression model - Calibration-2

The final calibration model had an average GEH of 2.6 during the peak hour and produced GEH less than 5 for 87% of the simulated values, this is higher than the 85% target – indicating that this model can be accepted as being valid. The travel time and speed as shown in Figure 6-27 ad Figure 6-29 were within 10% and 5km/h respectively for 100% of the simulated values. This is higher than the 85% target, thereby further confirming the validity of the model, even though the simulated speeds for the outer lane in Figure 6-28 are slightly higher than the average.

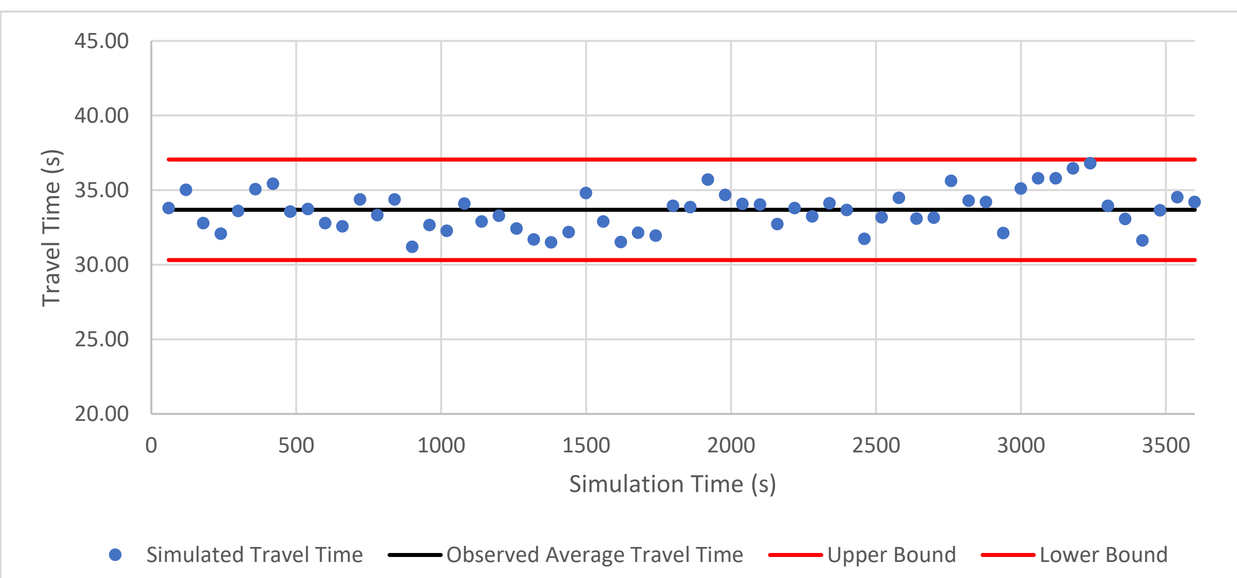

Figure 6-27: Travel time - Calibration-2

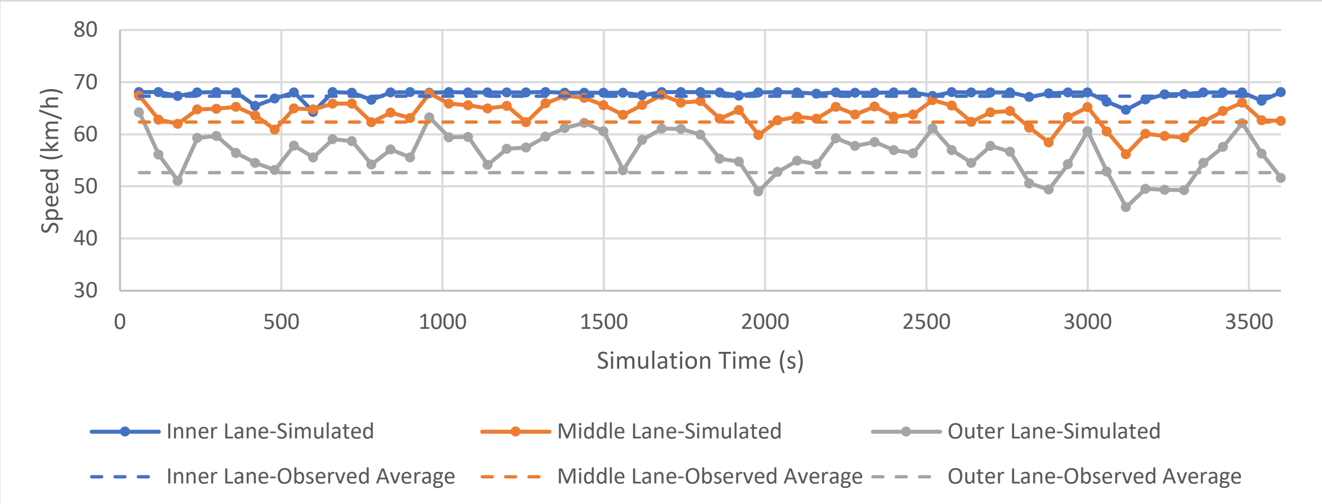

Figure 6-28: Lane speed - Calibration-2

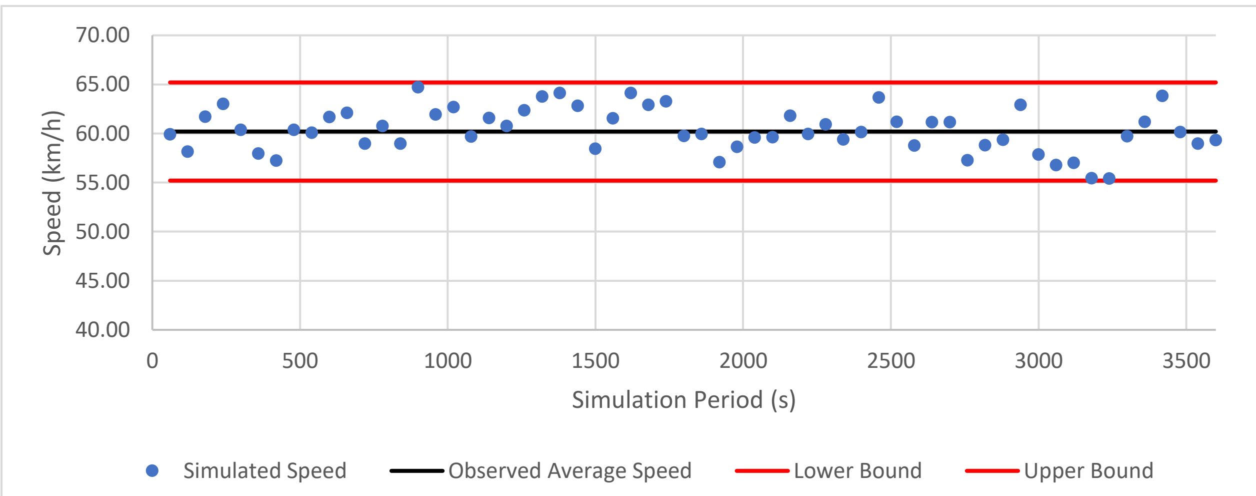

Figure 6-29: Speed - Calibration-2

All lane speeds above consistently show that the inner lane has higher and uniform speed profile, while the middle and outer lanes have lower speeds and fluctuating profiles. This confirms that most of the weaving occurs between the middle and outer lane, with vehicles wishing to take the M3 off-ramp often merging late and causing a disturbance and shockwaves in the outer lane, thus resulting in low and flatulating speeds and reduced capacity in both lanes. On the other hand, vehicles from the Liesbeek Parkway and N2 upstream, wishing to go to town move to the inner lane in order to avoid merging traffic in the middle and outer lane and drive at a higher and more uniform speed, since this lane experiences less disturbance.

Table 6-3 provides a list of the final parameter values after calibration and validation, while Table 6-4 shows a comparison of the three main model, the default, calibrated and validated models. The parameter in red signifies a change from the previous model. Parameters which were excluded from the list below were not included in the calibration and their default values were thus maintained. As mentioned previously, these parameters were excluded for one of two reasons; the first being that they were not applicable to this model as they are relevant for networks with specific features such as traffic lights or narrow lanes. The second reason pertained to the result of the sensitivity analysis, which demonstrated that some of the parameters did not influence the model output.

Table 6-3: Final calibration parameters

Parameter	Unit	Low Limit	High Limit	Parameter Values	Type 1	Type 2	Type 3	Type 4
Max. positive jump in acceleration per second	m/s^3	0.1	10	Default	1	0.6	0.6	0.5
				Calibrated	4	3	2	2
Linear following factor	s	0.1	10	Default	0.56	0.72	1.25	2.08
				Calibrated	0.7	0.9	1.28	1.2
Max. acceleration	m/s^2	0.1	8	Default	4	2.4	2.4	1
				Calibrated	4	3.5	3	2
Max. following deceleration	m/s^2	-2	0	Default	-0.5	-0.5	-0.5	-0.5
				Calibrated	-0.2	-0.4	-0.2	-0.2
Max. lane change deceleration	m/s^2	-8	0	Default	-3	-2.4	-2.4	-2
				Calibrated	-1	-1.2	-1	-1
Vehicle length	m	3	26	Default	4.4	4	4	8
				Calibrated	4.8	5.2	6	12
Static following factor	m	0.1	8	Default	3	3	3	3
				Calibrated	1.1	1.1	1.1	1.1
Quadratic following factor	s^2/m	0	0.02	Default	0.005	0.005	0.005	0.005
				Calibrated	0.018	0.018	0.018	0.018

Interestingly, Type 2 (minibus taxi) vehicle-driver combination exhibited higher values compared to Type 1 (passenger vehicle) for a few parameters. This is even though minibus taxis are larger and heavy-laden, which should make them less agile. Linear following factor, maximum following deceleration and maximum lane change deceleration are the three parameters which exhibit this phenomenon. These parameter values are a testament of the nature of minibus taxis in South Africa, which are generally characterized by their propensity for aggressive behaviour such as tailgating and cutting through one or more lanes in front of other vehicles. On the one hand, the high linear following factor speaks to the fact that minibus taxis accept smaller time headways by following too close behind the leading vehicle. On the other hand, high maximum following deceleration and maximum lane change deceleration speak to small gap acceptance and abrupt lane change behaviour.

Looking at the results presented in this chapter, one can clearly see that the model was gradually improved through an iterative process when compared to the first two models presented, that is, the default model and local calibration model. Interestingly, the model output prior to calibration showed a good fit when checked against traffic volumes only – with a GEH less than 5 for 97% of the simulated values – far higher than the 85% target and an R-squared value of 0.88. However, the simulated speed and travel time were significantly different from the field-measured average. This illustrates the danger of identifying the “best” parameter set based only on a single MoE – thereby highlighting the need to explore more MoEs to increase the explanatory power of the model on a wider range of metrics, thus providing a more representative set of parameters and an accurate model. Furthermore, the model shows that engineering judgement and a knowledge of local traffic conditions is paramount in identifying some of the major discrepancies in the model output.

Another clear distinction can be observed between Calibration-1 and Calibration-2 models. Calibration-1 being the model with the “best” parameters prior to validation, while Calibration-2 represent the model output after the validation process. Comparing Figure 6-12 and Figure 6-13 with Figure 6-25 and Figure 6-26, one can observe that Calibration-1 model exhibited a higher match in observed and simulated volumes than Claibration-2 model. While Calibration-1 had a GEH of less than 5 for 97% of the simulated values, Calibration-2 had a GEH of less than 5 for only 87% of the simulated volumes (a 10% difference). Similarly, the R-squared value decreased from 0.82 in Calibration-1 model to 0.72 in Calibration-2 model. This observation illustrates the importance of the validation process. Without, applying the parameter set obtained in the calibration process, it’s difficult to argue that the model would be valid in cases other than the data for which it was “trained”. This is because issues such as over-fitting of the model cannot be detected.

Table 6-4: Parameter comparison for the main models

Parameter	Unit	Low Limit	High Limit	Parameter Values	Type 1	Type 2	Type 3	Type 4
Max. positive jump in acceleration per second	m/s^3	0.1	10	Default	1	0.6	0.6	0.5
				Calibrated	4	3	2	2
				Validated	4	3	2	2
Linear following factor	s	0.1	10	Default	0.56	0.72	1.25	2.08
				Calibrated	0.7	0.9	1.28	1.2
				Validated	0.7	0.9	1.28	1.2
Max. acceleration	m/s^2	0.1	8	Default	4	2.4	2.4	1
				Calibrated	4	3.5	3	2
				Validated	4	3.5	3	2
Max. following deceleration	m/s^2	-2	0	Default	-0.5	-0.5	-0.5	-0.5
				Calibrated	-0.2	-0.4	-0.2	-0.2
				Validated	-0.2	-0.4	-0.2	-0.2
Max. lane change deceleration	m/s^2	-8	0	Default	-3	-2.4	-2.4	-2
				Calibrated	-1	-1.2	-1	-1
				Validated	-1	-1.2	-1	-1
Vehicle length	m	3	26	Default	4.4	4	4	8
				Calibrated	4.8	5.2	6	12
				Validated	4.8	5.2	6	12
Static following factor	m	0.1	8	Default	3	3	3	3
				Calibrated	1.2	1.2	1.2	1.2
				Validated	1.1	1.1	1.1	1.1
Quadratic following factor	s^2/m	0	0.02	Default	0.005	0.005	0.005	0.005
				Calibrated	0.018	0.018	0.018	0.018
				Validated	0.018	0.018	0.018	0.018

Just as underfitting produces a poor model, overfitting is also undesirable, because the model learns the details, noise and random fluctuations of the calibration data and accepts them as a concept to such an extent that it dents the model performance. In the observed scenario, these concepts do not always apply, so they pose a great hindrance to the model's ability to generalize when presented with new data. As a result, due to overfitting, a calibration model will not be able to achieve generalization, which means the model has limited applicability on new field data. In turn, this reduces the model's ability to discriminate patterns and predict correct results and could thus lead to catastrophic consequences in traffic infrastructure design and decisions.

Figure 6-30 shows a summary of the GEH statistic for the calibration models discussed above. The red straight line indicates the GEH of 5 while the rest of the curves show the different models from no calibration to the final calibrated model. The GEH statistic, a modified chi-squared statistic is an empirical formula that has proven useful in traffic modelling studies to compare modelled and observed traffic volumes by incorporating both relative and absolute differences. This is preferred as it avoids some pitfalls encountered when using simple percentages to compare two sets of volumes. For example, the analysis network in this study consists in mainline and off-ramp traffic – where the off-ramp traffic is only a fraction of that on the mainline. In these scenarios, it is generally difficult to choose a single variation percentage which is appropriate for both volumes because a specific level of percentage difference and absolute difference can have vastly different significance levels depending on the magnitude of the flows. Since GEH is non-linear, it reduces this problem by providing a practical self-scaling alternative. Thus, a single acceptance threshold based on GEH can be applied on a wider range of traffic scenarios.

The regression models presented in this chapter provide scatter plots of an indicative subset of the observed data and simulated output. Each of the points represent the field-observed traffic data plotted on the x-axis together with the corresponding simulated output value plotted on the y-axis. A diagonal line is drawn (at 45 degrees) to indicate the where the points would lie in the case of a perfect fit – this is where all the point would ideally lie. The goal behind a successful calibration model is to bring the observed and simulated points as close to the diagonal line as possible. In reality, it is unlikely that all the points will coincide with the diagonal line, however, the deviation of the points from the diagonal line in this study are well balance and distribute above and below the line, indicating that there is no bias in the models.

The regression models presented above make mention of the R-squared value on numerous occasions. Usually, the larger the R-squared, the better the regression model fits the data. However, this guideline comes with certain caveats, thus caution must be exercised when interpreting a regression model using R-squared only as a measure for a good fit. A high R-squared value does not necessarily imply that a model is good any more than a low value indicates a bad one.

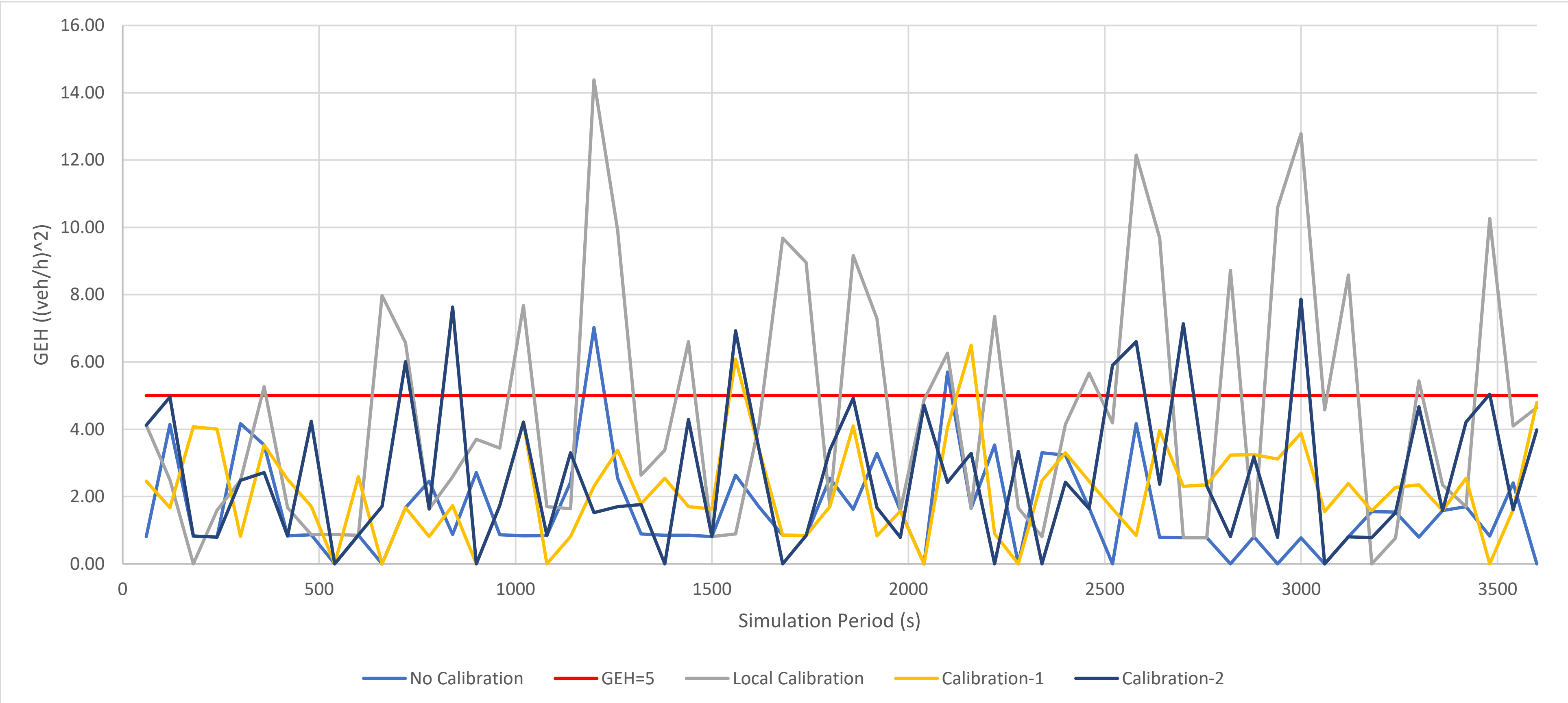

Figure 6-30: Summary of GEH values for different models

This research has already illustrated that high R-squared models could potentially suffer from other problems, such as overfitting. In other words, it is possible for a good model to have a low R-squared, while a biased model can have a high R-squared value. In fact, studies that try to explain human behaviour typically have R-squared values less than 0.5 (Ozili, 2023). These models possess an inherently greater amount of unexplainable variation since humans are simply harder to predict, compared to physical processes, for example.

Therefore, while a high R-squared is a good measure for initially facilitating comparisons between observed and simulated data, a more robust test would be to proceed further by assessing whether the regression model is statistically significant. A low R-squared can thus be accepted on condition that most of the explanatory variables are statistically significant. If this condition is not met, then the low R-squared model would not be accepted. All models in this study were tested for significance, regardless of the magnitude of the R-squared value. To illustrate, the statistical analysis for the model with the lowest R-squared presented in Figure 6-21 (Validation-2 model) is presented below. Table 6-5 provides the statistical table for the Validation-2 regression model and the values essential to testing the validity of the model are highlighted in red and discussed thereafter.

Table 6-5: Regression statistics - Validation-2 Model

Regression Statistics	
Multiple R	0.75627422
R Square	**0.57195069**
Adjusted R Square	0.56457053
Standard Error	222.165102
Observations	60

ANOVA

	df	*SS*	*MS*	*F*	*Significance F*
Regression	1	3825114.711	3825115	**77.49841**	**2.8037E-12**
Residual	58	2862725.289	49357.33		
Total	59	6687840			

	Coefficients	*Standard Error*	*t Stat*	*P-value*
Intercept	2025.72789	390.710876	5.184724	2.87E-06
X Variable 1	**0.62837005**	0.071378774	**8.803318**	**2.8E-12**

R-squared:

Answers the question: How much of the variance does this model explain?

In this instance 57.2% of the data can be explained by the model, which also means that 42.8% of the data cannot be explained by this model. As discussed above, this value does not imply that this model is unacceptable. Therefore, the analysis continues further to explore the F-statistic.

F-Statistic and Significance F:

Answers the question: Is this a good regression model?

In order to perform this test, the statement of hypothesis was formulated as follows:

H_0 – Null Hypothesis: The observed data variable model does not explain the variance in the simulated model any better than the intercept only model.

H_1 – Alternative Hypothesis: The observed data variable model does a better job (in a statistically significant way) of explaining the variance in the simulated model than the intercept only model.

The F-value for this model as indicated in Table 6-5 is 77.49. This value is higher than the F critical value at a 95% confidence interval (F-critical=1.53), which indicates some significance. The F value alone is, however, not sufficient in determining the significance of the model. It is important to remember that the F statistic is only one measure of significance which only compares the joint influence of all the variables together. A more complete test for significance takes account of the Significance F value (or p-value), which tests the probability that the model results could have emerged, due to random chance. In this case, the Significance F value of 2.80E-12 is smaller than any conventional level of significance - alpha (α), which implies that the observed data variable does indeed better explain the variance in the simulated model better than the intercept-only model and the null hypothesis thus ought to be rejected. In other words, if the level of significance is set to α=0.01, α=0.05 and α=0.10, the significance F value would still be smaller than all these values, therefore, the null hypothesis would be rejected in all three cases and the regression model deemed acceptable.

P-value:

Answers the question: Does the model have a good variable coefficient? Is there a relationship between the observed volumes and the simulated volumes?

The regression function shown in the plots above is of the following general form:

$$Y = \beta_1 x_1 + \beta_0 \qquad \textbf{6-1}$$

Where:

Y = Dependent variable

β_1 = Variable coefficient

x_1 = Independent variable

β_0 = Intercept

In order to test whether a relationship exists between the observed and simulated volumes, the statement of hypothesis was formulated as follows:

H_0: β_1 = 0 [No relationship between the observed and simulated values]

H_1 : β_1 coefficient is not equal to 0

The coefficient is tested by calculating the t-statistic and in turn, the t-statistic determines the p-value. Once again, the t value for this model is 8.8 which is larger than t- critical at a 95% confidence interval (t-critical =1.671) and the p-value of 2.8E-12 is smaller than any conventional level of significance, i.e., α=0.01, α=0.05 and α=0.10. Therefore, a relationship between the observed and simulated volumes does indeed exist and the null hypothesis is rejected.

Coefficient of slope

Answers the question: What is the nature of the relationship between the dependent and independent variable? Is it a positive or a negative relationship?

Since the equation has a positive slope, it is concluded that the relationship between the dependent and the independent variables is a positive one.

It can thus be concluded that the regression model as a whole is statistically significant based on the fact that the F-statistic and the coefficient tests show that the observed data contributes meaningful information in the prediction of the simulated values. The same tests were performed for each of the models discussed in this chapter and the results indicated that all regression models were statistically meaningful.

7. Conclusions

The primary objective of this research aimed at calibrating and validating a microsimulation model for a section of the N2 freeway using FOSIM. This would be achieved through the fine-tuning of default parameters until the model output aligned with the observed field measurements as close as possible, and then running a validation model to verify whether the model would be applicable in a different context. According to the quantitative and qualitative analysis of the available data and model output, it is concluded that the calibration and validation of the model was a success. In fact, the significance of the validation process is demonstrated in the differences between the calibration model before validation (Calibration-1) and after validation (Calibration-2). Even after many variations of parameters and iterations of the model, the calibration model maintained its validity, which speaks to the success of the technique applied.

The successful outcome of the study was achieved through a detailed series of steps, which have been sufficiently dealt with in the preceding chapters. Firstly, the aim and objectives of the research were established, and the relevant literature explored how similar studies have been done in the past. Secondly a detailed study of the FOSIM software was done in order to be better acquainted with its operations and limitations. A section of the N2 freeway between the M4 off-ramp and Hospital Bend (M3) in the inbound direction was selected as the analysis area of choice. Thereafter, the traffic counts were obtained from CCTV footage supplied by the Cape Town Freeway Management System and travel time and speed data obtained through floating car runs and supplemented by CCTV observations. Subsequently, the appropriate MoEs (volume, travel time & speed) were established based on the data available and the procedure and technique that the analysis would follow was set out. Prior to commencing with the calibration, a sensitivity analysis was performed to test the relative contribution of each parameter in the model output and the parameters which had no influence were excluded from the calibration. The model was then calibrated using a single-parameter search approach to determine the optimum range for each parameter. Finally, the model was validated, and the results were reported with the statistical analysis showing that the model was valid and acceptable.

The final calibration model (Calibration2) demonstrates a sufficiently calibrated model. This is evidenced by the fact that the observed and simulated traffic volume values plot close to one another and coincide in many instances, which directly address the research aim. The GEH statistic is testament of this with its value being less than 5 for 87% of the simulated values. Moreover, the R-squared value together with the statistical significance of the regression model further indicated that the model shows good explanatory power between the observed and simulated traffic volumes. In addition to this, the travel time and speed results demonstrated an excellent outcome with 100% of the data points falling within the acceptance limits.

Some differences were noted between the calibration model before and after validation. While on the one hand, Calibration-1 model exhibited extremely low GEH values and a strikingly high R-squared – thereby indicating a high correlation between the observed and simulated traffic volumes, Calibration-2 model data on the other hand, was slightly less fitting in comparison. The model-fit for Calibration-1 could only be attributed to overfitting since the possibility that it could have been obtained by random chance was ruled out after the model was tested for significance. As noted above, overfitting occurs when the model is fine-tuned to fit the current data and local traffic conditions so well that it fails to produce similarly good result when applied on a different data set. It is for this reason that one of the primary objectives of this research was to carry out a validation process of the calibrated model. Through validation, this research was able to verify whether the model actually achieves its intended purpose and if it could be generalized and applied in another context separate to that of calibration. This ultimately strengthened support for the calibration model and the reliability of its outputs.

The final list of the calibrated parameter values was presented, and the study showed that minibus taxis exhibited high linear following factor, maximum following deceleration and maximum lane change deceleration compared to passenger vehicles, which are smaller and lighter in weight. These findings demonstrate that minibus taxis accept smaller time headways as they tend to tailgate the leading vehicles – this was also observed on the CCTV footage. It also shows that minibus taxis accept smaller gaps for lane changes and are willing to apply the highest deceleration in order to perform a lane change.

This research demonstrated the importance of a sensitivity analysis in the calibration process. The sensitivity analysis determined the relative influence of model parameters, initial conditions, and other assumptions on the model. Through a sensitivity analysis, it was determined that not all the model parameters had a significant influence on the outcome of the model. Therefore, those parameters which were found to be of no significance to the overall accuracy of the model were omitted from the calibration process. As a result, the number of model parameters involved in the calibration was reduced by 36% - thereby reducing the time and calibration effort, which would have otherwise gone into calibrating these parameters. This was an iterative process which provided feedback that improved the model by comparing response variables from multiple model-runs.

In addition to the time saving benefit derived from conducting a sensitivity analysis, the methodology presented in this research has also shown that microscopic simulations can be achieved without the computational complexity and man hours, which are typically presented in other techniques. It challenged the conventional ideas about manual calibration processes being characterized by broad, time-consuming trial and error approach and the analyst’s experience, without exploring simple search function methods, which have the ability to narrow the search range for parameter values to the optimum. The establishment of a quicker and more accessible calibration approach is paramount as it offers an opportunity for transport agencies to easily evaluate the effects of proposed improvement on the road network before they could be implemented.

Another key finding demonstrated by this research was that the use of a single MoE as an assessment tool could have detrimental effects in the interpretation of the model output. The model output prior to calibration showed that it is possible for one MoE to fall perfectly within the acceptance range while another MoE fails completely. If the research only considered the MoE applicable in the former, the model could have been mistakenly accepted as being valid even though it was fundamentally flawed. The collection of more field data through floating car runs played a pivotal role in expanding the number of MoEs and ultimately producing a more representative and accurate model. However, there is a caveat that applies here because while the collection of more field data and increasing of MoEs might lead to a more accurate model result, an excessive number of MoEs could complicate the model due to the high computational effort and time required. The collection of field data is also a time-consuming and costly exercise, and the more MoEs are examined, the more field data collection would be required. The analyst thus needs to find an acceptable balance between these two competing needs.

In conclusion, the importance of microscopic model calibration to local conditions cannot be overemphasized. While it seems impossible to prescribe a fixed order in which model calibration and validation should be applied, and whereas practice shows that model calibration and validation techniques are applied in a haphazard manner, this research will hopefully stimulate analysts to pay more attention to the various aspects of calibrating and validating microscopic models and apply some of the techniques presented in this study. Based on this study, it is concluded that FOSIM is a useful tool which can be used for traffic management and operations.

8. Recommendations

The sensitivity analysis does not typically consider the potential calibration parameters' interactive effects when analysing the effects of extreme parameter values on the simulated results. For example, even though a number of parameters were not included in the calibration, since they did not exhibit any significant effects on the simulated model, when other values were held constant, the effect of those parameters could possibly be realized or strengthened when the other parameter values are changed at the simultaneously. Future studies should explore this interaction between parameters when conducting sensitivity analysis.

In addressing the issue of model overfitting, a question ought to be asked on whether it would be beneficial to find a way in which a model is calibrated to an optimal level of error, such that it establishes a parameter set, which might not necessarily offer the best possible model fit for a precise road and traffic condition, but can be generalized to provide an acceptable fit for a large network possessing similar characteristics. Future studies should develop a technique for establishing this optimal error which could produce a more widely applicable set of parameters.

With the availability of more data, future calibration of FOSIM should investigate the increase in spatial resolution of the study by extending the starting point beyond the Liesbeek Parkway off-ramp. This would enable the capturing of traffic operations at the termination of the BMT lane and the subsequent weaving of public transport vehicle moving from the inner lane to the outer lane to exit the freeway at the respective off ramps. The calibration would also account for the capacity drop near the on- and off-ramps caused by high traffic volumes from the Liesbeek Parkway and those exiting the N2 through the Main Road (M4) off-ramp, and the effect of the short weaving section between these two ramps. A longer could also eliminate the need of speed restriction in the model since downstream effects could be sufficiently measured.

This micro simulation model was successfully calibrated for a 3+1 (three-lane carriageway with one on-ramp) weaving section. However, other weaving interaction types with different traffic flow conditions might be different. FOSIM should, therefore, be calibrated for other locations with varying geometric features and weaving patterns, such as, 2+1 and 3+2 types to further improve the reliability of the FOSIM model.

References

Abaza, O., Arafat, M., & Uddin, M. S. (2019). *Survey and Economic Analysis of Pavement Impacts from Studded Tire Use in Alaska.* doi:FHWA-AK-RD-4000(175)

Alexiadis, V., Jeannotte, K., & Chandra, A. (2004). *Traffic Analysis Toolbox: Volume I: Traffic Analysis Tools Primer.* Department of Transportation. U.S: FHWA.

Ali, M. D., Zerpa, L. A., Kaisar, E. I., & Masters, K. O. (2018). Guidance for Identifying Corridor Conditions That Warrant Deploying Transit Signal Priority. *Transportation Research Board 97th Annual Meeting.* Washington D.C. doi:18-05194

Arafat, M., Nafis, S. R., Sadeghvaziri, E., & Tousif, F. (2020). A data-driven approach to calibrate microsimulation models based on the degree of saturation at signalized intersections. *Transportation Research Interdisciplinary Perspectives, 8*.

Barceló, J. (2010). *Fundamentals of Traffic Simulation.* New York: Springer.

Barcelo, J., & Casas, J. (2004). Methodological notes on the calibration and validation of microscopic traffic simulation models. *83rd Transportation Research Board Annual Meeting.* Washington, DC.

Ben-Akiva, M. E., Darda, D., Jha, M., Koutsopoulos, H. N., & Toledo, T. (2004). Calibration of microscopic traffic simulation models with aggregate data. *83rd TRB Annual Meeting.* Washington, DC.

Bloomberg, L., Swenson, M., & Haldors, B. (2003). Comparison of Simulation Models and the Highway Capacity Manual. *82nd Meeting of the Transportation Research Board.* Washington D.C.

Bourrel, E., & Lesort, J. B. (2003). Mixing Microscopic and Macroscopic Representations of Traffic Flow Hybrid Model Based on Lighthill-Whitham-Richards Theory. *Transportation Research Record: Journal of the Transportation Research Board, No. 1852* (pp. 193-200). Washington, D.C: Transportation Research Board of the National Academies.

Branston, D. (1976). Models of Single Lane Time Headway Distributions. *Transportation Science, 10*(2), 125-148.

Brockfeld, E., Kuhne, R. D., & Wagner, P. (2005). Calibration and Validation of Microscopic Models of Traffic Flow. *Transportation Research Record Journal of the Transportation Research Board*(1934), 179-187.

Buckley, D. J. (1968). A Semi-Poisson Model of Traffic Flow. *Transportation Science, 2*(2), 107-133.

Bullen, A. G. (1982). Development of Compact Microsimulation for Analyzing Freeway Operations and Design. *Transportation Research Record*(841), 15-18.

Burghout, W. (2005). *Mesoscopic Simulation Models for Short-Term Prediction.* PREDIKT Project Report.

Chander, R. E., Herman, R., & Montroll, E. W. (1958). Traffic Dynamics: Studies in Car Following. *Operations Research, 6*(2), 165-184.

Chanut, S., & Buisson, C. (2003). Macroscopic Model and Its Numerical Solution for Two-Flow Mixed Traffic with Different Speeds and Lengths. *Transportation Research Record: Journal of the Transportation Research Board, 1852*(1), 209-219.

Cheu, R. L., Jin, X., Ng, K. C., Ng, Y. L., & Srinivasan, D. (1998). Calibration of FRESIM for Singapore Expressway Using Genetic Algorithm. *Journal of Transportation Engineering, 124*(6), 526-535.

Chiappone, S., Giuffrè, O., Granà, A., Mauro, R., & Sferlazza, A. (2015). Traffic simulation models calibration using speed–density relationship: An automated procedure based on genetic algorithm. *Expert Systems With Applications, 44*, 147-155.

Chu, L., Liu, H. X., Oh, J. S., & Recker, W. (2004). A calibration procedure for microscopic traffic simulation. *83rd Transport Research Board Annual Meeting.* Washington, DC.

Ciuffo, B., & Punzo, V. (2010). Verification of traffic micro-simulation model calibration procedures: analysis of Goodness-of-fit measures. *89th Annual Meeting of the Transport Research Board*. Washington, D.C.

Ciuffo, B., Punzo, V., & Torrieri, V. (2008). Comparison of Simulation-Based and Model-Based Calibrations of Traffic-Flow Microsimulation Models. *Transportation Research Record: Journal of the Transportation Research Board*, *2088*(1), 36-44.

CORSIM User's Guide. (2006). *Federal Highway Administration*. Washington, D.C: U.S. Department of Transportation.

Cremer, M., & Ludwig, J. (1986). A Fast Simulation Model for Traffic Flow on the Basis of Boolean Operations. *Mathematics and Computers in Simulation*, *28*(4), 297-303.

Daganzo, C. F. (1994). The Cell Transmission Model: A Dynamic Representation of Highway Traffic Consistent with the Hydrodynamic Theory. *Transportation Research Part B: Methodological*, *28*(4), 269-287.

Daganzo, C. F. (2006). In Traffic Flow, Cellular Automata = Kinematic Waves. *Transportation Research Part B: Methodological*, *40*(5), 396-403.

de Leeuw, M., & Dijker, T. (2000). *Praktijkstudies fosim 4.* Delft, Netherlands: Delft University of Technology. doi: 0920-0592

del Castillo, J. M. (2012). Three New Models for the Flow–Density Relationship: Derivation and Testing for Freeway and Urban Data. *Transportmetrica*, *8*(6), 443-465.

Dijker, T., Bovy, P. H., & Vermijs, R. G. (1997). *Car-following under Non-congested and Congested Conditions.* Netherlands: Delft University of Technology.

Ding, L. (2003). *Evaluation of ITS Technologies In South Jersey Priority Corridor Project.* Masters Thesis, Rutgers, The State University of New Jersey.

Dowling, R., Skabardonis, A., & Alexiadis, V. (2004). *Traffic Analysis Toolbox Volume III: Guidelines for Applying Traffic Microsimulation Software.* Washington, D.C: Federal Highway Administration (FHWA).

Dowling, R., Skabardonis, A., Halkias, J., McHale, G., & Zammit, G. (2004). Guidelines for calibration of microsimulation models: framework and application. *83rd Transport Research Board Annual Meeting.* Washington, D.C.

Drake, J. S., Schofer, J. L., & May, A. D. (1967). A Statistical Analysis of Speed-Density Hypotheses in Vehicular Traffic Science. *Highway Research Record Proceedings, 154*, 112-117.

Drew, D. R. (1968). *Traffic Flow Theory and Control.* New York: McGraw-Hill Book Company.

Drud, A. S. (1994). CONOPT—A Large-Scale GRG Code. *ORSA Journal on Computing, 6*(2), 207-216.

Druitt, S. (1998). An Introduction to Microsimulation. *Traffic Engineering and Control, 39*(9), 480-483.

Edie, L. C. (1961). Car-Following and Steady-State Theory for Noncongested Traffic. *Operations Research, 9*(1), 66-76.

Espejel-Garcia, D., Saniger-Alba, J., Wenglas-Lara, G., Espejel-Garcia, V., & Villalobos-Aragon, A. (2017). A Comparison among Manual and Automatic Calibration Methods in VISSIM in an Expressway (Chihuahua, Mexico). *Open Journal of Civil Engineering*, *7*(4), 539-552.

Fritzsche, H. (1994). A Model for Traffic Simulation. *Traffic Engineering & Control, 35*(5), 317-321.

Gardes, Y., May, A. D., Dahlgren, J., & Skabardonis, A. (2002). Freeway Calibration and Application of the PARAMICS Model. *81st Transportation Research Board Meeting.*

Gazder, U., Saleh, M. H., Al Zoubi, Y. M., Mohammed, O., & Alhalabi, K. A. (2019). Calibrating Traffic Microsimulation Model for Bahrain and Estimating Traffic Impacts of a Mall on Road Network. *International Journal of Computing and Digital Systems, 8*(5), 516-523.

Gazis, D. C., Herman, R., & Rothery, R. W. (1961). Nonlinear Follow-The-Leader Models of Traffic Flow. *Operations Research, 9*(4), 545-567.

Gerlough, D. L., & Matthew, H. J. (1975). *Traffic Flow Theory: A Monograph.* Special Report 165, Transport Research Board, National Research Council, Washington D.C.

Gipps, P. G. (1981). A Behavioural Car-Following Model for Computer Simulation. *Transportation Research Part B: Methodology, 15*(2), 105-111.

Gipps, P. G. (1986). A model for the structure of lane-changing decisions. *Transportation Research Part B: Methodological, 20*(5), 403-414.

Glover, F. (1997). A Template for Scatter Search and Path Relinking in Artificial Evolution. *Third European Conference on Artificial Evolution* (pp. 3-57). Berlin, Heidelberg: Springer-Verlag.

Goldberg, D. E. (1989). *Genetic Algorithms in Search, Optimization and Machine Learning.* Boston, MA: Addison-Wesley Publishing.

Greenshields, B. D., Bibbins, J. R., Channing, W. S., & Miller, H. H. (1935). A Study of Traffic Capacity. *Highway Research Board Proceedings, 14,* 448-477.

Greenshields, B. D., Thompson, J. T., Dickinson, H. C., & Swinton, R. S. (1934). The Photographic Method of Studying Traffic Behavior. *Highway Research Board Proceedings, 13,* 382-399.

Halati, A., Lieu, H., & Walker, S. (1997). CORSIM- Corridor Traffic Simulation Model., (p. 76th Transportation Research Board Meeting). Washington, D.C.

Heikoop, H., & Henkens, N. (2016). Recent developments and history of the Dutch HCM. *Transportation Research Procedia, 15*, 51-62.

Hellinga, B. R. (1998). Requirements of the Validation and Calibration of Traffic Simulation Models. *Canada Society for Civil Engineering 1998 Anuual Conference*, (pp. 211-222). Halifax, Nova Scotia.

Helly, W. (1961). *Simulation of Bottlenecks in Single Lane Traffic Flow 1959.* Amsterdam: Elsevier.

Herman, R., Montroll, E. W., Potts, R. B., & Rothery, R. W. (1959). Traffic Dynamics: Analysis of Stability in Car Following. *Operations Research*, *7*(1), 86-106.

Hourdakis, J., Michalopoulos, P. G., & Kottommannil, J. (2003). Practical procedure for calibrating microscopic traffic simulation models. *Transportation Research Record: Journal of the Transportation Research Board, 1852*, 130-139.

Jobanputra, R., & Vanderschuren , M. (2012). Calibration and Validation of Micro-Simulation Model for a Local Arterial in Cape Town. *31st Southern African Transport Conference*, (pp. 12-23). Pretoria.

Jobanputra, R., & Vanderschuren, M. (2014). The Development and Calibration of an Agent-Based Microsimulation Model for Vehicle-Pedestrian Interaction. In U. Weidmann, U. Kirsch, & M. Schreckenberg (Eds.), *Pedestrian and Evacuation Dynamics 2012* (pp. 1001-1011). Switzerland: Springer.

Kan, S., & Bhan, G. (2007). Evaluation of microscopic lane change models using NGSIM data. *18th conference on Proceedings of the 18th IASTED International Conference: modeling and simulation*, (pp. 592-597). Montreal, Canada.

Kaseko, M. S. (2002). *A Comparative Evaluation of Simulation Software for Traffic Operations.* Research Division, Nevada Department of Transportation. doi:RDT 03-032

Kerner, B. S. (2009). *Introduction to Modern Traffic Flow Theory and Control: The Long Road to Three-Phase Traffic Theory.* New York: Springer.

Kerner, B. S., & Rehborn, H. (1997). Experimental Properties of Phase Transitions in Traffic Flow. *Physical Review Letters*, *79*(20), 4030-4033.

Kiefer, J., & Wolfowitz, J. (1952). Stochastic estimation of the maximum of a regression function. *Annals of Mathematical Statistics, 23*, 462-466.

Kikuchi, S., Uno, N., & Tanaka, M. (2003). Impacts of Shorter Perception-Reaction Time of Adapted Cruise Controlled Vehicles on Traffic Flow and Safety. *ASCE Journal of Transportation Engineering, 129*(2), 109-221.

Kim, K. O., & Rilett, L. R. (2003). Simplex-based calibration of traffic microsimulation models with intelligent transportation systems data. *Transportation Research Record: Journal of the Transportation Research Board, 1855*(1), 80-89.

Kim, K. O., & Rilett, L. R. (2004). A genetic algorithm based approach to traffic micro-simulation calibration using ITS data. *83rd Transport Research Board Annual Meeting.* Washington, DC.

Kim, S. J., Kim, W., & Rilett, L. R. (2005). Calibration of Microsimulation Models Using Nonparametric Statistical Techniques. *Transportation Research Record: Journal of the Transportation Research Board, 1935*(1).

Knospe, W., Santen, L., Schadschneider, A., & Schreckenberg, M. (2004). Empirical Test for Cellular Automaton Models of Traffic Flow. *Physical Review E: Statistical, Nonlinear, and Soft Matter Physics, 70*(1), 1-25.

Lagarias, J. C., Reeds, J. A., Wright, M. H., & Wright, P. E. (1998). Convergence Properties of the Nelder-Mead Simplex Method in Low Dimensions. *SIAM Journal of Optimization, 9*(1), 112-147.

Leclercq, L. (2007). Hybrid Approaches to the Solutions of the “Lighthill–Whitham–Richards” Models. *Transportation Research Part B: Methodological, 41*(7), 701-709.

Leclercq, L., Laval, J. A., & Chevallier, E. (2007). The Lagrangian Coordinates and What It Means for First Order Traffic Flow Models. *Transportation and Traffic Theory 2007* (pp. 735-753). Oxford, U.K: Elsevier.

Lee, D., Yang, X., & Chandrasekar, P. (2001). Parameter Calibration for PARAMICS Using Genetic Algorithm. *80th Annual Meeting of the Transportation Research Board.* Washington D.C.

Lieberman, E. B. (2015). Brief History of Traffic Simulation. *Transport Research Circular: Transport Research Board 93rd Annual Meeting* (pp. 17-29). Washington, D.C: Transport Research Board of the National Academies.

Ma, J. T., Dong, H., & Zhang, H. M. (2007). Calibration of Microsimulation with Heuristic Optimization Methods. *Transportation Research Record: Journal of the Transportation Research Board, 1999*(1), 208-217.

Ma, T., & Abdulhai, B. (2002). Genetic Algorithm-Based Optimization Approach and Generic Tool for Calibrating Traffic Microscopic Simulation Parameters. *Transportation Research Record: Journal of the Transportation Research Board, 1800*(1), 6-15.

Merritt, E. (2004). Calibration and validation of CORSIM for Swedish road traffic conditions. *83rd Transport Research Board Annual Meeting.* Washington, DC.

Miliam, R. T., & Choa, F. (2000). Recommended Guidelines for the Calibration and Validation of Traffic Simulation Models. *Institute of Transportation Engineers 2000, District 6 Annual Meeting.* Washington, DC.

Mitchell, M. (1997). *An Introduction to Genetic Algorithms.* Cambridge, Massachusetts: The MIT Press.

Nagel, K., & Schreckenberg, M. (1992). A Cellular Automaton Model for Freeway Traffic. *Journal de Physique I France, 2*(12), 2221-2229.

Nelder, J. A., & Mead, R. (1965). A simplex method for function minimization. *Computer Journal, 7*, 308-313.

Newell, G. F. (1961). Nonlinear Effects in the Dynamics of Car Following. *Operations Research, 9*(2), 209-229.

Newell, G. F. (1965). Instability in Dense Highway Traffic: A Review. *2nd International Symposium on the Theory of Traffic Flow 1963*, (pp. 73-83). London.

Newell, G. F. (2002). A Simplified Car-Following Theory: A Lower-Order Model. *Transportation Research Part B: Methodological, 36*(3), 195-205.

Ossen, S. J., & Hoogendoorn, S. P. (2008). Validity of Trajectory-Based Calibration Approach of Car-Following Models in the Presence of Measurement Errors. *Transportation Research Records: Journal of the Transportation Research Board, 2088*(1).

Owen, L. E., Zhang, Y., Rao, L., & McHale, G. (2000). Traffic Flow Simulation Using CORSIM. *2000 Winter Simulation Conference*, (pp. 1143-1147). Singapore.

Owen, L. E., Zhang, Y., Rao, L., & McHale, G. (2000). Traffic Flow Simulation Using CORSIM. *2000 Winter Simulation Conference Proceedings.* Orlando, FL, USA.

Ozili, K. (2023). The Acceptable R-Square in Empirical Modelling for Social Science Research. In C. A. Saliya, *Social Research Methodology and Publishing Results.* Singapore: Springer. doi:10.4018/978-1-6684-6859-3.ch009

Park, B., & Qi, H. (2005). Development and Evaluation of a Procedure for the Calibration of Simulation Models. *Transportation Research Record: Journal of the Transportation Research Board, 1934*(1), 208-217.

Park, B., & Schneeberger, J. (2003). Microscopic Simulation Model Calibration and Validation: Case Study of VISSIM Simulation Model for a Coordinated Actuated Signal System. *Transportation Research Record: Journal of the Transportation Research Board, 1856*(1), 185-192.

Park, B., & Won, J. (2006). *Microscopic Simulation Model Calibration and Validation Handbook.* FHWA, U.S Department of Transportation, Washington D.C. doi:FHWA/VTRC 07-CR6

Pipes, L. A. (1953). An Operational Analysis of Traffic Dynamics. *Journal of Applied Physics, 24*(3), 274-281.

Prigogine, I., & Andrews, F. C. (1960). A Boltzmann-Like Approach for Traffic Flow. *Operations, 8*(6), 789-797.

Punzo, V., & Simonelli, F. (2005). Analysis and comparison of microscopic traffic flow models with real traffic microscopic data. *Transportation Research Record Journal of the Transportation Research Board*(1934), 53-63.

Punzo, V., & Tripodi, A. (2007). Steady-state solutions and multi-class calibration of Gipps' microscopic traffic flow model. *Transportation Research Record Journal of the Transportation Research Board*(1999), 104-114.

Rakha, H. (n.d.). *INTEGRATION DYNAMIC TRAFFIC ASSIGNMENT AND SIMULATION SOFTWARE*. Retrieved May 21, 2022, from HESHAM A. RAKHA, PH.D., P.ENG., F.IEEE: https://sites.google.com/a/vt.edu/hrakha/software

Rakha, H., & Crowther, B. (2002). Comparison of Greenshields, Pipes, and Van Aerde Car following and Traffic Stream Models. *Transportation Research Record, 1802*(1), 248-262.

Rrecaj, A. A., & Bombol, K. M. (2015). Calibration and Validation of the VISSIM Parameters—State of the Art. *TEM Journal-Technology Education Management Informatics, 4*(3), 255-269.

Sanwal, K. K., Petty, K., Walrand, J., & Fawaz, Y. (1996). An Extended Macroscopic Model for Traffic Flow. *Transportation Research Part B, 30*(1), 1-9.

Schultz, G. G., & Rilett, L. R. (2004). Analysis of Distribution and Calibration of Car - Following Sensitivity Parameters in Microscopic Traffic Simulation Models. *Transportation Research Record: Journal of Transportation Research Board, 1876*, 41-51.

Shaaban, K. S., & Radwan, E. (2005). A calibration and validation procedure for microscopic simulation model: a case study of sim traffic arterial streets. *84rd Transport Research Board Annual Meeting.* Washington, DC.

Smith, S., & Lasdon, L. (1992). Solving Large Sparse Nonlinear Programs Using GRG. *ORSA Journal on Computing, 4*(1), 2-15.

Smulders, S. (1990). Control of Freeway Traffic Flow by Variable Speed Signs. *Transportation Research Part B: Methodological*, *24*(2), 111-132.

Spall, J. C. (1992). Multivariate Stochastic Approximation Using a Simultaneous Perturbation Gradient Approximation. *IEEE Transactions on Automatic Control, 37*(3), 332-341.

Spall, J. C. (2003). *Introduction to Stochastic Search and Optimization.* Wiley-Interscience.

Tichauer, C. R., & Watters, M. (2008). N2 BMT Lane - A First for South Africa. *27th Southern African Transport Conference*, (pp. 537-546). Pretoria, South Africa.

Toledo, T., & Koutsopoulos, H. N. (2004). Statistical validation of traffic simulation models. *83rd Transport Research Board Annual Meeting.* Washington, DC.

Toledo, T., Ben-Akiva, M. E., Darda, D., Jah, M., & Koutsopoulos, H. N. (2004). Calibration of Microscopic Traffic Simulation Models with Aggregate Data. *Transportation Research Record: Journal of the Transportation Research Board, 1876*(1), 10-19.

Toledo, T., Koutsopoulos, H. N., Davol, A., Ben-Akiva, M. E., Burghout, W., Andreasson, I., . . . Lundin, C. (2003). Calibration and validation of microscopic traffic simulation tools – Stockholm case study. *Transportation Research Record: Journal of the Transportation Research Board, 1831*(1), 65-75.

Treiber, M., Kesting, A., & Helbing, D. (2006). Understanding Widely Scattered Traffic Flows, the Capacity Drop, and Platoons as Effects of Variance-Driven Time Gaps. *Physical Review E: Statistical, Nonlinear, and Soft Matter Physics, 74*(1).

Treiterer, J., & Myers, J. A. (1974). The Hysteresis Phenomenon in Traffic Flow. *Proc., 6th International Symposium on Transportation and Traffic Theory 1974.* Oxford, U.K: Elsevier.

Ugray, Z., Lasdon, L., Plummer, J., Glover, F., Kelly, J., & Marti, R. (2002). Scatter Search and Local NLP Solvers: A MultistartFramework for Global Optimization. *INFORMS Journal on Computing*, *19*(3), 328-340.

Van Aerde, M. (1995). A single regime speed-flow-density relationship for freeways and arterials. *74th TRB Annual Meeting.* Washington, D.C.

Van Aerde, M. (1995). Single regime speed-flow-density relationship for congested and uncongested highways. *Presented at the 74th TRB Annual Conference.* Washington, D.C.

Van Aerde, M., & Rakha, H. (1995). Multivariate calibration of single regime speed-flow density relationships. *Vehicle Navigation and Information Systems (VNIS) Conference.* Seattle, WA, USA.

Van Aerde, M., Hellinga, B., Baker, M., & Rakha, H. (1996). INTEGRATION: Overview of Simulation Features. *1996 Transportation Research Board Annual Meeting.* Washington, D.C.

van Wageningen-Kessels, F., Hoogendoorn, S. P., Vuik, K., & van Lint, H. (2015). Traffic Flow Modeling: Genealogy. *Transport Research Circular: Transport Research Board 93rd Annual Meeting* (pp. 1-16). Washington, D.C: Transport Research Board of the National Academies.

Vanderschuren , M. (2007). Calibrating Microscopic Simulation Models. *26th Southern African Transport Conference*, (pp. 610-620). Pretoria.

Vermijs, R. G. (1991). The Use of Micro Simulation for the Design of Weaving Sections. In U. Brannolte, *Highway Capacity and Level of Service* (pp. 419-427). Karlsruhe: CRC Press.

Vissim User Manual - V10. (2018). Karlsruhe, Germany.

Wiedemann, R. (1974). *Simulation des Strassenverkehrsflusses*. Institute for Traffic Engineering, University of Karlsruhe.

Wohl, M., & Martin, B. V. (1967). *Traffic Systems Analysis for Engineers and Planners.* New York: McGraw-Hill Book Company.

10. Appendix A: Traffic Count Data

24 Jan Traffic Count Data - Cape Town Destination						
Start	**End**	**Passenger vehicles**	**Taxis**	**Buses**	**Trucks**	**All vehicles**
07h00	07h01	59	12	3	1	75
07h01	07h02	50	16	0	0	66
07h02	07h03	65	4	3	0	72
07h03	07h04	64	12	0	1	77
07h04	07h05	63	10	0	0	73
07h05	07h06	50	10	0	0	60
07h06	07h07	50	16	2	0	68
07h07	07h08	43	15	0	0	58
07h08	07h09	54	8	0	0	62
07h09	07h10	56	7	1	0	64
07h10	07h11	55	7	2	2	66
07h11	07h12	55	5	2	0	62
07h12	07h13	57	16	0	0	73
07h13	07h14	55	4	0	0	59
07h14	07h15	42	9	0	0	51
07h15	07h16	47	14	2	1	64
07h16	07h17	52	10	1	0	63
07h17	07h18	55	13	1	0	69
07h18	07h19	65	8	1	0	74
07h19	07h20	73	10	1	0	84
07h20	07h21	47	14	0	0	61
07h21	07h22	47	12	0	1	60
07h22	07h23	47	12	0	0	59
07h23	07h24	52	11	1	0	64
07h24	07h25	59	6	2	0	67
07h25	07h26	49	11	1	0	61
07h26	07h27	64	6	1	0	71
07h27	07h28	42	17	2	0	61
07h28	07h29	58	9	1	0	68
07h29	07h30	56	8	2	0	66
07h30	07h31	61	9	0	0	70
07h31	07h32	52	10	1	0	63
07h32	07h33	67	7	1	0	75
07h33	07h34	65	6	1	0	72
07h34	07h35	67	7	1	0	75
07h35	07h36	50	19	0	0	69
07h36	07h37	50	10	0	0	60
07h37	07h38	63	3	3	1	70
07h38	07h39	51	10	0	0	61
07h39	07h40	58	17	0	0	75

24 Jan Traffic Count Data - Cape Town Destination						
Start	**End**	**Passenger vehicles**	**Taxis**	**Buses**	**Trucks**	**All vehicles**
07h40	07h41	53	11	1	0	65
07h41	07h42	58	9	1	0	68
07h42	07h43	61	10	1	0	72
07h43	07h44	64	11	0	1	76
07h44	07h45	69	11	0	2	82
07h45	07h46	58	14	0	0	72
07h46	07h47	57	16	0	0	73
07h47	07h48	57	15	1	0	73
07h48	07h49	75	7	0	0	82
07h49	07h50	71	9	0	0	80
07h50	07h51	56	17	3	1	77
07h51	07h52	71	9	0	0	80
07h52	07h53	62	13	0	0	75
07h53	07h54	70	17	1	0	88
07h54	07h55	71	9	2	0	82
07h55	07h56	71	11	0	1	83
07h56	07h57	57	8	1	0	66
07h57	07h58	61	12	3	0	76
07h58	07h59	66	9	0	0	75
07h59	07h60	70	8	0	0	78
Total		**3493**	**636**	**50**	**12**	**4191**
Modal Split		**83%**	**15%**	**1%**	**0%**	

24 Jan Traffic Count Data - M3 Destination						
Start	End	Passenger vehicles	Taxis	Buses	Trucks	All vehicles
07h00	07h01	16	0	0	0	16
07h01	07h02	19	0	0	0	19
07h02	07h03	15	0	1	0	16
07h03	07h04	19	0	0	0	19
07h04	07h05	14	1	1	0	16
07h05	07h06	14	0	1	0	15
07h06	07h07	19	0	0	0	19
07h07	07h08	21	0	1	1	23
07h08	07h09	16	0	0	0	16
07h09	07h10	17	1	0	0	18
07h10	07h11	15	0	0	0	15
07h11	07h12	23	0	0	0	23
07h12	07h13	18	0	0	0	18
07h13	07h14	20	0	0	0	20
07h14	07h15	20	0	0	1	21
07h15	07h16	12	2	1	0	15
07h16	07h17	24	0	0	0	24
07h17	07h18	15	0	0	0	15
07h18	07h19	16	0	0	0	16
07h19	07h20	15	2	0	2	19
07h20	07h21	21	0	0	0	21
07h21	07h22	16	0	0	0	16
07h22	07h23	20	3	0	0	23
07h23	07h24	20	0	0	0	20
07h24	07h25	22	1	1	0	24
07h25	07h26	15	0	0	0	15
07h26	07h27	13	1	0	0	14
07h27	07h28	22	0	0	0	22
07h28	07h29	17	0	0	0	17
07h29	07h30	16	0	0	0	16
07h30	07h31	22	0	0	0	22
07h31	07h32	24	0	0	0	24
07h32	07h33	22	0	0	0	22
07h33	07h34	21	1	0	0	22
07h34	07h35	19	0	0	0	19
07h35	07h36	17	1	0	0	18
07h36	07h37	15	0	0	0	15
07h37	07h38	18	0	0	0	18
07h38	07h39	27	2	0	0	29
07h39	07h40	15	0	0	0	15

24 Jan Traffic Count Data - M3 Destination						
Start	**End**	**Passenger vehicles**	**Taxis**	**Buses**	**Trucks**	**All vehicles**
07h40	07h41	23	0	0	0	23
07h41	07h42	19	0	1	0	20
07h42	07h43	12	0	0	0	12
07h43	07h44	21	1	0	0	22
07h44	07h45	18	0	0	0	18
07h45	07h46	26	1	0	0	27
07h46	07h47	16	1	0	0	17
07h47	07h48	20	0	0	0	20
07h48	07h49	15	0	0	0	15
07h49	07h50	19	2	1	0	22
07h50	07h51	23	0	0	0	23
07h51	07h52	13	0	0	0	13
07h52	07h53	21	2	0	0	23
07h53	07h54	15	0	0	0	15
07h54	07h55	14	0	0	0	14
07h55	07h56	14	0	0	0	14
07h56	07h57	16	0	0	0	16
07h57	07h58	12	0	0	0	12
07h58	07h59	17	0	0	0	17
07h59	07h60	17	1	1	0	19
Total		**1081**	**23**	**9**	**4**	**1117**
Modal Split		**96.8%**	**2.1%**	**0.8%**	**0.4%**	

25 January Traffic Count Data – Cape Town Destination						
Start	**End**	**Passenger vehicles**	**Taxis**	**Buses**	**Trucks**	**All vehicles**
07h00	07h01	61	2	0	0	63
07h01	07h02	62	11	1	0	74
07h02	07h03	65	4	3	1	73
07h03	07h04	46	19	1	0	66
07h04	07h05	52	18	2	0	72
07h05	07h06	44	13	0	0	57
07h06	07h07	61	13	1	0	75
07h07	07h08	67	9	0	1	77
07h08	07h09	56	20	0	0	76
07h09	07h10	51	11	0	0	62
07h10	07h11	43	20	0	0	63
07h11	07h12	53	15	1	0	69
07h12	07h13	67	12	1	0	80
07h13	07h14	57	24	2	0	83
07h14	07h15	49	9	2	0	60
07h15	07h16	62	12	0	2	76
07h16	07h17	50	16	1	0	67
07h17	07h18	62	11	0	0	73
07h18	07h19	61	4	2	0	67
07h19	07h20	59	8	2	1	70
07h20	07h21	49	17	1	0	67
07h21	07h22	70	6	0	0	76
07h22	07h23	58	7	1	0	66
07h23	07h24	60	17	1	0	78
07h24	07h25	59	13	2	0	74
07h25	07h26	61	10	0	0	71
07h26	07h27	42	12	2	0	56
07h27	07h28	65	7	2	0	74
07h28	07h29	51	6	1	0	58
07h29	07h30	72	13	2	0	87
07h30	07h31	54	18	0	0	72
07h31	07h32	59	10	1	0	70
07h32	07h33	66	7	0	0	73
07h33	07h34	61	7	0	1	69
07h34	07h35	67	6	0	0	73
07h35	07h36	57	15	0	0	72
07h36	07h37	61	19	2	0	82
07h37	07h38	61	10	0	0	71
07h38	07h39	61	11	1	0	73
07h39	07h40	60	14	1	0	75

25 January Traffic Count Data – Cape Town Destination						
Start	**End**	**Passenger vehicles**	**Taxis**	**Buses**	**Trucks**	**All vehicles**
07h40	07h41	54	12	1	0	67
07h41	07h42	52	16	1	0	69
07h42	07h43	56	9	0	0	65
07h43	07h44	70	11	1	0	82
07h44	07h45	68	8	1	0	77
07h45	07h46	62	14	0	0	76
07h46	07h47	65	15	2	0	82
07h47	07h48	52	16	0	0	68
07h48	07h49	55	18	0	0	73
07h49	07h50	66	19	1	2	88
07h50	07h51	56	19	0	0	75
07h51	07h52	53	19	0	0	72
07h52	07h53	64	7	0	0	71
07h53	07h54	52	8	1	0	61
07h54	07h55	67	4	0	0	71
07h55	07h56	61	10	1	0	72
07h56	07h57	57	2	4	1	64
07h57	07h58	74	5	1	0	80
07h58	07h59	50	10	2	0	62
07h59	07h60	65	7	2	0	74
Total		**3521**	**705**	**54**	**9**	**4289**
Modal Split		**82%**	**16%**	**1%**	**0%**	

25 Jan Traffic Count Data - M3 Destination						
Start	**End**	**Passenger vehicles**	**Taxis**	**Buses**	**Trucks**	**All vehicles**
07h00	07h01	20	0	1	0	21
07h01	07h02	18	0	0	0	18
07h02	07h03	12	1	0	0	13
07h03	07h04	20	2	0	0	22
07h04	07h05	10	0	0	0	10
07h05	07h06	15	1	1	0	17
07h06	07h07	17	0	0	0	17
07h07	07h08	13	0	0	1	14
07h08	07h09	22	1	0	0	23
07h09	07h10	17	0	0	0	17
07h10	07h11	22	0	1	0	23
07h11	07h12	25	1	0	0	26
07h12	07h13	17	2	0	0	19
07h13	07h14	19	0	0	0	19
07h14	07h15	24	0	1	0	25
07h15	07h16	11	0	0	1	12
07h16	07h17	17	1	0	0	18
07h17	07h18	21	0	0	0	21
07h18	07h19	20	0	0	0	20
07h19	07h20	19	0	0	0	19
07h20	07h21	20	1	0	0	21
07h21	07h22	19	0	0	0	19
07h22	07h23	22	1	0	0	23
07h23	07h24	24	0	1	0	25
07h24	07h25	23	0	0	0	23
07h25	07h26	19	0	0	0	19
07h26	07h27	31	0	0	1	32
07h27	07h28	19	0	0	0	19
07h28	07h29	23	3	0	0	26
07h29	07h30	16	1	0	0	17
07h30	07h31	23	0	0	0	23
07h31	07h32	13	3	2	0	18
07h32	07h33	23	1	0	0	24
07h33	07h34	23	1	0	0	24
07h34	07h35	16	1	0	0	17
07h35	07h36	20		0	0	20
07h36	07h37	22	1	0	0	23
07h37	07h38	25	1	0	0	26
07h38	07h39	20	1	0	0	21
07h39	07h40	15		0	0	15

25 Jan Traffic Count Data - M3 Destination						
Start	**End**	**Passenger vehicles**	**Taxis**	**Buses**	**Trucks**	**All vehicles**
07h40	07h41	22	0	0	0	22
07h41	07h42	18	0	0	0	18
07h42	07h43	25	0	0	0	25
07h43	07h44	20	1	0	0	21
07h44	07h45	16	1	0	0	17
07h45	07h46	17	2	0	0	19
07h46	07h47	15	0	0	0	15
07h47	07h48	15	0	0	0	15
07h48	07h49	17	1	0	0	18
07h49	07h50	12	0	0	0	12
07h50	07h51	18	0	0	0	18
07h51	07h52	14	2	1	0	17
07h52	07h53	16	1	2	0	19
07h53	07h54	13	0	0	0	13
07h54	07h55	19	0	1	0	20
07h55	07h56	19	0	0	0	19
07h56	07h57	19	0	0	0	19
07h57	07h58	16	2	1	0	19
07h58	07h59	16	1	0	0	17
07h59	07h60	18	0	0	0	18
Total		**1120**	35	12	3	**1170**
Modal Split		**95.7%**	**3.0%**	**1.0%**	**0.3%**	

24-Jan-23 Hourly-Equivalent Traffic Volume for all Destinations							
Start	**End**	**Passenger vehicles**	**Taxis**	**Buses**	**Trucks**	**Total Vehicles per minute**	**Hourly Equivalent Volume**
07h00	07h01	75	12	3	1	91	5460
07h01	07h02	69	16	0	0	85	5100
07h02	07h03	80	4	4	0	88	5280
07h03	07h04	83	12	0	1	96	5760
07h04	07h05	77	11	1	0	89	5340
07h05	07h06	64	10	1	0	75	4500
07h06	07h07	69	16	2	0	87	5220
07h07	07h08	64	15	1	1	81	4860
07h08	07h09	70	8	0	0	78	4680
07h09	07h10	73	8	1	0	82	4920
07h10	07h11	70	7	2	2	81	4860
07h11	07h12	78	5	2	0	85	5100
07h12	07h13	75	16	0	0	91	5460
07h13	07h14	75	4	0	0	79	4740
07h14	07h15	62	9	0	1	72	4320
07h15	07h16	59	16	3	1	79	4740
07h16	07h17	76	10	1	0	87	5220
07h17	07h18	70	13	1	0	84	5040
07h18	07h19	81	8	1	0	90	5400
07h19	07h20	88	12	1	2	103	6180
07h20	07h21	68	14	0	0	82	4920
07h21	07h22	63	12	0	1	76	4560
07h22	07h23	67	15	0	0	82	4920
07h23	07h24	72	11	1	0	84	5040
07h24	07h25	81	7	3	0	91	5460
07h25	07h26	64	11	1	0	76	4560
07h26	07h27	77	7	1	0	85	5100
07h27	07h28	64	17	2	0	83	4980
07h28	07h29	75	9	1	0	85	5100
07h29	07h30	72	8	2	0	82	4920
07h30	07h31	83	9	0	0	92	5520
07h31	07h32	76	10	1	0	87	5220
07h32	07h33	89	7	1	0	97	5820
07h33	07h34	86	7	1	0	94	5640
07h34	07h35	86	7	1	0	94	5640
07h35	07h36	67	20	0	0	87	5220
07h36	07h37	65	10	0	0	75	4500
07h37	07h38	81	3	3	1	88	5280
07h38	07h39	78	12	0	0	90	5400
07h39	07h40	73	17	0	0	90	5400

24-Jan-23 Hourly-Equivalent Traffic Volume for all Destinations							
Start	**End**	**Passenger vehicles**	**Taxis**	**Buses**	**Trucks**	**Total Vehicles per minute**	**Hourly Equivalent Volume**
07h40	07h41	76	11	1	0	88	5280
07h41	07h42	77	9	2	0	88	5280
07h42	07h43	73	10	1	0	84	5040
07h43	07h44	85	12	0	1	98	5880
07h44	07h45	87	11	0	2	100	6000
07h45	07h46	84	15	0	0	99	5940
07h46	07h47	73	17	0	0	90	5400
07h47	07h48	77	15	1	0	93	5580
07h48	07h49	90	7	0	0	97	5820
07h49	07h50	90	11	1	0	102	6120
07h50	07h51	79	17	3	1	100	6000
07h51	07h52	84	9	0	0	93	5580
07h52	07h53	83	15	0	0	98	5880
07h53	07h54	85	17	1	0	103	6180
07h54	07h55	85	9	2	0	96	5760
07h55	07h56	85	11	0	1	97	5820
07h56	07h57	73	8	1	0	82	4920
07h57	07h58	73	12	3	0	88	5280
07h58	07h59	83	9	0	0	92	5520
07h59	07h60	87	9	1	0	97	5820
Total		**4574**	**659**	**59**	**16**	**5308**	
Modal Split		**86.2%**	**12.4%**	**1.1%**	**0.3%**		

Destination Fractions							
		Passenger vehicles	**Taxis**	**Buses**	**Trucks**	**All Vehicles**	
	Town	76%	97%	85%	75%	79%	
	M3	24%	3%	15%	25%	21%	

25-Jan-23 Hourly-Equivalent Traffic Volume for all Destinations							
Start	End	Passenger vehicles	Taxis	Buses	Trucks	Total Vehicles	Hourly Equivalent Volume
07h00	07h01	81	2	1	0	84	5040
07h01	07h02	80	11	1	0	92	5520
07h02	07h03	77	5	3	1	86	5160
07h03	07h04	66	21	1	0	88	5280
07h04	07h05	62	18	2	0	82	4920
07h05	07h06	59	14	1	0	74	4440
07h06	07h07	78	13	1	0	92	5520
07h07	07h08	80	9	0	2	91	5460
07h08	07h09	78	21	0	0	99	5940
07h09	07h10	68	11	0	0	79	4740
07h10	07h11	65	20	1	0	86	5160
07h11	07h12	78	16	1	0	95	5700
07h12	07h13	84	14	1	0	99	5940
07h13	07h14	76	24	2	0	102	6120
07h14	07h15	73	9	3	0	85	5100
07h15	07h16	73	12	0	3	88	5280
07h16	07h17	67	17	1	0	85	5100
07h17	07h18	83	11	0	0	94	5640
07h18	07h19	81	4	2	0	87	5220
07h19	07h20	78	8	2	1	89	5340
07h20	07h21	69	18	1	0	88	5280
07h21	07h22	89	6	0	0	95	5700
07h22	07h23	80	8	1	0	89	5340
07h23	07h24	84	17	2	0	103	6180
07h24	07h25	82	13	2	0	97	5820
07h25	07h26	80	10	0	0	90	5400
07h26	07h27	73	12	2	1	88	5280
07h27	07h28	84	7	2	0	93	5580
07h28	07h29	74	9	1	0	84	5040
07h29	07h30	88	14	2	0	104	6240
07h30	07h31	77	18	0	0	95	5700
07h31	07h32	72	13	3	0	88	5280
07h32	07h33	89	8	0	0	97	5820
07h33	07h34	84	8	0	1	93	5580
07h34	07h35	83	7	0	0	90	5400
07h35	07h36	77	15	0	0	92	5520
07h36	07h37	83	20	2	0	105	6300
07h37	07h38	86	11	0	0	97	5820
07h38	07h39	81	12	1	0	94	5640
07h39	07h40	75	14	1	0	90	5400

25-Jan-23 Hourly-Equivalent Traffic Volume for all Destinations							
Start	**End**	**Passenger vehicles**	**Taxis**	**Buses**	**Trucks**	**Total Vehicles**	**Hourly Equivalent Volume**
07h40	07h41	76	12	1	0	89	5340
07h41	07h42	70	16	1	0	87	5220
07h42	07h43	81	9	0	0	90	5400
07h43	07h44	90	12	1	0	103	6180
07h44	07h45	84	9	1	0	94	5640
07h45	07h46	79	16	0	0	95	5700
07h46	07h47	80	15	2	0	97	5820
07h47	07h48	67	16	0	0	83	4980
07h48	07h49	72	19	0	0	91	5460
07h49	07h50	78	19	1	2	100	6000
07h50	07h51	74	19	0	0	93	5580
07h51	07h52	67	21	1	0	89	5340
07h52	07h53	80	8	2	0	90	5400
07h53	07h54	65	8	1	0	74	4440
07h54	07h55	86	4	1	0	91	5460
07h55	07h56	80	10	1	0	91	5460
07h56	07h57	76	2	4	1	83	4980
07h57	07h58	90	7	2	0	99	5940
07h58	07h59	66	11	2	0	79	4740
07h59	07h60	83	7	2	0	92	5520
Total		**4641**	**740**	**66**	**12**	**5459**	
Modal Split		**85.0%**	**13.6%**	**1.2%**	**0.2%**		
Destination Fractions							
		Passenger vehicles	**Taxis**	**Buses**	**Trucks**	**All Vehicles**	
	Town	76%	95%	82%	75%	79%	
	M3	24%	5%	18%	25%	21%	